

GEORGIA INSTITUTE OF TECHNOLOGY
OFFICE OF CONTRACT ADMINISTRATION
SPONSORED PROJECT INITIATION

Date: 8/7/78

Project Title: Powerhouse Penstock and Tunnel Junctions

Project No: E-20-638 (Co-project w/E-20-637/Mayer/CE)

Project Director: Dr. C. S. Martin

Sponsor: Southern Company Services

Agreement Period: From 6/30/78 Until 7/1/80
5/1/79

Type Agreement: Standard Industrial Research Agreement dated 7/24/78

Amount: \$58,500

Reports Required: Initial Results, Final Report

Sponsor Contact Person (s):

Technical Matters

Contractual Matters
(thru OCA)

Mr. G. B. Dougherty, Manager
Hydro-Projects Department
Southern Company Services
P. O. Box 2625
Birmingham, AL 35202

Defense Priority Rating: None

Assigned to: Civil Engineering (School/Laboratory)

COPIES TO:

Project Director
Division Chief (EES)
School/Laboratory Director
Dean/Director-EES
Accounting Office
Procurement Office
Security Coordinator (OCA)✓
Reports Coordinator (OCA)

Library, Technical Reports Section
EES Information Office
EES Reports & Procedures
Project File (OCA)
Project Code (GTRI)
Other _____

GEORGIA INSTITUTE OF TECHNOLOGY
OFFICE OF CONTRACT ADMINISTRATION
SPONSORED PROJECT TERMINATION

Date: 10/3/80

Project Title: Powerhouse Penstock and Tunnel Junctions

Project No: E-20-638 (Co-project w/E-20/637/Mayer/CE)

Project Director: Dr. C.S. Martin

Sponsor: Southern Company Services

Effective Termination Date: 7/31/80

Clearance of Accounting Charges: 7/31/80

Grant/Contract Closeout Actions Remaining:

- ☒ Final Invoice and Closing Documents
- ☐ Final Fiscal Report
- ☐ Final Report of Inventions
- ☐ Govt. Property Inventory & Related Certificate
- ☐ Classified Material Certificate
- ☐ Other _____

Assigned to: Civil Engineering (School/~~Laboratory~~)

COPIES TO:

Project Director
Division Chief (EES)
School/Laboratory Director
Dean/Director—EES
Accounting Office
Procurement Office
✓ Security Coordinator (OCA)
✓ Reports Coordinator (OCA)

Library, Technical Reports Section
EES Information Office
Project File (OCA)
Project Code (GTRI)
Other C.E. Smith

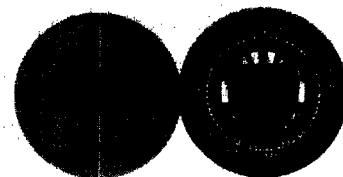
**HYDRAULIC MODEL STUDY —
POWER TUNNEL BIFURCATION
ROCKY MOUNTAIN PROJECT
GEORGIA POWER COMPANY**

**By
C. S. Martin**

**Prepared for
SOUTHERN COMPANY SERVICES, INC.
Birmingham, Alabama 35202**

March 1980

**GEORGIA INSTITUTE OF TECHNOLOGY
SCHOOL OF CIVIL ENGINEERING
ATLANTA, GEORGIA 30682**



HYDRAULIC MODEL STUDY - POWER TUNNEL BIFURCATION

ROCKY MOUNTAIN PROJECT

GEORGIA POWER COMPANY

by

C. S. Martin

Prepared for

SOUTHERN COMPANY SERVICES, INC.
Birmingham, Alabama 35202

March 1980

School of Civil Engineering
Georgia Institute of Technology
Atlanta, Georgia 30332

FOREWORD

Hydraulic model studies of the Power Tunnel Bifurcation of the Rocky Mountain Project were conducted in the Old Hydraulics Laboratory, School of Civil Engineering, Georgia Institute of Technology for the Georgia Power Company under the administration of Southern Company Services, Inc.

Dr. C. S. Martin, Professor of Civil Engineering, was the principal investigator for the project. Mr. Frank D. Lewis of the Lockheed-Georgia Corporation supervised the design and construction of the initial model scheme. Mr. Homer J. Bates, Senior Laboratory Technician, fabricated and installed the remaining three schemes. Mr. D. E. Tamplin assisted in the construction of the model and the collection of data. Most of the data exhibits were prepared by Mr. M. E. Blalock with the aid of a digital plotter.

The guidance and advice of Mr. Gale B. Dougherty of Southern Company Services, Inc. throughout the conduct of the project is appreciated. The assistance of Dr. C. S. Chiou of the same organization is likewise acknowledged. The writer also would like to recognize the able advice and assistance of Mr. A. W. Elkins of the Georgia Power Company.

TABLE OF CONTENTS

	Page
FOREWORD.	i
LIST OF EXHIBITS.	iii
LIST OF TABLES.	viii
SUMMARY	ix
CHAPTER	
I. INTRODUCTION	1
II. DESCRIPTION OF MODEL	3
Flow Measurement	4
Piezometric Head Measurement	4
Test Conditions.	5
III. TEST RESULTS FOR MODIFIED B-1 SCHEME	15
Head-Loss Data	15
Flow Patterns in Bifurcation Model	17
Pressure Distribution in Trunk	19
IV. TEST RESULTS FOR SCHEME B-2.	43
Head-Loss Data	43
Flow Patterns in Bifurcation Model	43
Pressure Distribution in Trunk	44
V. TEST RESULTS FOR SCHEME C-1.	64
Head-Loss Data	64
Flow Patterns in Bifurcation Model	64
VI. TEST RESULTS FOR SCHEME A-i.	81
Head-Loss Data	81
Flow Patterns in Bifurcation Model	81
Pressure Distribution in Trunk	82
VII. COMPARISON OF FOUR SCHEMES	110
VIII. PERFORMANCE OF ELBOW BETWEEN VERTICAL SHAFT AND TUNNEL	113
IX. CONCLUSIONS AND RECOMMENDATIONS.	115
APPENDIX.	116

LIST OF EXHIBITS

Exhibit	Title	Page
1	Geometries of Four Bifurcation Schemes Tested.	2
2	Layout of Model in Laboratory.	6
3	View of Model Tunnel and Vertical Shaft.	7
4	View of Model Trunk and Penstocks.	8
5	Location of Pressure Taps in Straight Legs of Schemes B-1 and B-2	9
6	Location of Pressure Taps in Straight Legs of Scheme A-1.10
7	Location of Pressure Taps in Trunk of Modified Scheme B-1.11
8	Location of Pressure Taps in Trunk of Scheme B-212
9	Location of Pressure Taps in Trunk of Scheme A-113
10	Hydraulic and Energy Grade Lines in Modified Scheme B-1 for Three Units Generating.20
11	Hydraulic and Energy Grade Lines in Modified Scheme B-1 for Units 1 and 2 Generating.21
12	Hydraulic and Energy Grade Lines in Modified Scheme B-1 for Units 1 and 3 Generating.22
13	Hydraulic and Energy Grade Lines in Modified Scheme B-1 for Units 2 and 3 Generating.23
14	Hydraulic and Energy Grade Lines in Modified Scheme B-1 for Single Unit Generating.24
15	Hydraulic and Energy Grade Lines in Modified Scheme B-1 for Three Units Pumping25
16	Hydraulic and Energy Grade Lines in Modified Scheme B-1 for Units 1 and 2 Pumping26
17	Hydraulic and Energy Grade Lines in Modified Scheme B-1 for Units 1 and 3 Pumping27
18	Hydraulic and Energy Grade Lines in Modified Scheme B-1 for Units 2 and 3 Pumping28

Exhibit	Title	Page
19	Hydraulic and Energy Grade Lines in Modified Scheme B-1 for Single Unit Pumping.	29
20	View of Tuft and Air Bubble Patterns in Trunk of Modified Scheme B-1 for Three Units Generating.	32
21	View of Tuft Pattern in Trunk of Modified Scheme B-1 for Units 1 and 2 Generating	33
22	View of Tuft Pattern in Trunk of Modified Scheme B-1 for Unit 3 Generating.	34
23	View of Tuft and Air Bubble Patterns in Trunk of Modified Scheme B-1 for Three Units Pumping	35
24	View of Tuft and Air Bubble Patterns in Trunk of Modified Scheme B-1 for Units 1 and 2 Pumping	36
25	View of Tuft and Air Bubble Patterns in Trunk of Modified Scheme B-1 for Units 1 and 3 Pumping	37
26	View of Tuft and Air Bubble Patterns in Trunk of Modified Scheme B-1 for Units 2 and 3 Pumping	38
27	View of Tuft and Air Bubble Patterns in Trunk of Modified Scheme B-1 for Unit 1 Pumping.	39
28	View of Tuft and Air Bubble Patterns in Trunk of Modified Scheme B-1 for Unit 2 Pumping.	40
29	View of Tuft and Air Bubble Patterns in Trunk of Modified Scheme B-1 for Unit 3 Pumping.	41
30	Hydraulic and Energy Grade Lines in Scheme B-2 for Three Units Generating	45
31	Hydraulic and Energy Grade Lines in Scheme B-2 for Units 1 and 2 Generating	46
32	Hydraulic and Energy Grade Lines in Scheme B-2 for Units 1 and 3 Generating	47
33	Hydraulic and Energy Grade Lines in Scheme B-2 for Units 2 and 3 Generating	48
34	Hydraulic and Energy Grade Lines in Scheme B-2 for Single Unit Generating.	49
35	Hydraulic and Energy Grade Lines in Scheme B-2 for Three Units Pumping.	50
36	Hydraulic and Energy Grade Lines in Scheme B-2 for Units 1 and 2 Pumping.	51

Exhibit	Title	Page
37	Hydraulic and Energy Grade Lines in Scheme B-2 for Units 1 and 3 Pumping.	52
38	Hydraulic and Energy Grade Lines in Scheme B-2 for Units 2 and 3 Pumping.	53
39a	Hydraulic and Energy Grade Lines in Scheme B-2 for Single Units 1 and 2 Pumping	54
39b	Hydraulic and Energy Grade Lines in Scheme B-2 for Unit 3 Pumping	55
40	View of Tuft Pattern in Trunk of Scheme B-2 for Three Units Generating	58
41	View of Tuft Pattern in Trunk of Scheme B-2 for Unit 3 Generating.	59
42	View of Tuft Pattern in Trunk of Scheme B-2 for Three Units Pumping.	60
43	View of Tuft Pattern in Trunk of Scheme B-2 for Units 2 and 3 Pumping.	61
44	View of Tuft Pattern in Trunk of Scheme B-2 for Unit 3 Pumping	62
45	Hydraulic and Energy Grade Lines in Scheme C-1 for Three Units Generating	66
46	Hydraulic and Energy Grade Lines in Scheme C-1 for Units 1 and 2 Generating	67
47	Hydraulic and Energy Grade Lines in Scheme C-1 for Units 1 and 3 Generating	68
48	Hydraulic and Energy Grade Lines in Scheme C-1 for Units 2 and 3 Generating	69
49	Hydraulic and Energy Grade Lines in Scheme C-1 for Single Unit Generating	70
50	Hydraulic and Energy Grade Lines in Scheme C-1 for Three Units Pumping.	71
51	Hydraulic and Energy Grade Lines in Scheme C-1 for Units 1 and 2 Pumping.	72
52	Hydraulic and Energy Grade Lines in Scheme C-1 for Units 1 and 3 Pumping.	73
53	Hydraulic and Energy Grade Lines in Scheme C-1 for Units 2 and 3 Pumping.	74

Exhibit	Title	Page
54	Hydraulic and Energy Grade Lines in Scheme C-1 for Single Unit Pumping.	75
55	View of Tuft Pattern in Trunk of Scheme C-1 for Three Units Generating	78
56	View of Tuft Pattern in Trunk of Scheme C-1 for Three Units Pumping.	79
57	View of Tuft Pattern in Trunk of Scheme C-1 for Unit 3 Pumping	80
58	Hydraulic and Energy Grade Lines in Scheme A-1 for Three Units Generating	83
59	Hydraulic and Energy Grade Lines in Scheme A-1 for Units 1 and 2 Generating	84
60	Hydraulic and Energy Grade Lines in Scheme A-1 for Units 1 and 3 Generating	85
61	Hydraulic and Energy Grade Lines in Scheme A-1 for Units 2 and 3 Generating	86
62	Hydraulic and Energy Grade Lines in Scheme A-1 for Single Unit Generating	87
63	Hydraulic and Energy Grade Lines in Scheme A-1 for Three Units Pumping.	88
64	Hydraulic and Energy Grade Lines in Scheme A-1 for Units 1 and 2 Pumping.	89
65	Hydraulic and Energy Grade Lines in Scheme A-1 for Units 1 and 3 Pumping.	90
66	Hydraulic and Energy Grade Lines in Scheme A-1 for Units 2 and 3 Pumping.	91
67	Hydraulic and Energy Grade Lines in Scheme A-1 for Single Unit Pumping.	92
68	View of Tuft Pattern in Trunk of Scheme A-1 for Three Units Generating	95
69	View of Tuft Pattern in Trunk of Scheme A-1 for Units 1 and 2 Generating	96
70	View of Tuft Pattern in Trunk of Scheme A-1 for Units 1 and 3 Generating	97
71	View of Tuft Pattern in Trunk of Scheme A-1 for Units 2 and 3 Generating	98

Exhibit	Title	Page
72	View of Tuft Pattern in Trunk of Scheme A-1 for Unit 1 Generating.	99
73	View of Tuft Pattern in Trunk of Scheme A-1 for Unit 2 Generating.100
74	View of Tuft Pattern in Trunk of Scheme A-1 for Unit 3 Generating.101
75	View of Tuft Pattern in Trunk of Scheme A-1 for Three Units Pumping.102
76	View of Tuft Pattern in Trunk of Scheme A-1 for Units 1 and 2 Pumping.103
77	View of Tuft Pattern in Trunk of Scheme A-1 for Units 1 and 3 Pumping.104
78	View of Tuft Pattern in Trunk of Scheme A-1 for Units 2 and 3 Pumping.105
79	View of Tuft Pattern in Trunk of Scheme A-1 for Unit 1 Pumping106
80	View of Tuft Pattern in Trunk of Scheme A-1 for Unit 2 Pumping107
81	View of Tuft Pattern in Trunk of Scheme A-1 for Unit 3 Pumping108
82	Design Drawings and Model Cross Sections for Modified Scheme B-1.117
83	Design Drawings and Model Cross Sections for Scheme B-2121
84	Design Drawings and Model Cross Sections for Scheme A-1124

LIST OF TABLES

Table	Title	Page
1	List of Possible Test Conditions.....	14
2	Summary of Actual Loss Coefficients for Modified B-1 Scheme.....	30
3	Summary of Relative Loss Coefficients for Modified B-1 Scheme.....	31
4	Values of Relative Hydraulic Grade Line in Trunk of Modified B-1 Scheme.....	42
5	Summary of Actual Loss Coefficients for B-2 Scheme.....	56
6	Summary of Relative Loss Coefficients for B-2 Scheme.....	57
7	Values of Relative Hydraulic Grade Line in Trunk of B-2 Scheme.....	63
8	Summary of Actual Loss Coefficients for C-1 Scheme.....	76
9	Summary of Relative Loss Coefficients for C-1 Scheme.....	77
10	Summary of Actual Loss Coefficients for A-1 Scheme.....	93
11	Summary of Relative Loss Coefficients for A-1 Scheme.....	94
12	Values of Relative Hydraulic Grade Line in Trunk of A-1 Scheme.....	109
13	Comparison of Performance of Schemes A-1, B-1, B-2, and C-1 Based on Relative Loss Coefficients.....	112

SUMMARY

A hydraulic model study of four bifurcation schemes of the Rocky Mountain Pumped Storage Project was conducted. For each design the head losses and the hydraulic performance of the three-penstock bifurcation were determined. Head loss coefficients were based upon the extrapolation of the energy grade lines from the straight tunnel and three straight penstocks to the bifurcation itself. Careful measurement of the linear HGLs in each straight leg allowed for the construction and extrapolation of representative EGLs to the bifurcation. By means of observing tuft glued to the inside walls of the trunk of the bifurcation and air bubbles injected into the flowing water flow patterns in the model were photographed and studied.

Based upon an extensive research program that included 14 tests for each configuration, Scheme A-1 was judged to be the best overall. Although for several modes of operation this scheme was outperformed by one of the others, Scheme A-1 is recommended as having the lowest overall hydraulic losses and the best hydraulic performance.

CHAPTER I

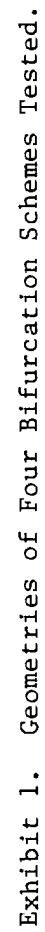
INTRODUCTION

The Rocky Mountain Project is a pumped storage development of the Georgia Power Company. This hydroelectric facility is to be located some ten miles northwest of Rome, Georgia. Hydraulic model studies were conducted at the Georgia Institute of the following three main components of the project: Lower Reservoir Main Spillway, Upper Reservoir Intake Structure, and Power Tunnel Bifurcation. This report includes only the results of the hydraulic model investigation of the Power Tunnel Bifurcation. The results of the other hydraulic model studies of the Rocky Mountain Project are contained in companion reports.

The purpose of this model study was to evaluate the head losses and hydraulic performance of three-tunnel bifurcation schemes. The vertical shaft, tunnel, bifurcations, and penstocks were modeled with a pressurized piping system that did not include the upper reservoir and its intake. The model was constructed at a scale ratio of 39.6:1, corresponding to a ten-inch conduit representing the model tunnel and vertical shaft.

The model was constructed so that flow in both the generating and pumping modes could be investigated. By the use of pumps, and control valves on each penstock, various combinations of one, two, or three unit operation in either mode could be established.

Four schemes were extensively tested for energy efficiency and flow distribution in the bifurcations. Exhibit 1 shows the shape of the four geometries, which are referred to as Schemes C-1, B-2, B-1, (Modified) and A-1. In the Appendix the detailed designs of Schemes B-1, B-2, and A-1 are compared with the actual scaled cross sections of the model as built.



CHAPTER II

DESCRIPTION OF MODEL

The entire hydraulic model was built at an undistorted scale of 1:39.6. Although gravity does not affect the flow patterns in a pressurized flow of the type present in tunnel bifurcations, the Froude law was used to establish the model flows. From the length scale $L_R = 39.6$, the prototype-to-model ratios of velocity V_R , discharge Q_R , and head H_R are

$$V_R = \sqrt{L_R} = 6.29 \quad (1)$$

$$Q_R = L_R^{5/2} = 9868 \quad (2)$$

$$H_R = L_R = 39.6 \quad (3)$$

The above relationships were used in specifying model flows and in the conversion of model data to prototype conditions. Testing was frequently conducted at flows higher than those dictated by equation (2) in order to create greater differences in head for ease of measurement. For the range of Reynolds numbers covered in the test program the flow was always turbulent. The bifurcation losses, which are mainly a result of turbulence caused by separated flow, should vary as the velocity squared. All flow rates and heads are reported in prototype units.

The free-surface condition and the intake of the upper reservoir were not simulated in this model as the principal objective was the hydraulic performance of the various bifurcation schemes, which should not have been influenced measurably by the entrance flow patterns in the generation mode. A schematic of the model layout is shown in Exhibit 2. Because of the limitation in space both the vertical shaft and the tunnel had to be fore-shortened somewhat. In order to improve the flow conditions in the

generating mode straightening vanes were installed in the upper elbow of the model. The lower elbow shown in the background of Exhibit 3 was fabricated to scale out of clear plastic.

The entire bifurcation model was made out of clear plastic, as shown in the photograph in Exhibit 4. Standard size commercial piping was used for the three penstocks, which were connected to PVC elbows and piping, terminating with the three pinch valves, which simulated the pump-turbines. By closing the discharge valve on the pump situated in the laboratory sump flow could be produced in the generating mode from the constant head tank outside the laboratory. In this mode the dump valve at the sump was open, allowing the flow through the respective units to be controlled by the three pinch valves.

By closing the dump valve and opening the pump discharge valve the sump pump produced flow in the pumping mode to the head tank. The flow rate in each unit could be systematically set to a prescribed value.

Flow Measurement

As shown in Exhibit 2 a bend meter was installed on each unit. Each bend meter was connected to an air-water manometer for direct reading. By use of the large laboratory weighing tank the discharge coefficient of each meter was accurately determined for flow in both directions. Based upon calibration and the accuracy of reading the manometer it is estimated that the uncertainty in flow measurement is no more than ± 100 cfs for each bend meter. In order to simulate the identical approach flow conditions to the meters the entire PVC pipe assembly upstream and downstream of each meter was in place during calibration.

Piezometric Head Measurement

Piezometer taps were installed in the walls of the vertical shaft, the tunnel, and the penstocks for the determination of the head loss

characteristics of the model. Exhibits 5 and 6 illustrate the location of the piezometer taps for Schemes B-1 and B-2, and A-1, respectively. The only difference between the two is the location of piezometers 4, 8, 12 and 13 relative to the bifurcation model. During measurement each of the piezometer tubes was connected to a 20-tube manometer board, where the water level could be read to 0.1 inch model units.

For bifurcation schemes B-1, B-2, and A-1 the piezometric-head distribution in the trunk of the model, which is defined by cross hatching on Exhibits 7, 8, and 9 for Schemes B-1, B-2, and A-1, respectively, was also measured using the 20-tube air-water manometer board. The exact location of the various piezometers are also indicated on the exhibits.

Test Conditions

For each of the schemes there were fourteen possible combinations of flow for the three-unit system operating in either the generating or pumping mode, as listed in Table 1.

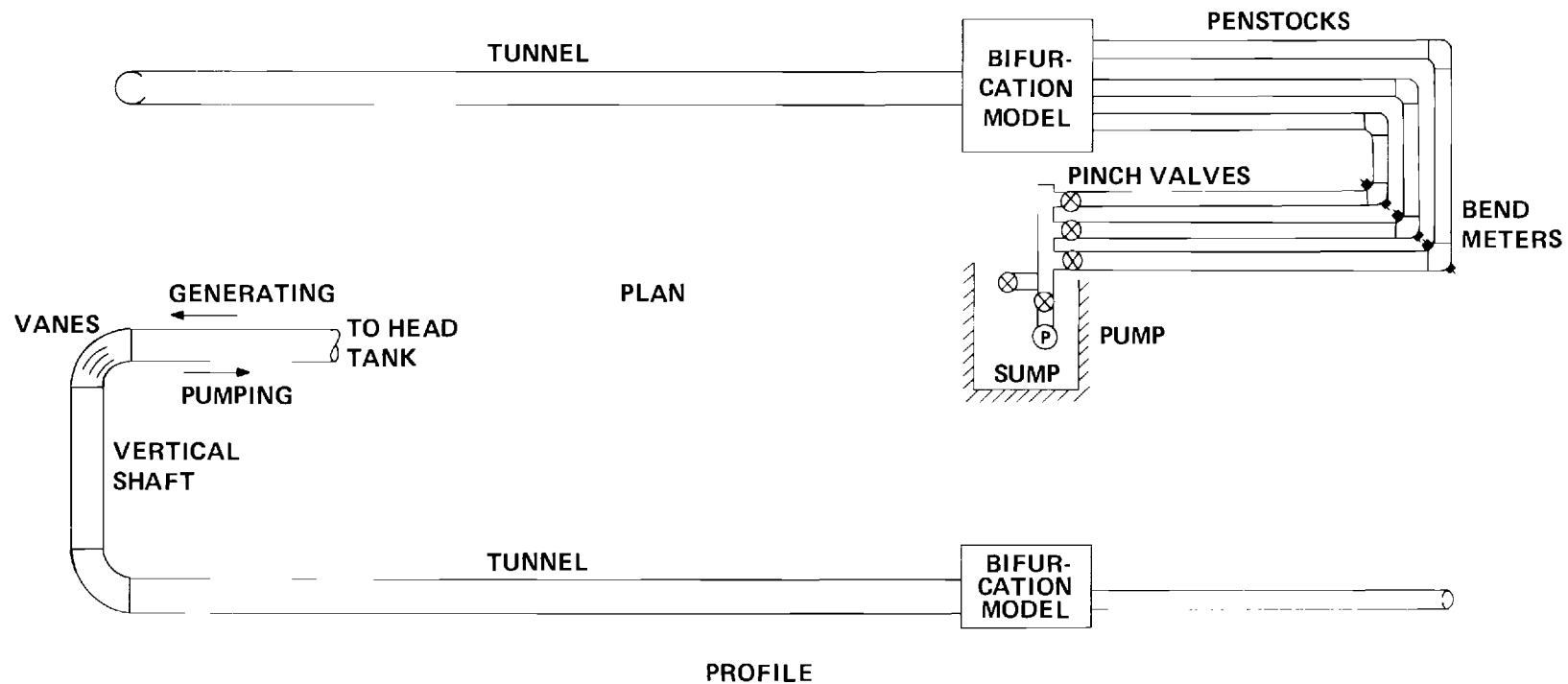


Exhibit 2. Layout of Model in Laboratory.

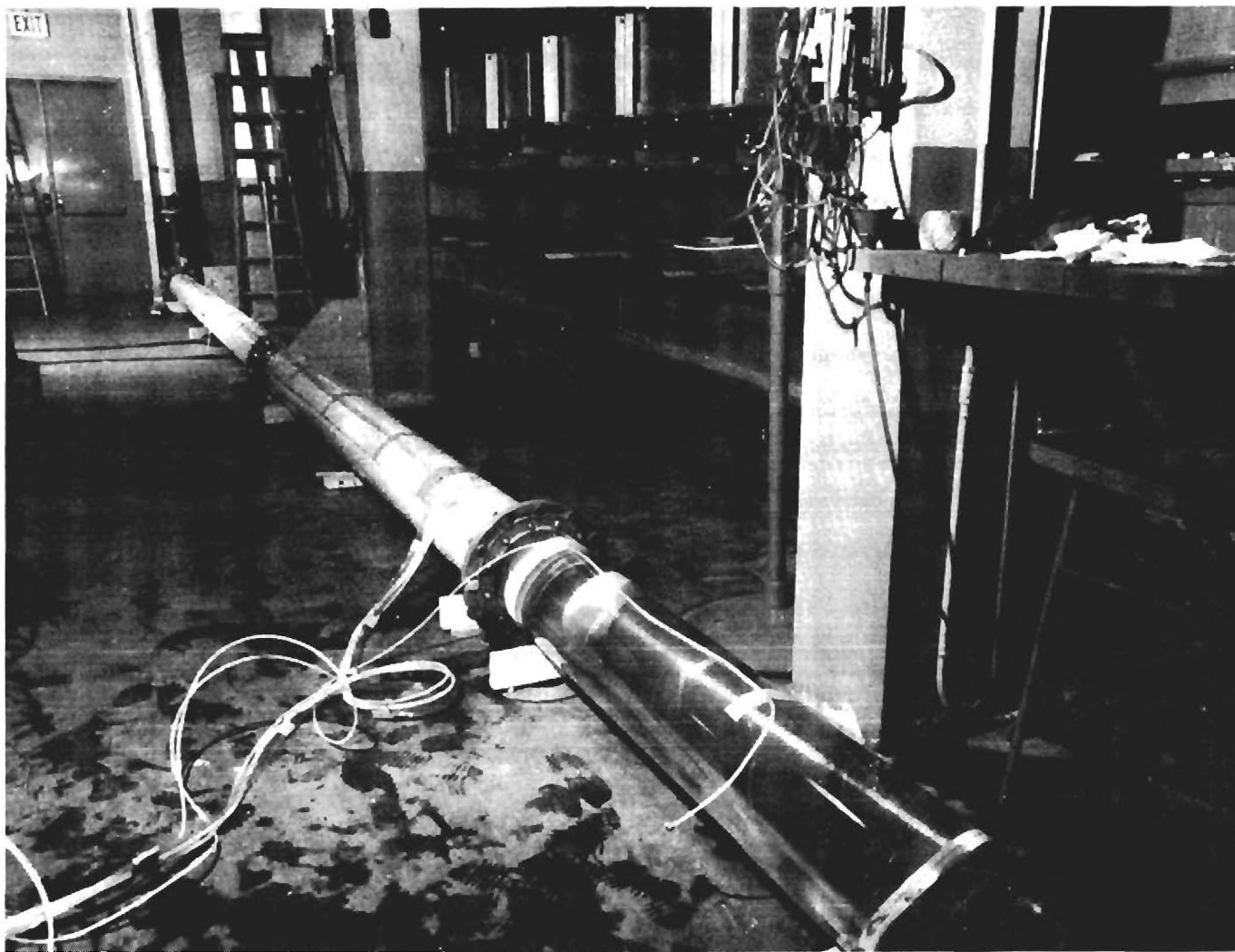


Exhibit 3. View of Model Tunnel and Vertical Shaft.

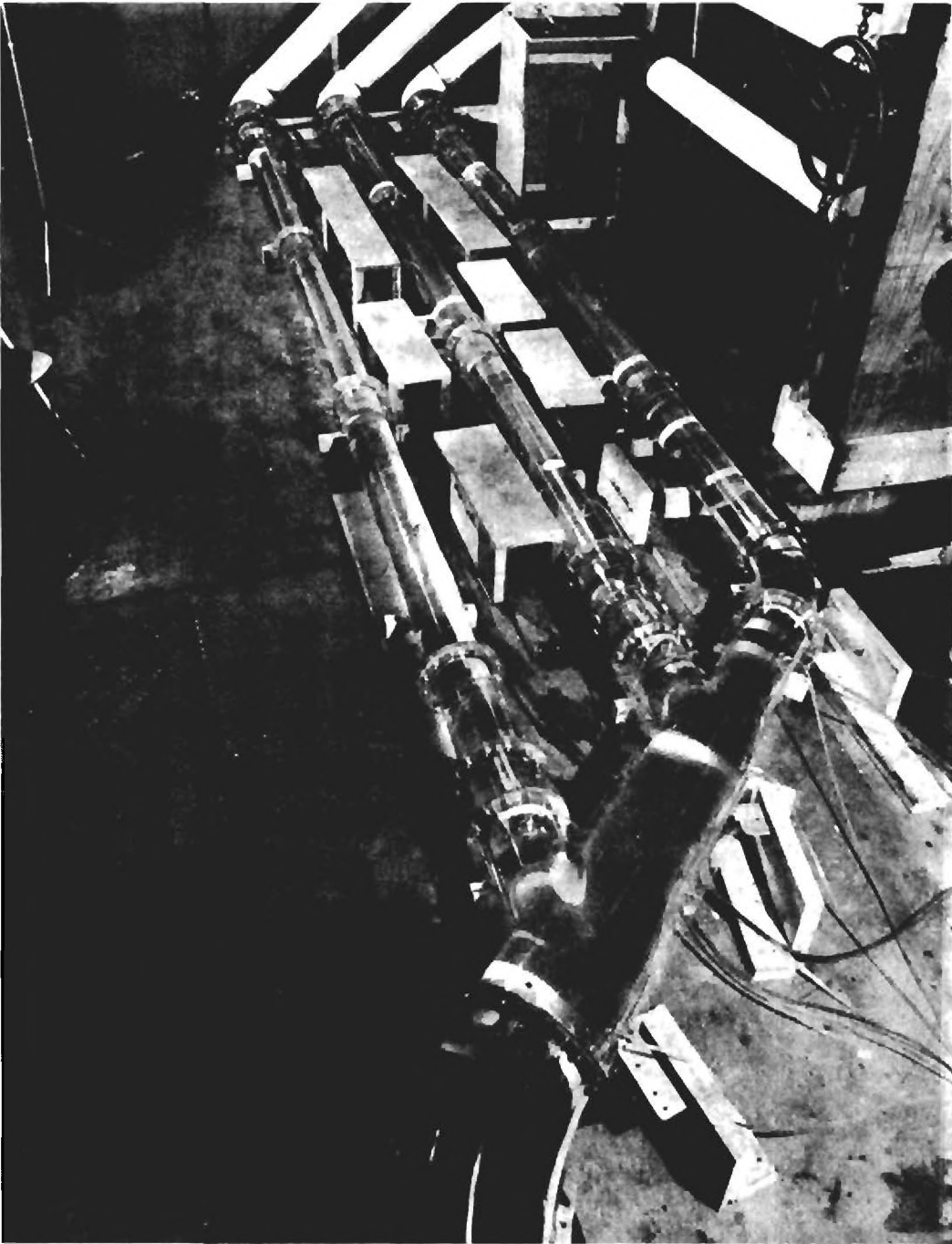


Exhibit 4. View of Model Trunk and Penstocks.

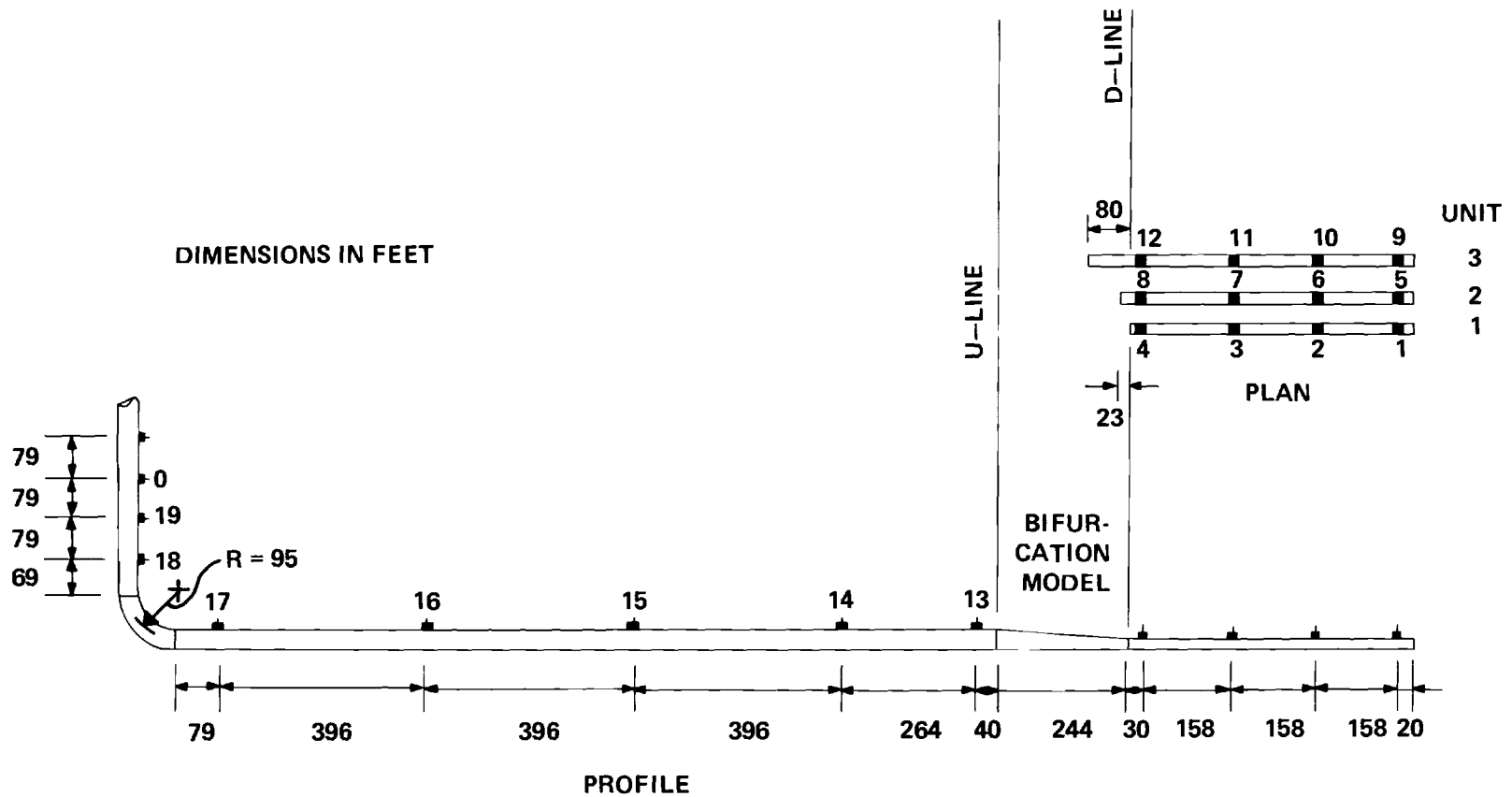


Exhibit 5. Location of Pressure Taps in Straight Legs of Schemes B-1 and B-2.

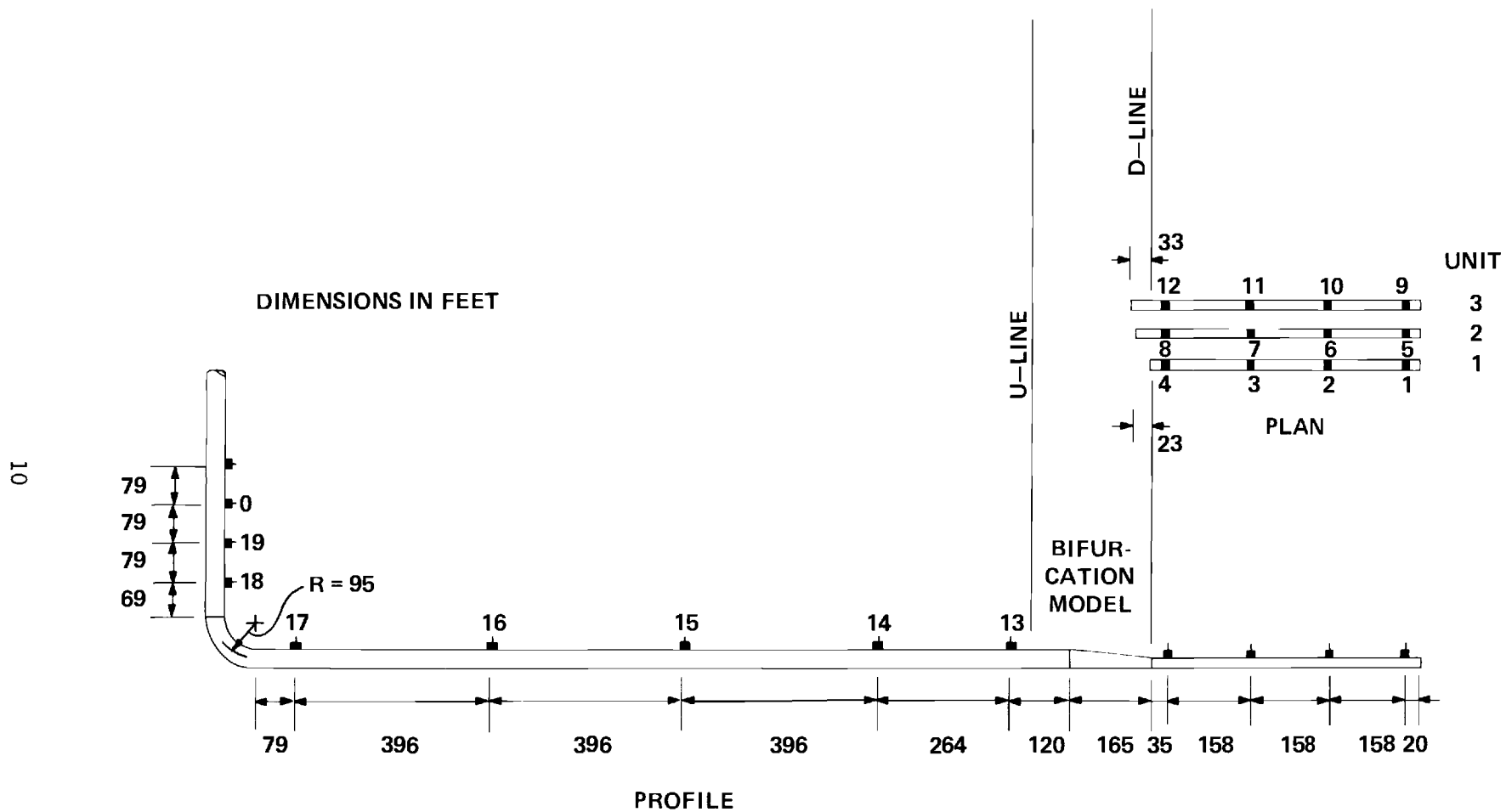


Exhibit 6. Location of Pressure Taps in Straight Legs of Scheme A-1.

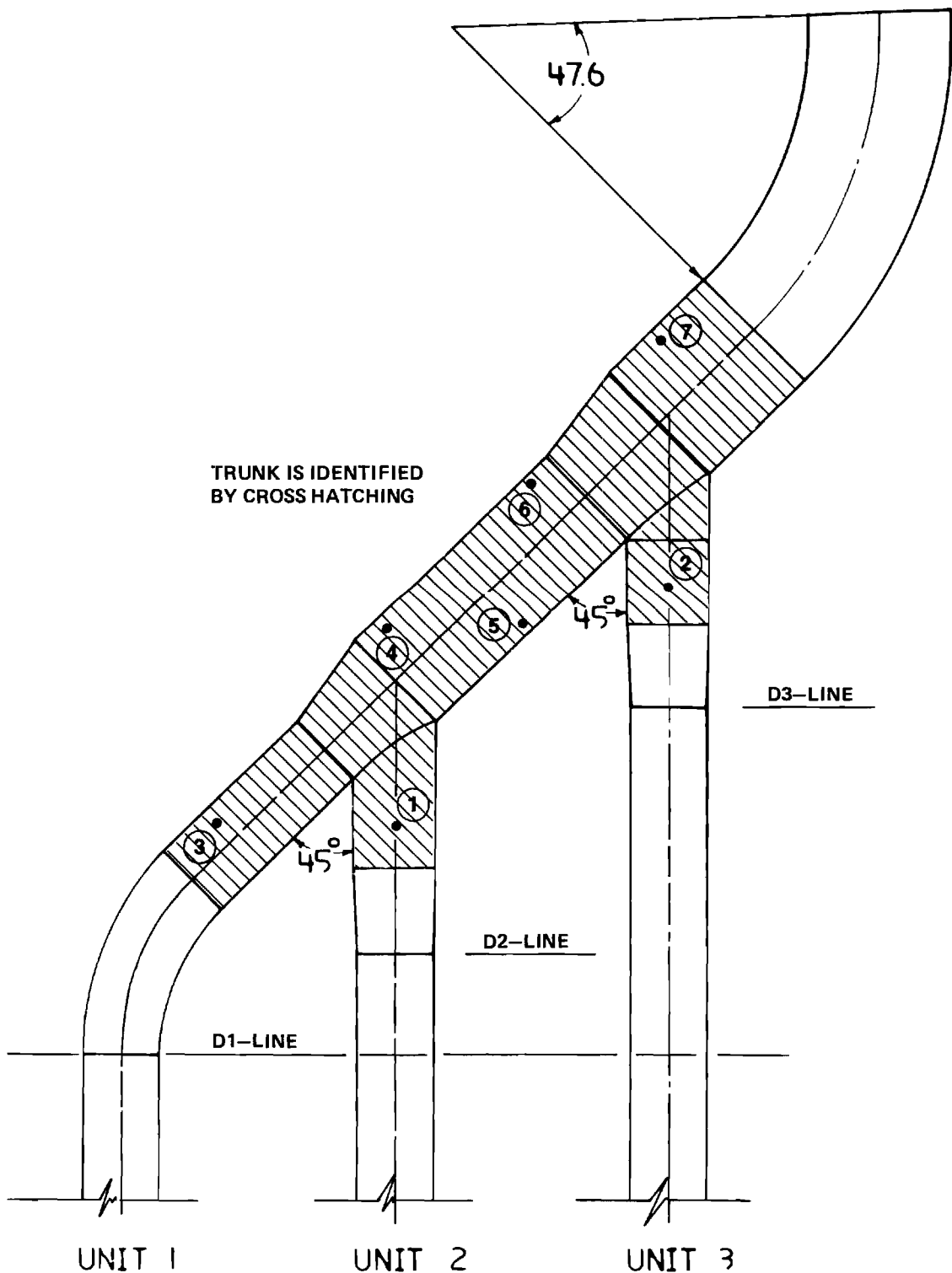


Exhibit 7. Location of Pressure Taps in Trunk of Modified Scheme B-1.

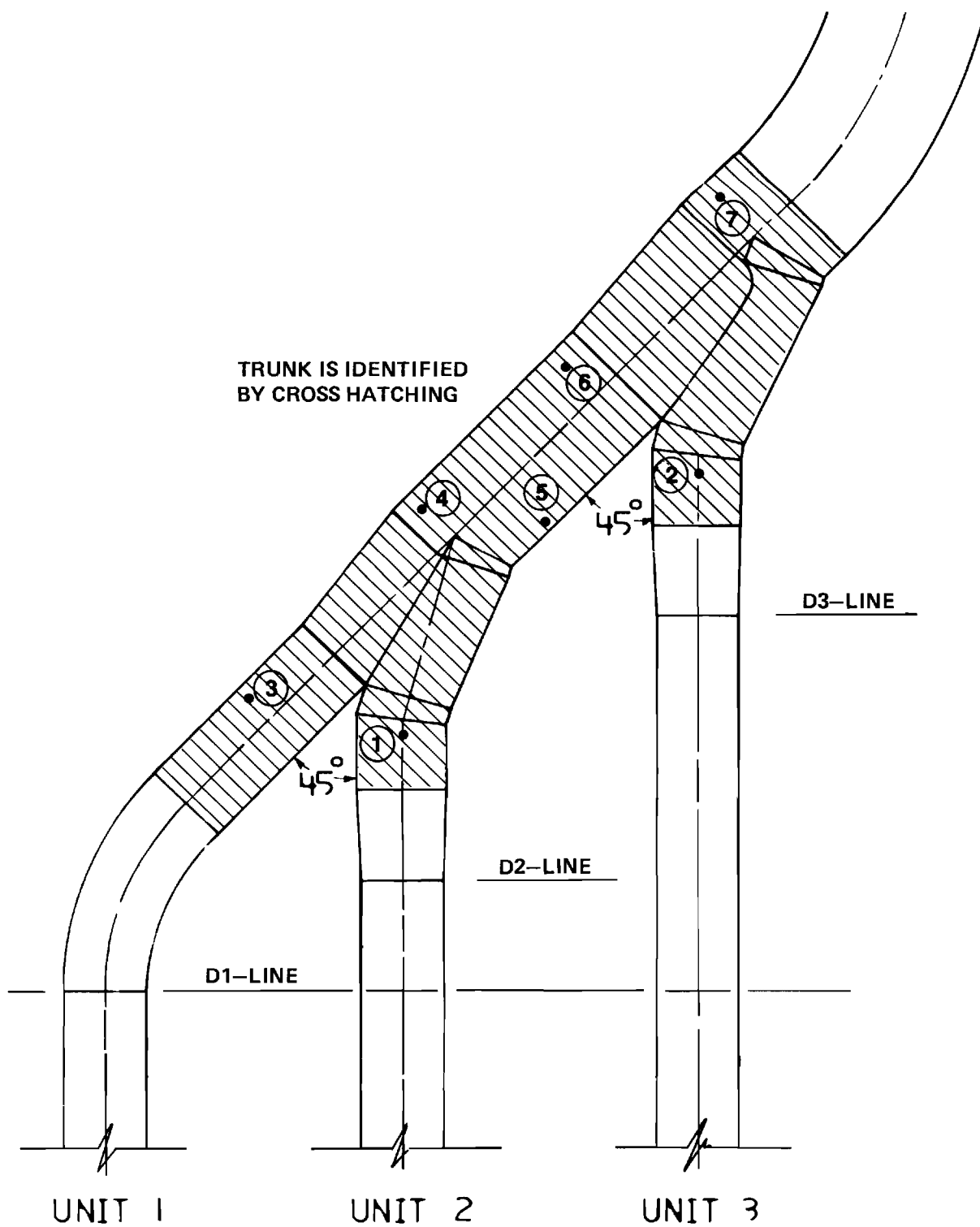


Exhibit 8. Location of Pressure Taps in Trunk of Scheme B-2.

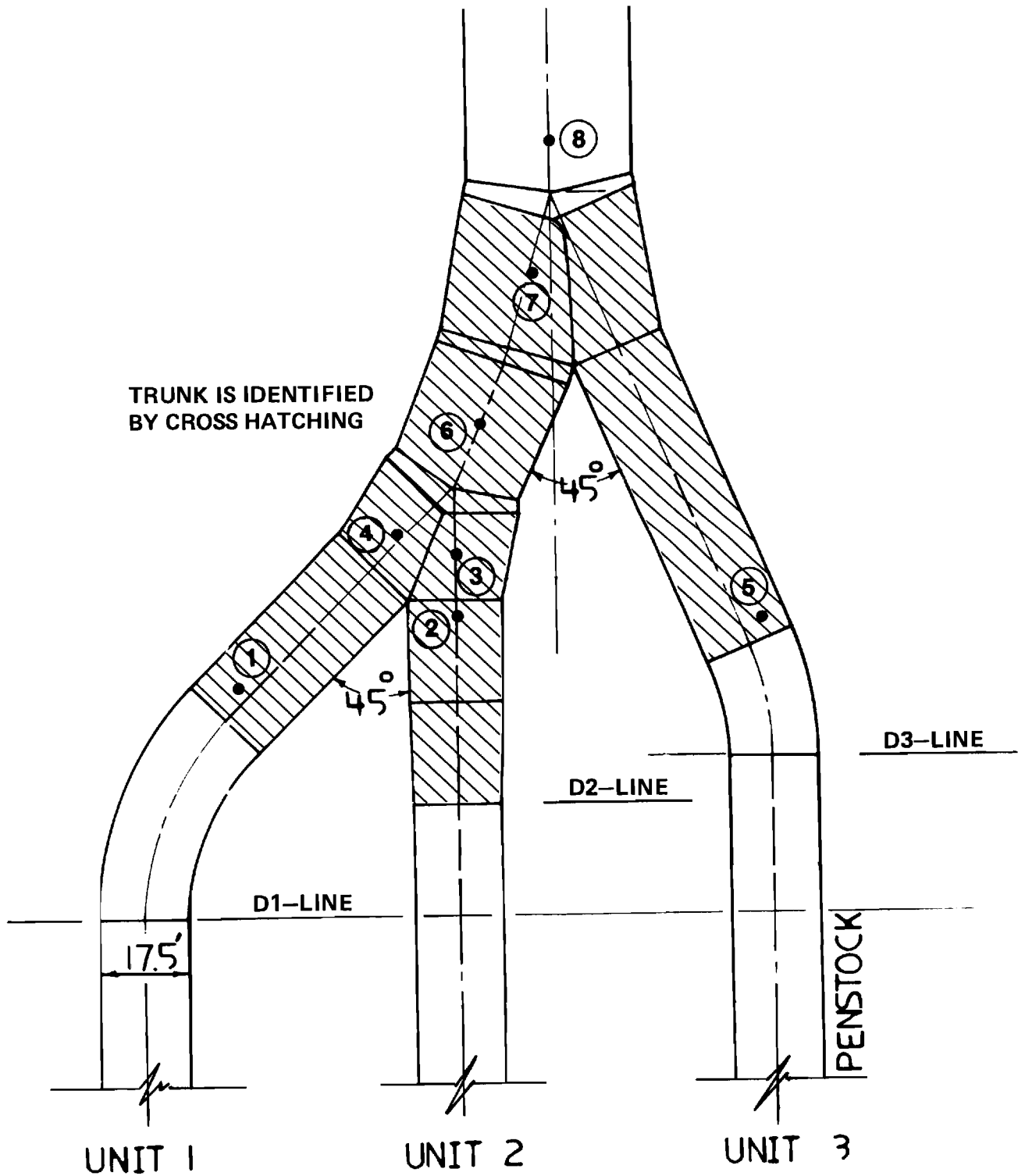


Exhibit 9. Location of Pressure Taps in Trunk of Scheme A-1.

TABLE 1
LIST OF POSSIBLE TEST CONDITIONS

<u>Mode</u>	<u>Units Operating</u>
Generating	1, 2 and 3
Generating	1 and 2
Generating	1 and 3
Generating	2 and 3
Generating	1
Generating	2
Generating	3
Pumping	1, 2 and 3
Pumping	1 and 2
Pumping	1 and 3
Pumping	2 and 3
Pumping	1
Pumping	2
Pumping	3

CHAPTER III

TEST RESULTS FOR MODIFIED B-1 SCHEME

The B-1 Scheme as tested is referred to as a modified scheme as the transition from the trunk to the penstock of Unit 3 was not fabricated precisely according to design drawings. In order to produce a more streamlined flow in that region the transition was improved somewhat by grinding and reforming the model, the result of which can be seen on some of the following photographs. Exhibit 82 in the Appendix illustrates more precisely the actual difference between the model as tested and the bifurcation as designed.

Head-Loss Data

The fourteen possible test conditions for the three-unit system operating in either the generating or pumping mode listed in Table 1 were tested for Scheme B-1. Maximum possible model flows rather than design flows were produced in each case in order to improve the accuracy of measurement. The results for each test are plotted along the straight portions of the vertical shaft, tunnel, and penstocks of the comprehensive model in Exhibits 10-19. For ease of reference and for the sole purpose of comparison of head loss between schemes, the value of the HGL at piezometer number 0 in Exhibit 5 is arbitrarily assigned a value of 1000 ft. Therefore, the values of the HGL throughout the system are not actual, but relative.

As shown in Exhibit 10, which corresponds to three units generating, the piezometric-head line or hydraulic grade line (HGL) is essentially a straight line in the various legs of the model for this test condition. For each leg a best fit straight line is drawn through the points on the HGL which appear to be in a developed flow region. Using the measured discharge through the respective conduit the energy grade line (EGL) is then drawn parallel to the HGL one velocity head higher.

The elbow head loss is determined by extrapolating the EGL's from the vertical shaft and the tunnel to the bend, which is assumed to have no length in this analysis. The loss coefficient K_L for the elbow is defined by

$$H_L = K_L \frac{V^2}{2g} \quad (4)$$

in which V is the mean velocity in the tunnel and in the shaft. As shown in Exhibit 10 the difference in EGL's at the location of the elbow is defined as the bend head loss, which was 3.4 ft in this instance. Based upon the velocity head in the tunnel, which is the same as that in the shaft, the loss coefficient is 0.15.

The head loss coefficients for the tunnel bifurcation are defined on the basis of the velocity head in the respective penstock. The actual head loss is defined as the difference in the extrapolated EGL at the right end of the tunnel (beginning of bend) and the extrapolated EGL at the left end of the 17.5 ft diameter penstock (Lines D1, D2, or D3 in Exhibit 7) in question, as shown by Exhibit 5. For each penstock the actual head loss coefficient is

$$H_{L_1} = K_{L_1} \frac{V_1^2}{2g} \quad \text{defined by:} \quad (5)$$

$$H_{L_2} = K_{L_2} \frac{V_2^2}{2g} \quad (6)$$

$$H_{L_3} = K_{L_3} \frac{V_3^2}{2g} \quad (7)$$

in which V_1 , V_2 , and V_3 are the mean velocities in the penstocks for Units 1, 2, and 3, respectively.

In Exhibits 10-19 the values of the HGL are plotted relative to the beginning of the penstocks in order to calculate the actual head loss across the model. The relative loss coefficients, which are useful in

comparing performance of the three units, are instead referred to the head loss between the common locations designated by the U-Line and D-Line shown on Exhibit 1, and are defined by

$$H_{R_1} = K_{R_1} \frac{v_1^2}{2g} \quad (8)$$

$$H_{R_2} = K_{R_2} \frac{v_2^2}{2g} \quad (9)$$

$$H_{R_3} = K_{R_3} \frac{v_3^2}{2g} \quad (10)$$

in which K_{R_1} , K_{R_2} , and K_{R_3} are the relative head loss coefficients.

The head-loss coefficients tabulated on Exhibits 10-19 are based upon the actual head loss across the bifurcation model. Tables 2 and 3 provide a summary of the actual and relative loss coefficients for the fourteen test conditions for the Modified B-1 Scheme, respectively. Since the D-Line crosses the plane of the beginning of the penstock of Unit 1 there is no difference in the actual and relative loss coefficients K_{L_1} and K_{R_1} for this unit. The rather abrupt transition from the penstocks of Units 2 and 3, especially that of Unit 3, created unusually bad flow conditions, particularly in the pumping mode.

Flow Patterns in Bifurcation Model

The flow patterns in the model were determined by (1) observing the direction of tuft glued to the inside wall of the trunk and penstocks and (2) by photographing air bubbles that were injected upstream of the model.

For scheme B-1 the air bubbles clearly illustrated the severe turbulence under several modes of operation.

Exhibit 20 shows both the orientation of the various tuft and a time exposure of air bubbles which were injected into the flow for the case of three units generating. The bad flow condition at the juncture of penstock #3 and the trunk is illustrated by the tuft swirling in the eddy caused by the flow separation at that location. Exhibit 21 shows the flow pattern for Units 1 and 2 in the generating mode. The values of the loss coefficients listed in Tables 2 and 3 indicate lower losses for single unit flow than for multiple unit flow in the generating mode. Exhibit 22 clearly shows, in comparison with Exhibit 20, that the eddy at the beginning of penstock #3 is quite weak for flow through that unit alone.

The flow patterns in the model were more clearly exhibited in the pumping mode by the air bubbles because of the ability to inject air into each penstock. Moreover, the severe turbulence generated in the expanded flow regions at the junction of penstocks #2 and #3 with the trunk could be easily observed. Exhibit 23 clearly illustrates the turbulence in the trunk for the condition of all three units pumping. Even when Unit 3 is not pumping the fairly sudden expansion in the trunk area creates a considerable amount of turbulence, as shown by Exhibit 24 for Units 1 and 2 pumping. The flow pattern changes considerably when Units 1 and 3 are pumping (Exhibit 25) or Units 2 and 3 (Exhibit 26). The corresponding redistribution of the head losses is reflected by the changes in the loss coefficients (Tables 2 and 3).

For single unit pumping the loss coefficients for Units 2 and 3 increase significantly because of the steep expansion angle from the penstocks to the trunk. Exhibits 27 and 28 show the flow patterns for

the cases of Unit 1 pumping and Unit 2 pumping, respectively. The worst flow condition of the entire set of test conditions is shown by Exhibit 29 -- Unit 3 pumping. In this case the turbulence, as marked by the air bubbles, persisted as a strong vortex core up the tunnel for a number of diameters. This nonuniform flow condition is reflected by the much higher values of the HGL in the tunnel for Unit 1 pumping than for either Unit 2 or Unit 3 pumping, as clearly shown by Exhibit 19.

Pressure Distribution in Trunk

For the seven piezometer locations indicated on Exhibit 7 the piezometric head was measured for all of the pumping conditions and one of the generating conditions listed in Table 1. The results are listed in Table 4 relative to the same 1000 ft datum for piezometer number 0 in the vertical shaft. The differences in pressure throughout the trunk are not significant from a design standpoint. The values of the piezometric head at piezometers 4 and 7 in the pumping mode are in particular greater than at the remaining locations because of a stagnation effect as the flow enters the trunk from penstocks 2 and 3, respectively.

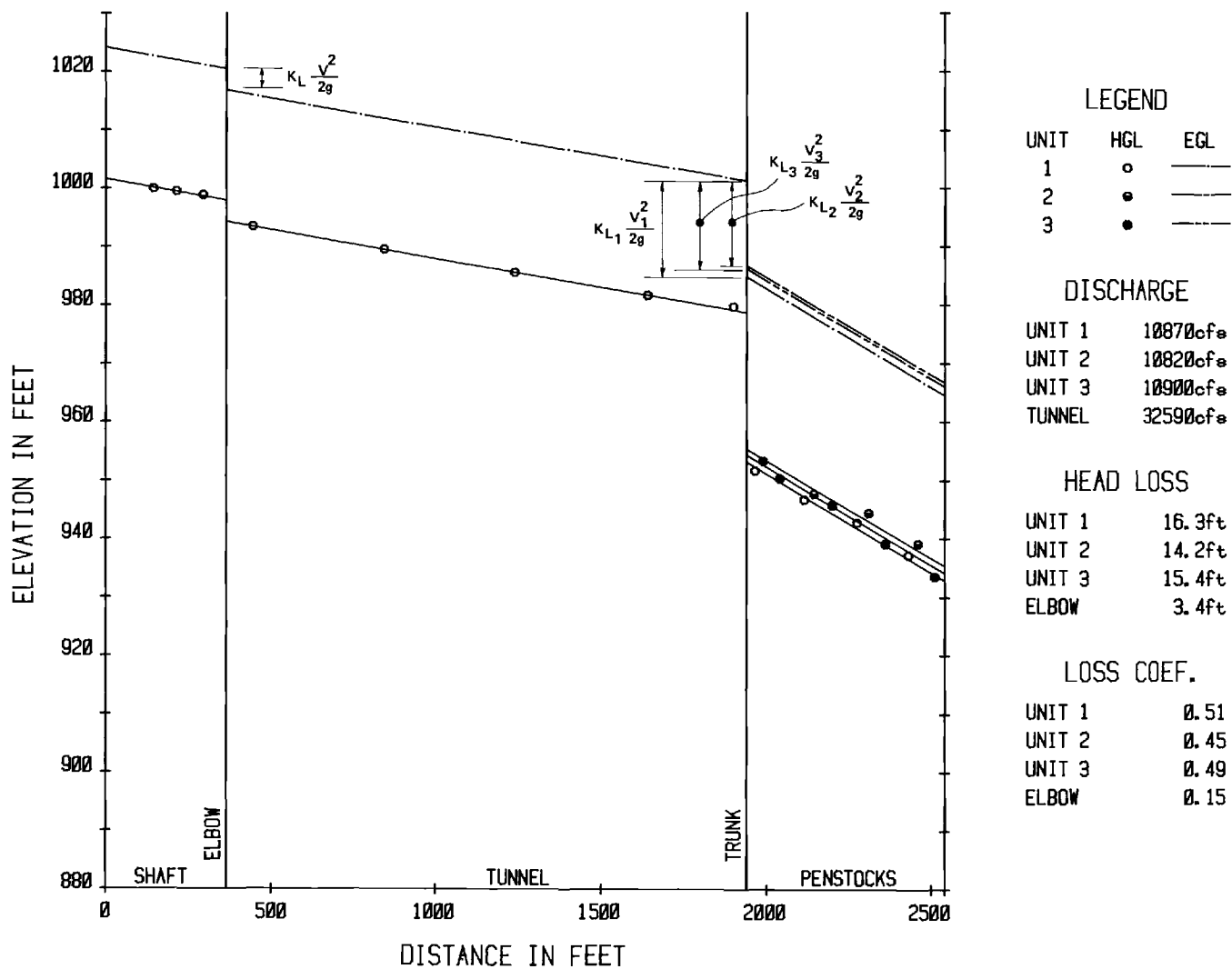


Exhibit 10. Hydraulic and Energy Grade Lines in Modified Scheme B-1 for Three Units Generating.

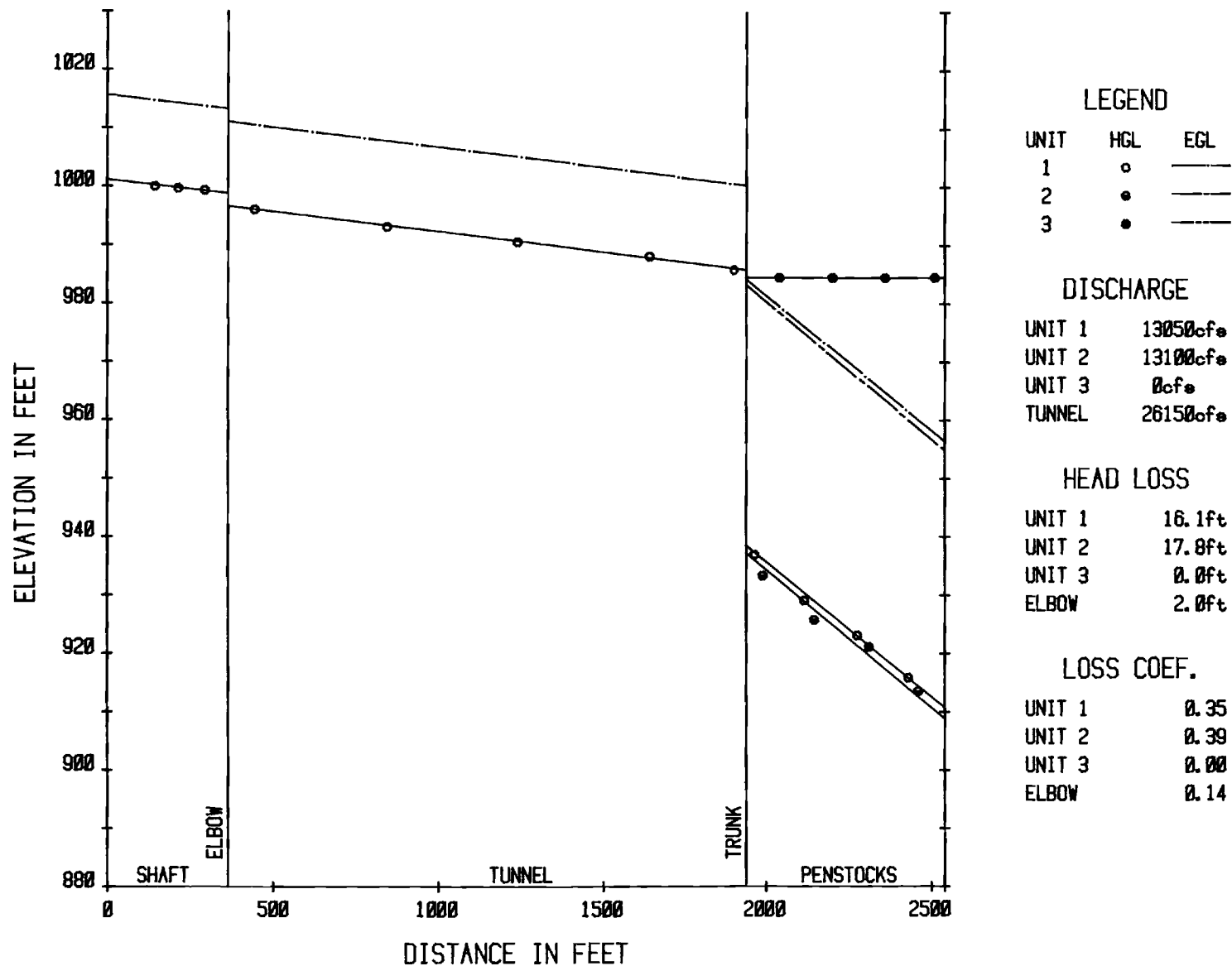


Exhibit 11. Hydraulic and Energy Grade Lines in Modified Scheme B-1 for Units 1 and 2 Generating.

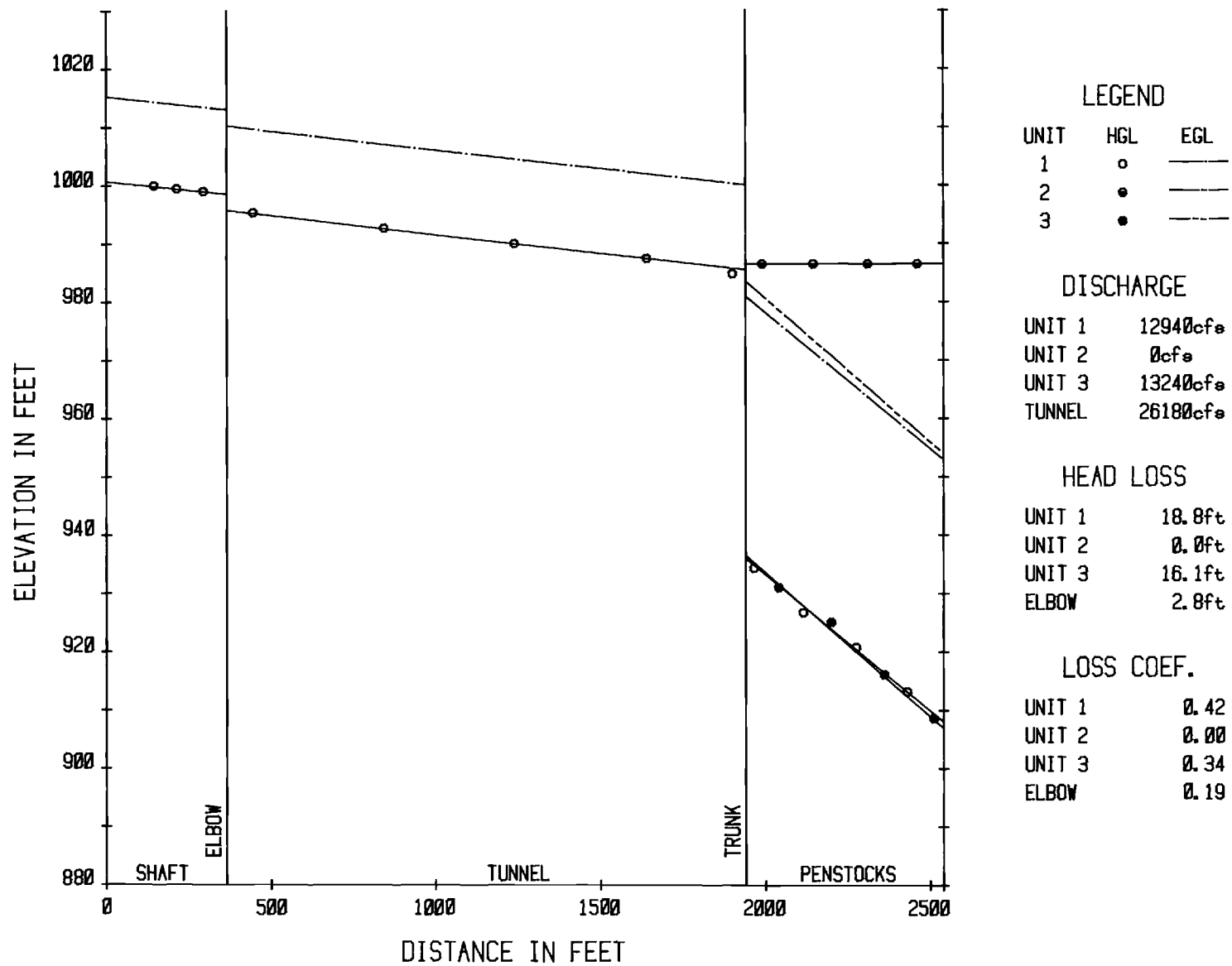


Exhibit 12. Hydraulic and Energy Grade Lines in Modified Scheme B-1 for Units 1 and 3 Generating.

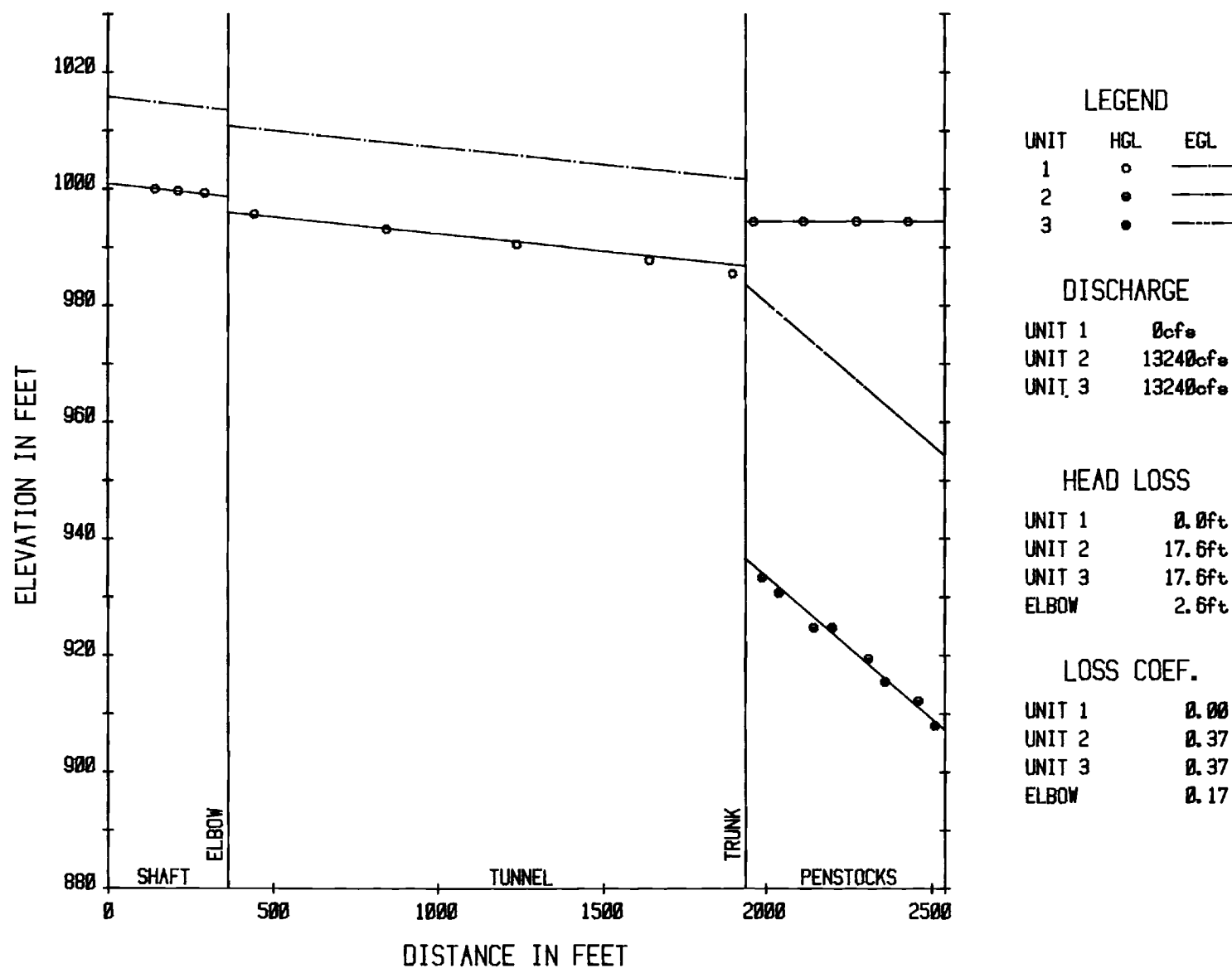


Exhibit 13. Hydraulic and Energy Grade Lines in Modified Scheme B-1 for Units 2 and 3 Generating.

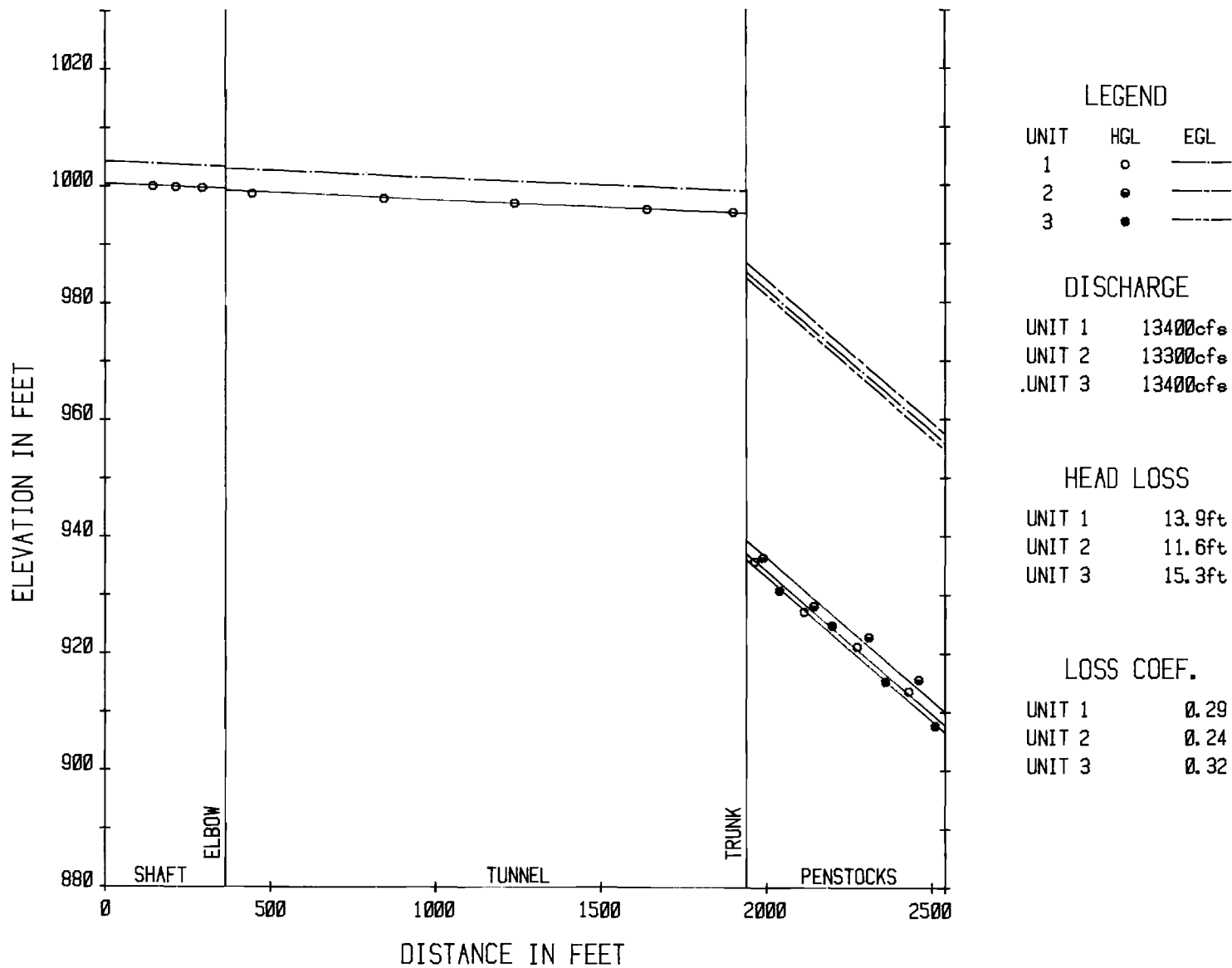


Exhibit 14. Hydraulic and Energy Grade Lines in Modified Scheme B-1 for Single Unit Generating.

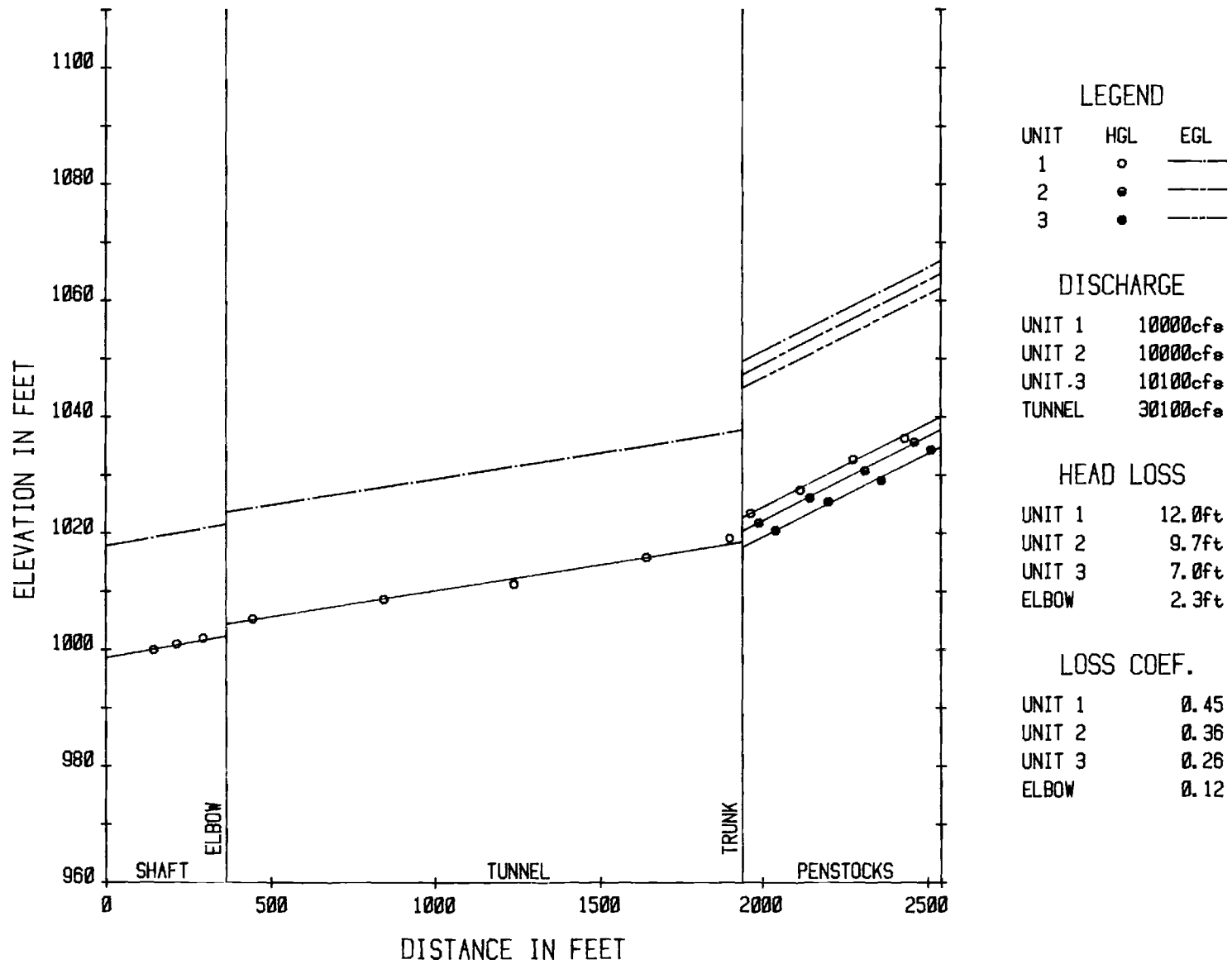


Exhibit 15. Hydraulic and Energy Grade Lines in Modified Scheme B-1 for Three Units Pumping.

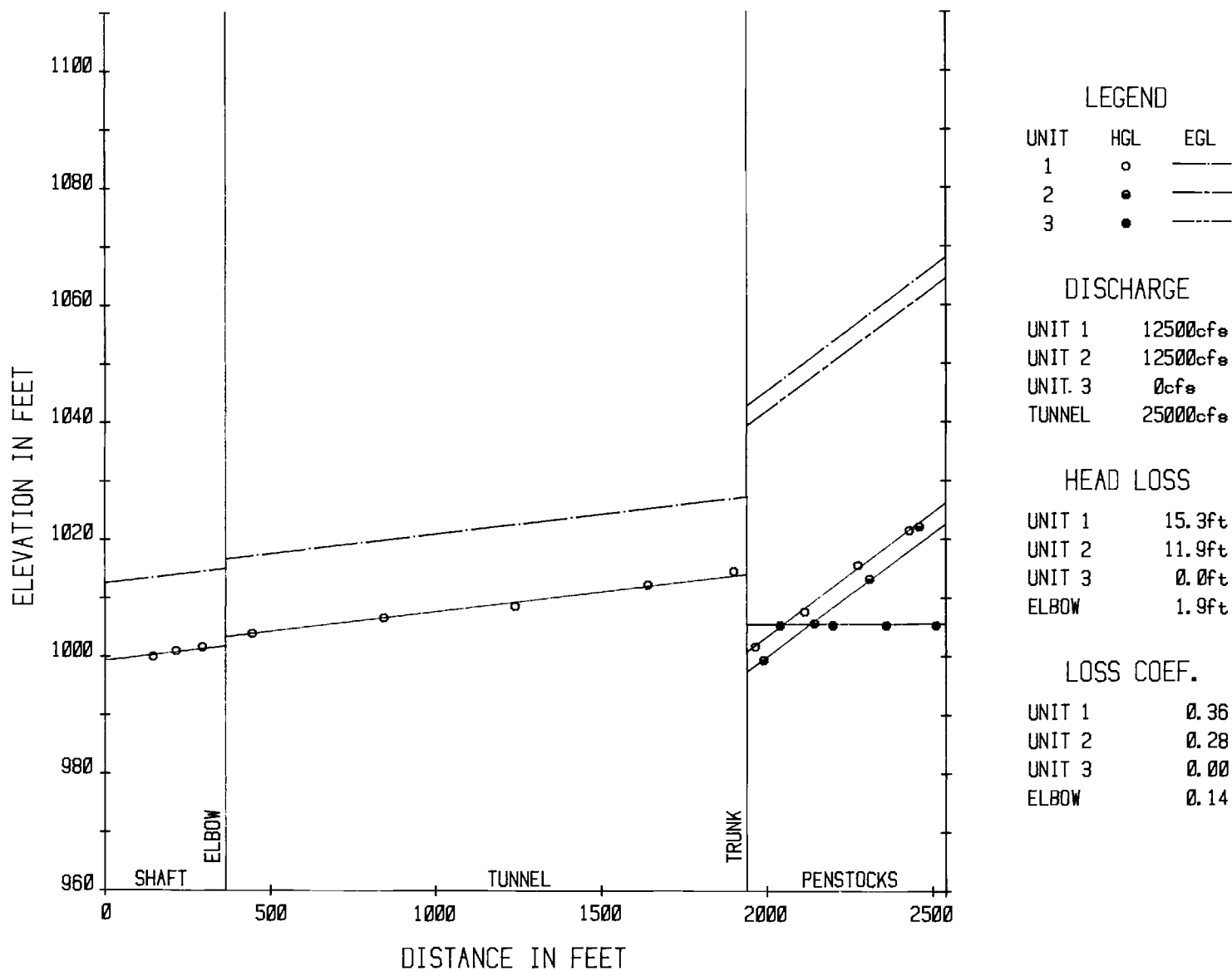


Exhibit 16. Hydraulic and Energy Grade Lines in Modified Scheme B-1 for Units 1 and 2 Pumping.

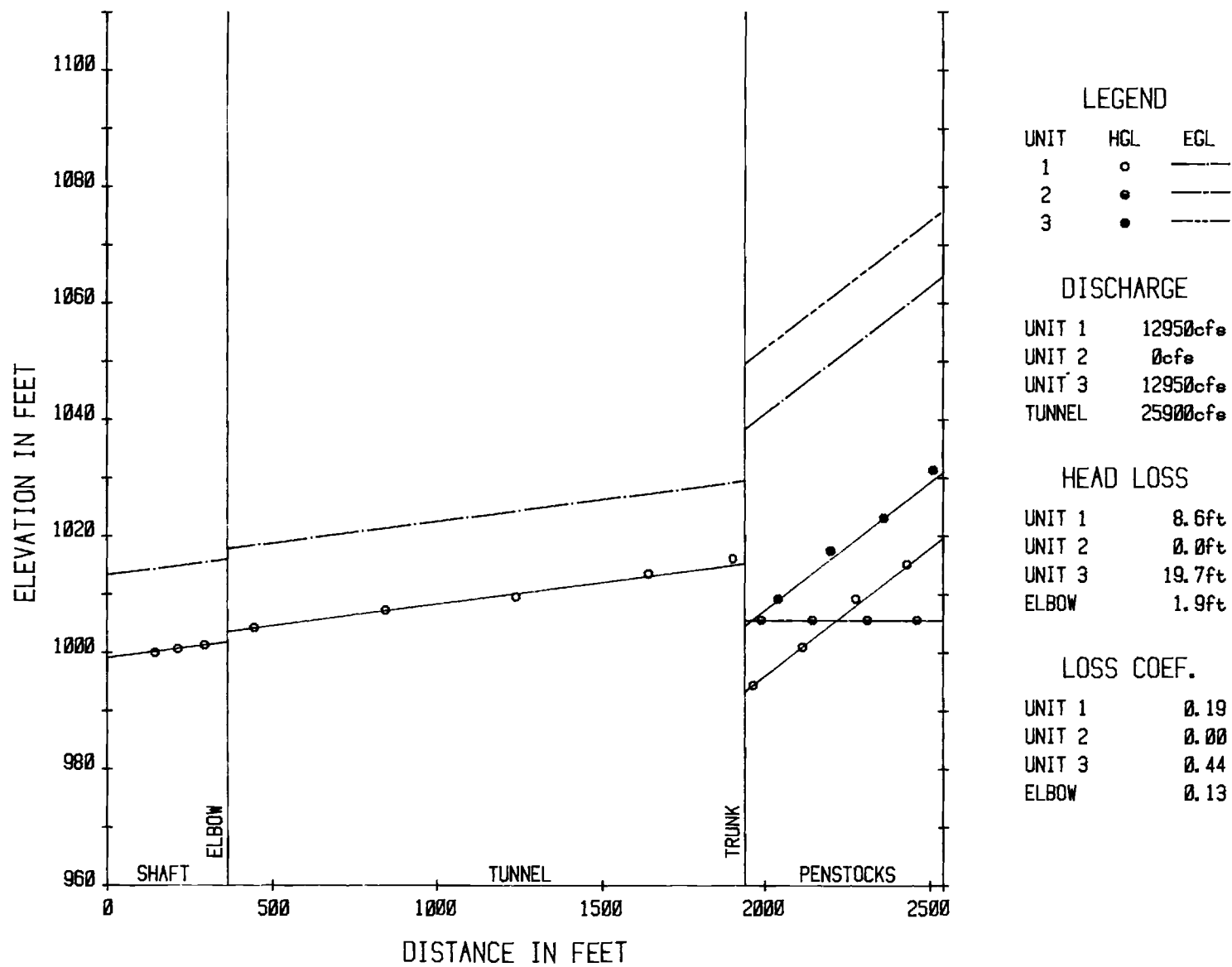


Exhibit 17. Hydraulic and Energy Grade Lines in Modified Scheme B-1 for Units 1 and 3 Pumping.

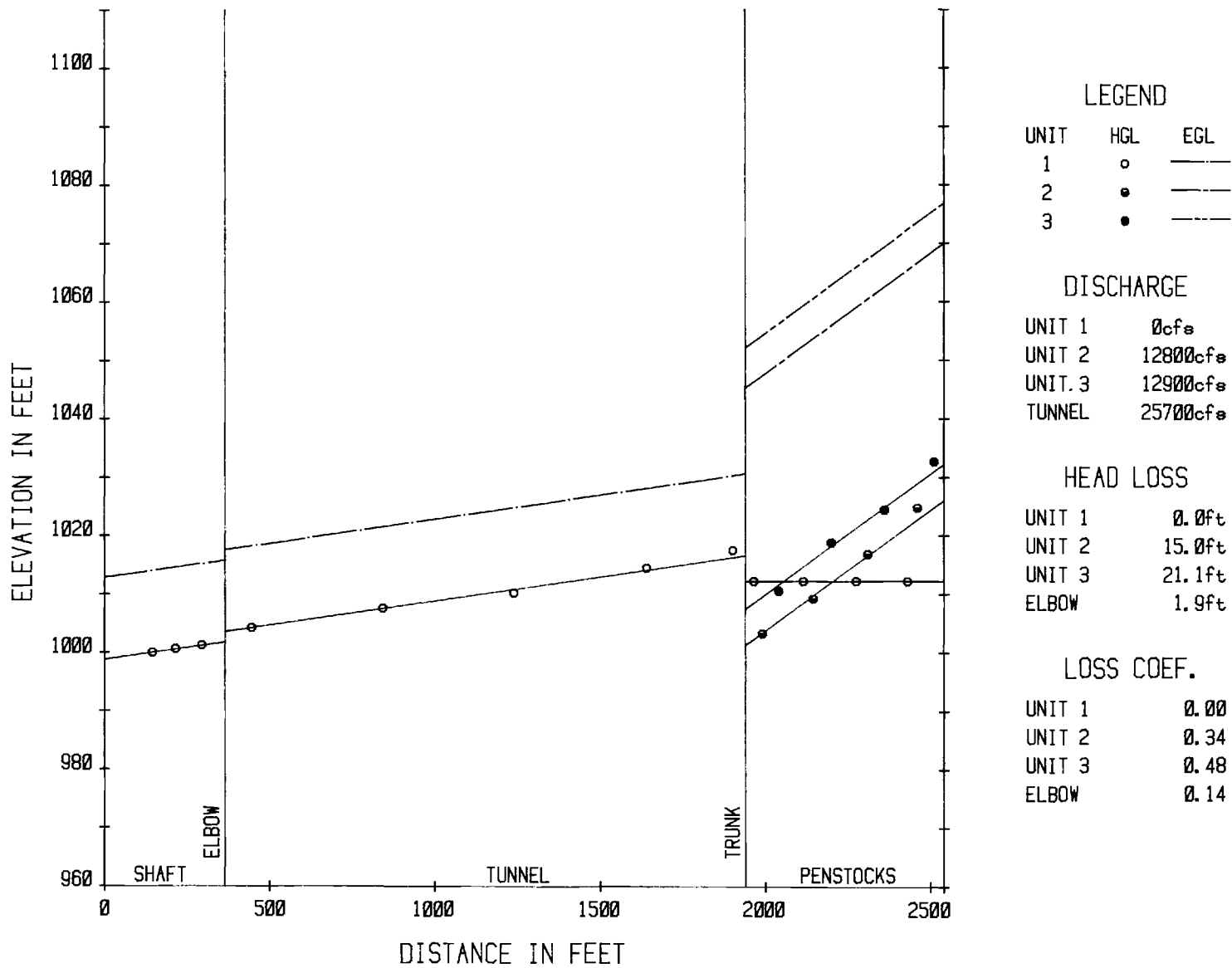


Exhibit 18. Hydraulic and Energy Grade Lines in Modified Scheme B-1 for Units 2 and 3 Pumping.

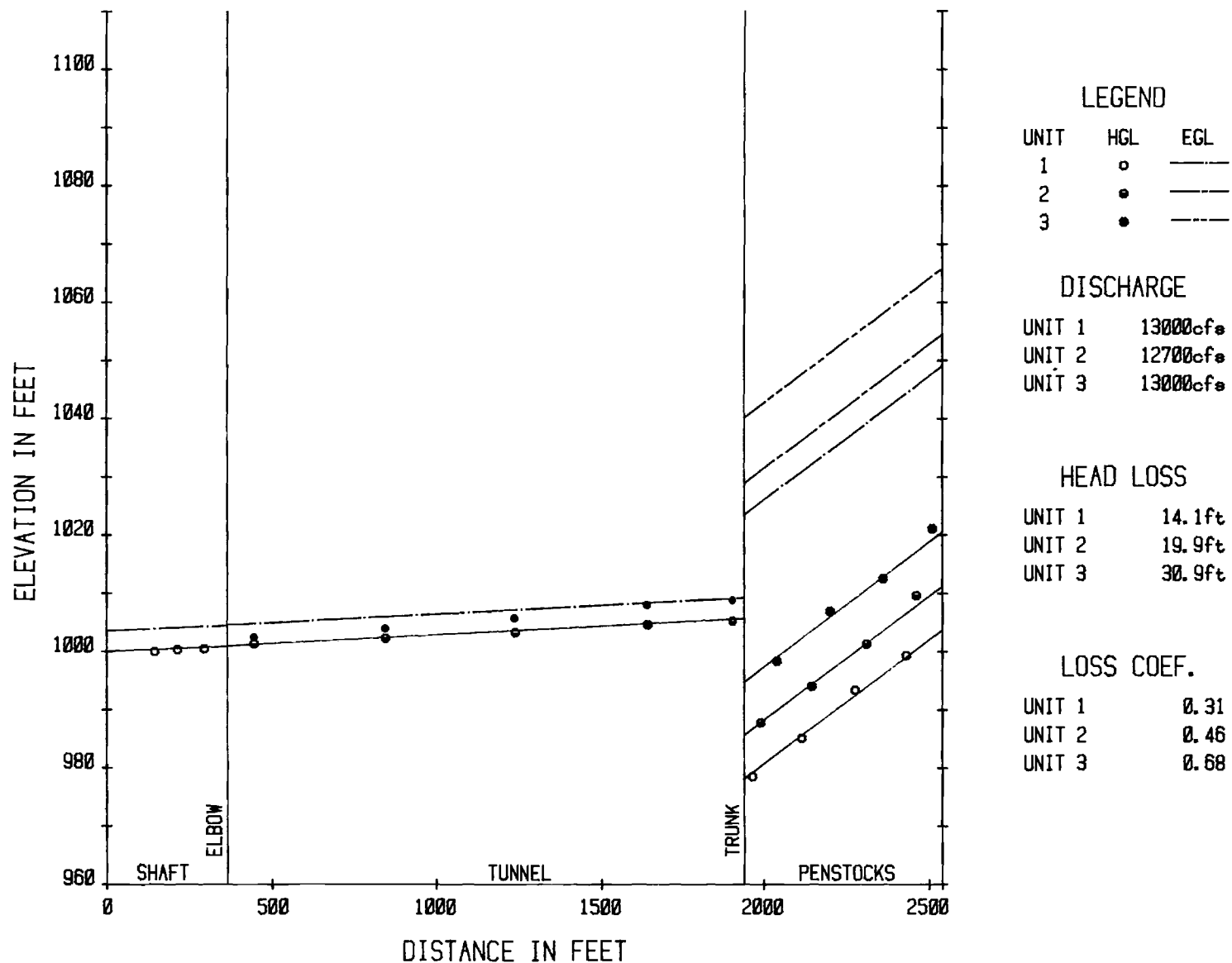


Exhibit 19. Hydraulic and Energy Grade Lines in Modified Scheme B-1 for Single Unit Pumping.

TABLE 2
SUMMARY OF ACTUAL LOSS COEFFICIENTS
FOR MODIFIED B-1 SCHEME

<u>MODE</u>	K_{L_1} (<u>UNIT 1</u>)	K_{L_2} (<u>UNIT 2</u>)	K_{L_3} (<u>UNIT 3</u>)
Three Units Generating	0.51	0.45	0.49
Units 1 and 2 Generating	0.35	0.39	--
Units 1 and 3 Generating	0.42	--	0.34
Units 2 and 3 Generating	--	0.37	0.37
Single Unit Generating	0.29	0.24	0.32
Three Units Pumping	0.45	0.36	0.26
Units 1 and 2 Pumping	0.36	0.28	--
Units 1 and 3 Pumping	0.19	--	0.44
Units 2 and 3 Pumping	--	0.34	0.48
Single Unit Pumping	0.31	0.46	0.68

TABLE 3
SUMMARY OF
RELATIVE LOSS COEFFICIENTS
FOR MODIFIED B-1 SCHEME

<u>MODE</u>	K_{R_1} (<u>UNIT 1</u>)	K_{R_2} (<u>UNIT 2</u>)	K_{R_3} (<u>UNIT 3</u>)
Three Units Generating	0.51	0.47	0.57
Units 1 and 2 Generating	0.35	0.41	--
Units 1 and 3 Generating	0.42	--	0.42
Units 2 and 3 Generating	--	0.39	0.45
Single Unit Generating	0.29	0.26	0.40
Three Units Pumping	0.45	0.38	0.34
Units 1 and 2 Pumping	0.36	0.30	--
Units 1 and 3 Pumping	0.19	--	0.52
Units 2 and 3 Pumping	--	0.36	0.56
Single Unit Pumping	0.31	0.48	0.74



Exhibit 20. View of Tuft and Air Bubble Patterns in Trunk of Modified Scheme B-1 for Three Units Generating.



Exhibit 21. View of Tuft Pattern in Trunk of Modified Scheme B-1 for Units 1 and 2 Generating.



Exhibit 22. View of Tuft Pattern in Trunk of Modified Scheme B-1
for Unit 3 Generating.



Exhibit 23. View of Tuft and Air Bubble Patterns in Trunk of Modified Scheme B-1 for Three Units Pumping.



Exhibit 24. View of Tuft and Air Bubble Patterns in Trunk of Modified Scheme B-1 for Units 1 and 2 Pumping.

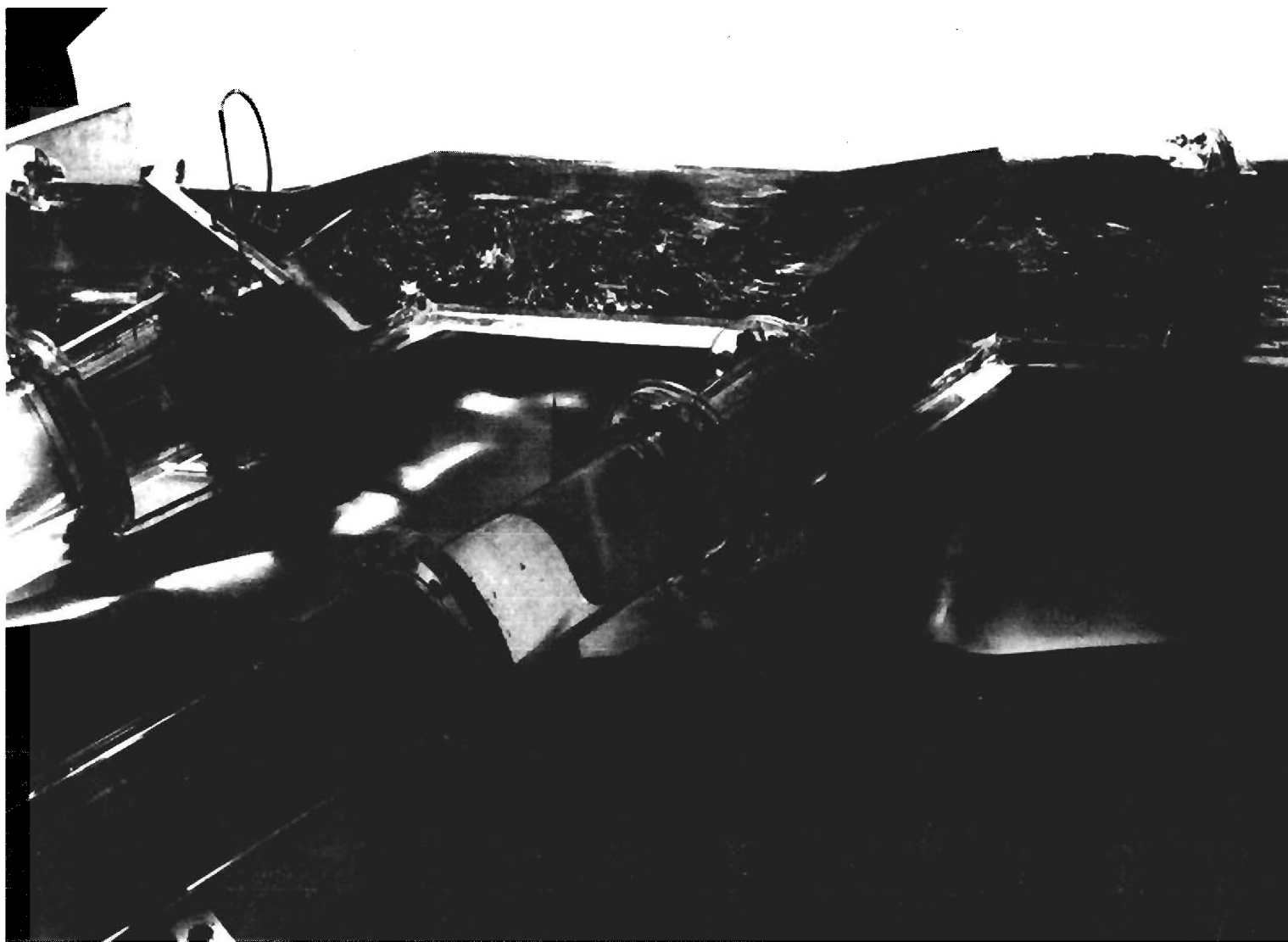


Exhibit 25. View of Tuft and Air Bubble Patterns in Trunk of Modified Scheme B-1 for Units 1 and 3 Pumping.



Exhibit 26. View of Tuft and Air Bubble Patterns in Trunk of Modified Scheme B-1 for Units 2 and 3 Pumping.



Exhibit 27. View of Tuft and Air Bubble Patterns in Trunk of Modified Scheme B-1 for Unit 1 Pumping.



Exhibit 28. View of Tuft and Air Bubble Patterns in Trunk of Modified Scheme B-1 for Unit 2 Pumping.



Exhibit 29. View of Tuft and Air Bubble Patterns in Trunk of Modified Scheme B-1 for Unit 3 Pumping.

Table 4. Values of Relative Hydraulic Grade
Line in Trunk of Modified B-1 Scheme.

TRUNK HYDRAULIC GRADE LINE SCHEME B-1 (MOD)

UNIT 1	UNIT 2	UNIT 3	PIEZOMETER NUMBER						
(cfs)	(cfs)	(cfs)	1	2	3	4	5	6	7
PUMPING MODE									
10000	9990	10010	1027.7	1025.4	1028.7	1031.7	1024.1	1023.1	1023.4
9950	9990	9970	1027.4	1025.1	1028.7	1031.4	1023.8	1023.1	1023.4
12710	0	0	990.8	1002.3	983.8	998.0	998.4	1000.0	1004.6
0	12580	0	993.1	1001.3	995.1	1022.4	999.7	1001.3	1003.3
0	0	16110	1002.3	1003.6	1001.7	1003.0	1003.6	1002.0	1041.6
12310	12360	0	1006.9	1008.9	1008.9	1013.2	1002.0	1002.0	1015.8
12280	12360	0	1007.3	1008.9	1008.9	1013.2	1002.0	1001.3	1015.2
12440	0	12550	1006.3	1013.2	1001.0	1014.9	1014.9	1016.2	1018.2
0	12690	12800	1008.6	1015.5	1011.9	1039.3	1017.2	1018.5	1019.5
6030	3220	6060	1011.9	1010.6	1011.9	1012.9	1009.9	1009.9	1009.6
GENERATING MODE									
10870	10790	10760	965.0	970.0	968.0	976.2	972.3	972.3	975.6

HYDRAULIC GRADE LINE ELEVATIONS ARE IN FEET

CHAPTER IV

TEST RESULTS FOR SCHEME B-2

The B-2 Scheme, shown on Exhibit 1, is more streamlined than the Modified Scheme B-1 at the junction of penstocks 2 and 3 and the bifurcation trunk. Hence in general the flow patterns were better and the head losses were smaller for Scheme B-2 than for Modified Scheme B-1.

Head-Loss Data

The hydraulic grade lines for the fourteen test conditions outlined in Table 1 are plotted in Exhibits 30-39. Again the piezometer scheme of Exhibit 5 applies, and the head at piezometer number 0 in the vertical shaft is assigned an arbitrary value of 1000 ft for all test results. The actual and relative loss coefficients are summarized in Tables 5 and 6, respectively. The performance of Scheme B-2 relative to the Modified Scheme B-1 will be discussed later.

Flow Patterns in Bifurcation Model

During initial stages of the testing of this scheme the trunk of the model failed structurally. It was subsequently repaired by means of reinforcing bands and pieces of clear plastic glued to the body of the trunk along the failure line, as shown by the photograph of Exhibit 40, which illustrates somewhat poorly the flow pattern for the case of three units generating. Exhibit 41 shows the flow in the approach to Unit 3 when it is the sole unit generating.

The flow in the pumping mode is still fairly turbulent, as illustrated by the air bubbles of Exhibits 42-44, which correspond to three units pumping, Units 2 and 3 pumping, and Unit 3 pumping, respectively.

Pressure Distribution in Trunk

For the seven piezometer locations shown on Exhibit 8 the values of the hydraulic grade line in trunk of Scheme B-2 are listed in Table 7. The greatest value of the HGL occurs at piezometer number 4 for Units 2 and 3 pumping because of the effect of stagnation from the flow out of penstock number 2.

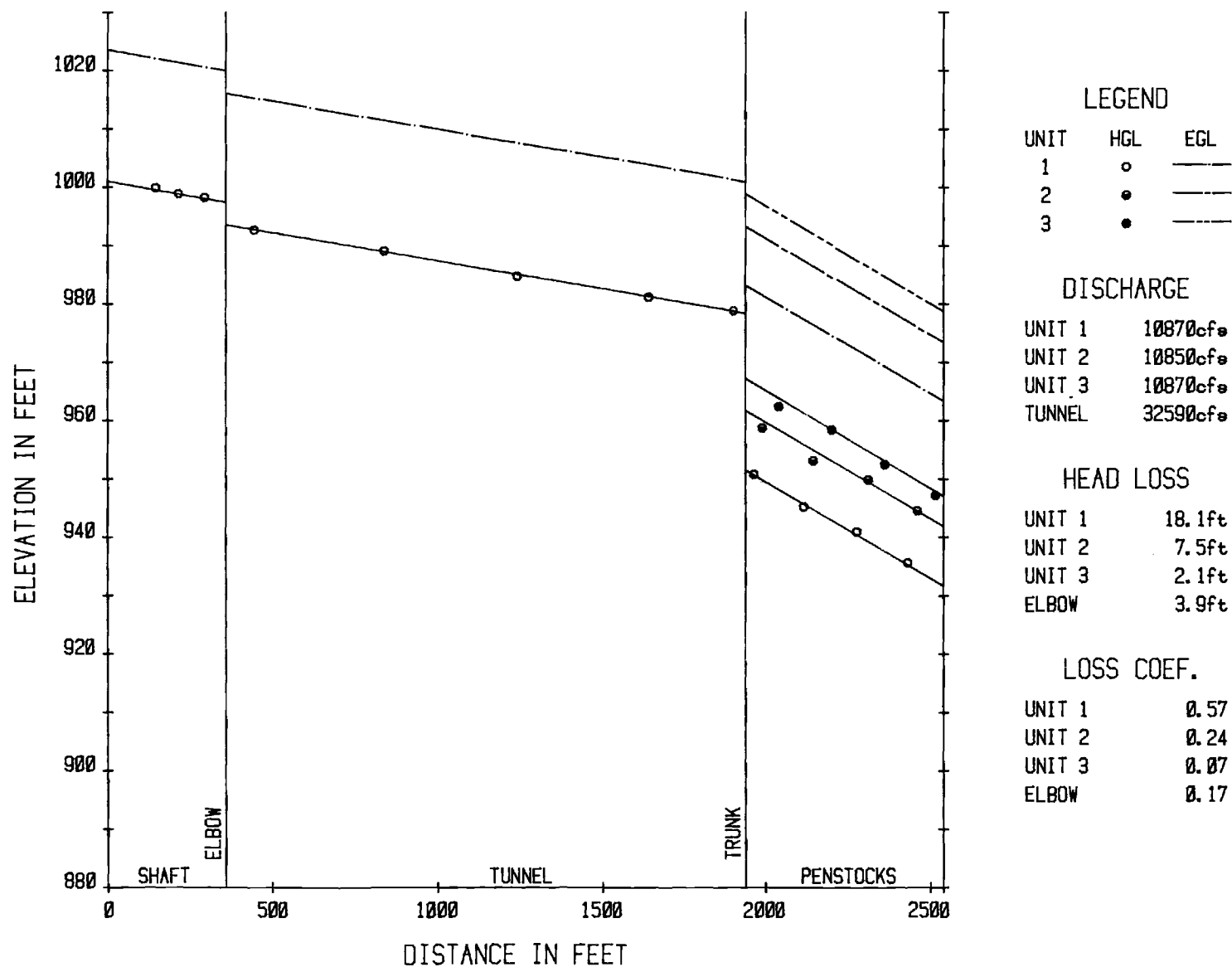


Exhibit 30. Hydraulic and Energy Grade Lines in Scheme B-2 for Three Units Generating.

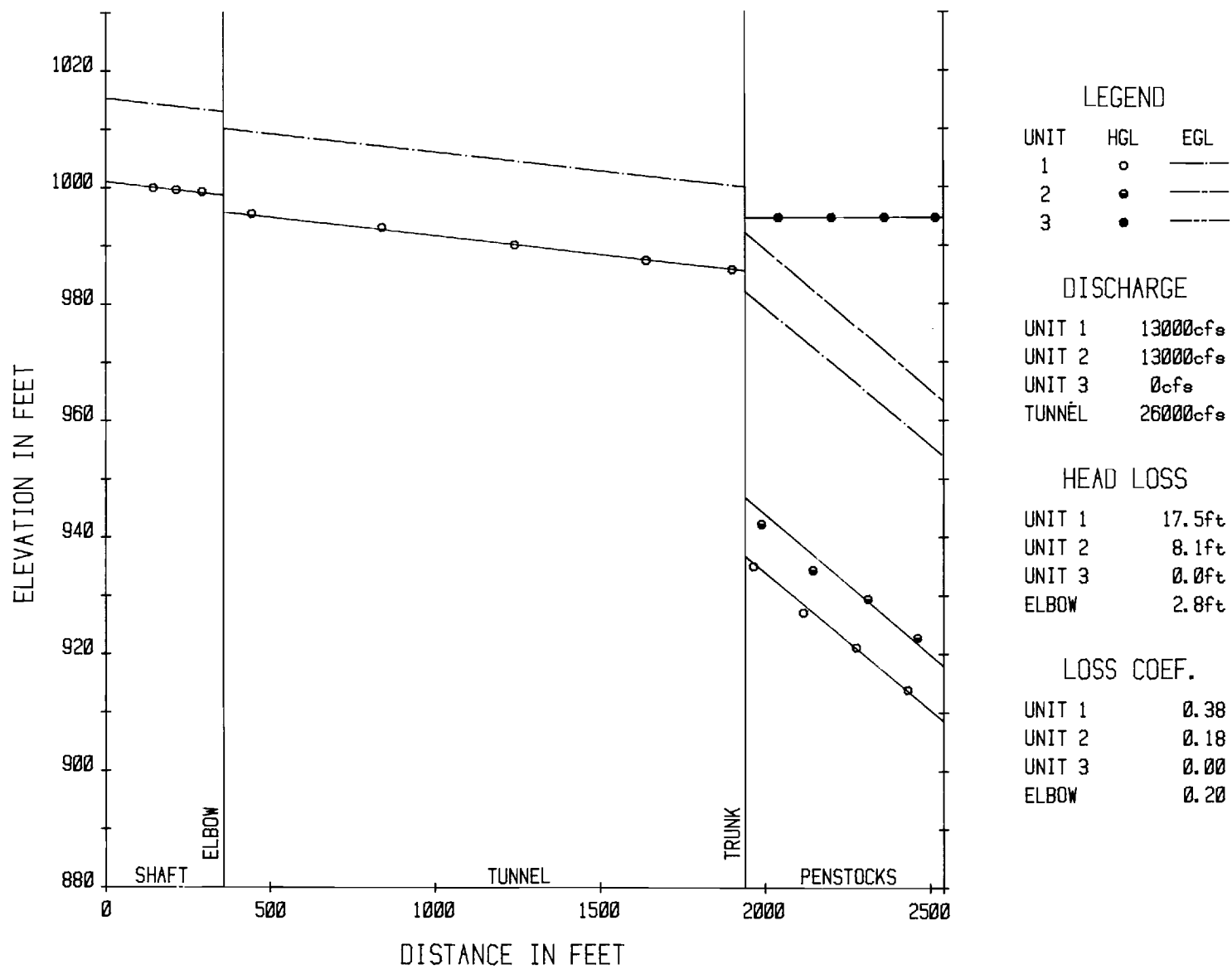


Exhibit 31. Hydraulic and Energy Grade Lines in Scheme B-2 for Units 1 and 2 Generating.

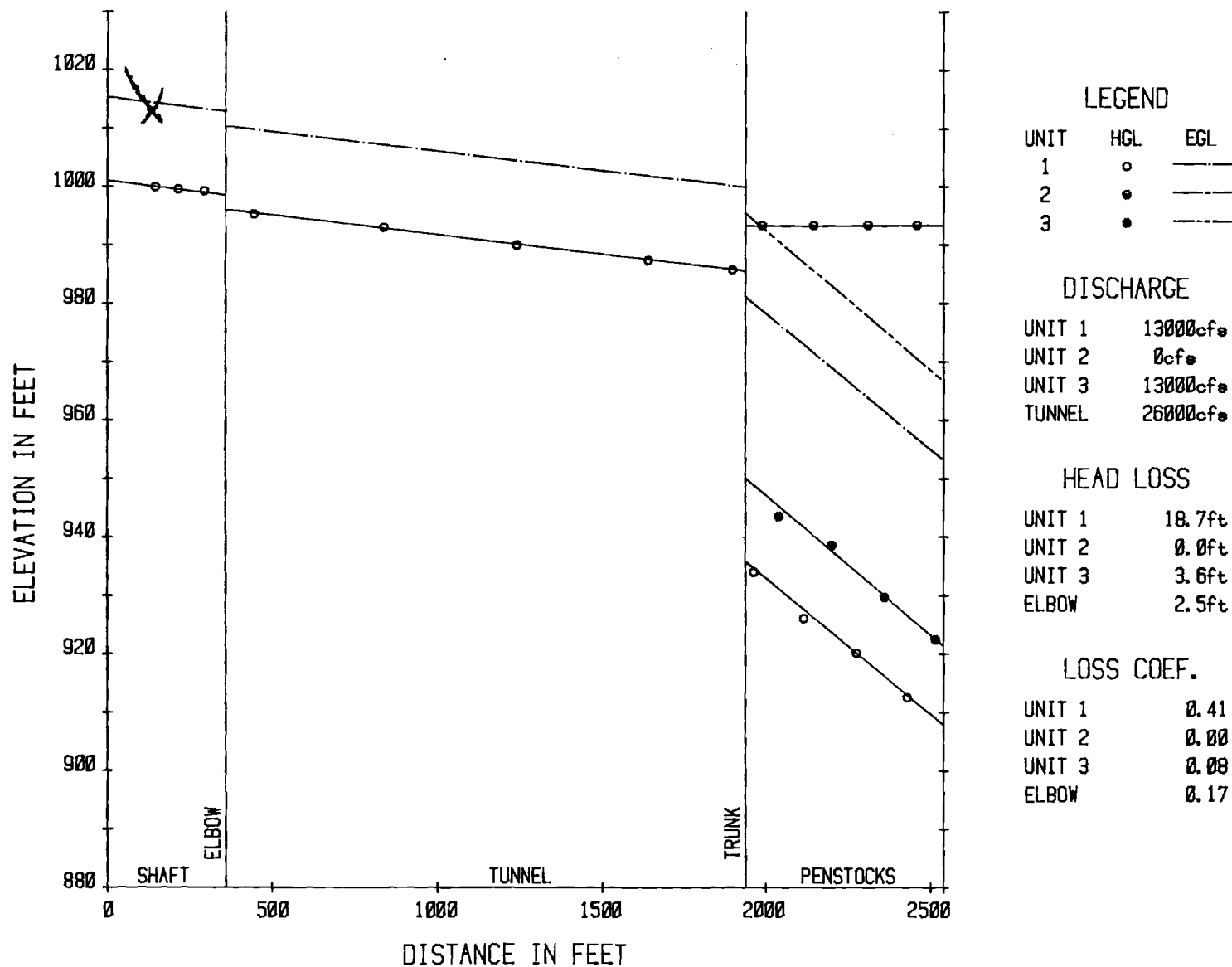


Exhibit 32. Hydraulic and Energy Grade Lines in Scheme B-2 for Units 1 and 3 Generating.

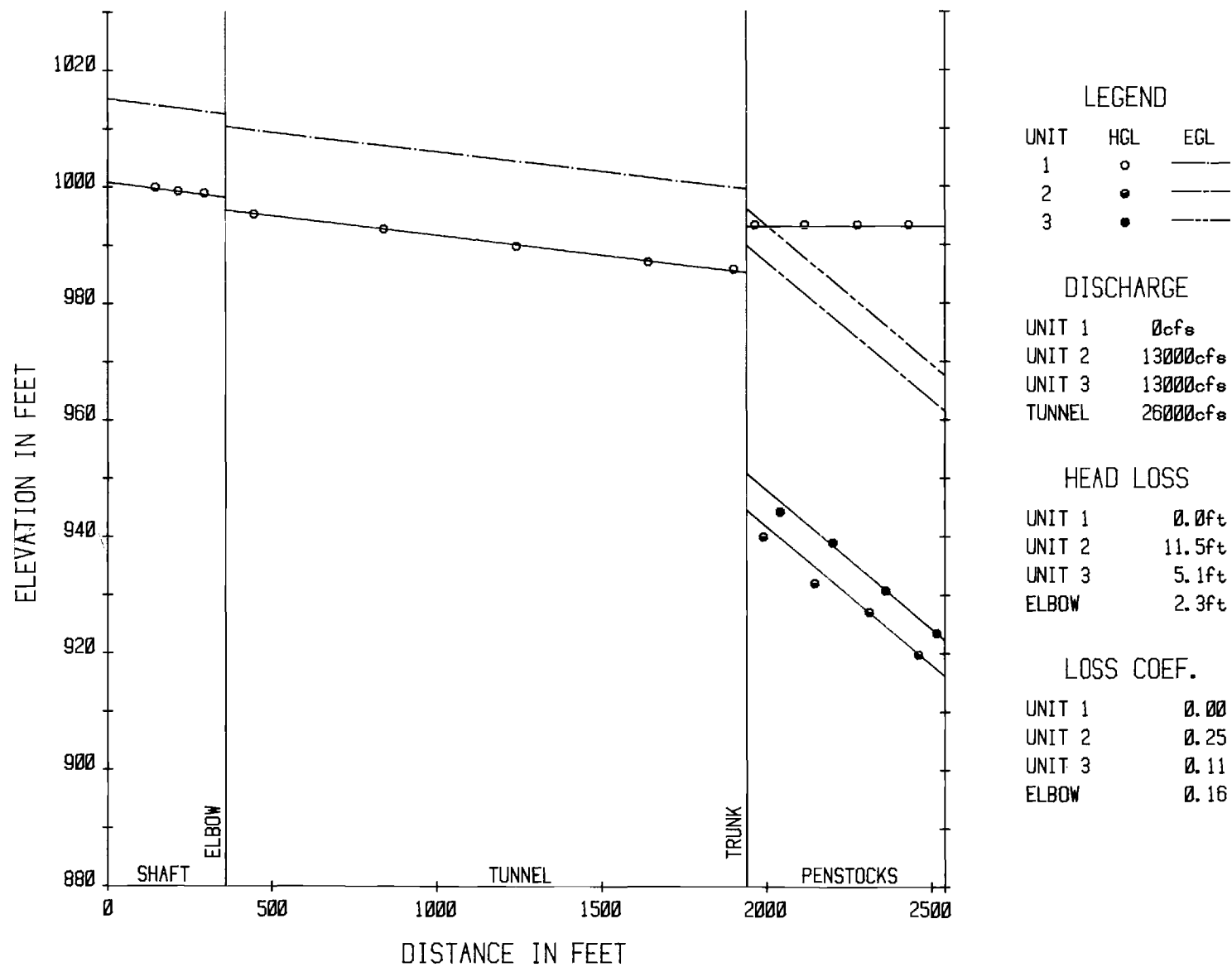


Exhibit 33. Hydraulic and Energy Grade Lines in Scheme B-2 for Units 2 and 3 Generating.

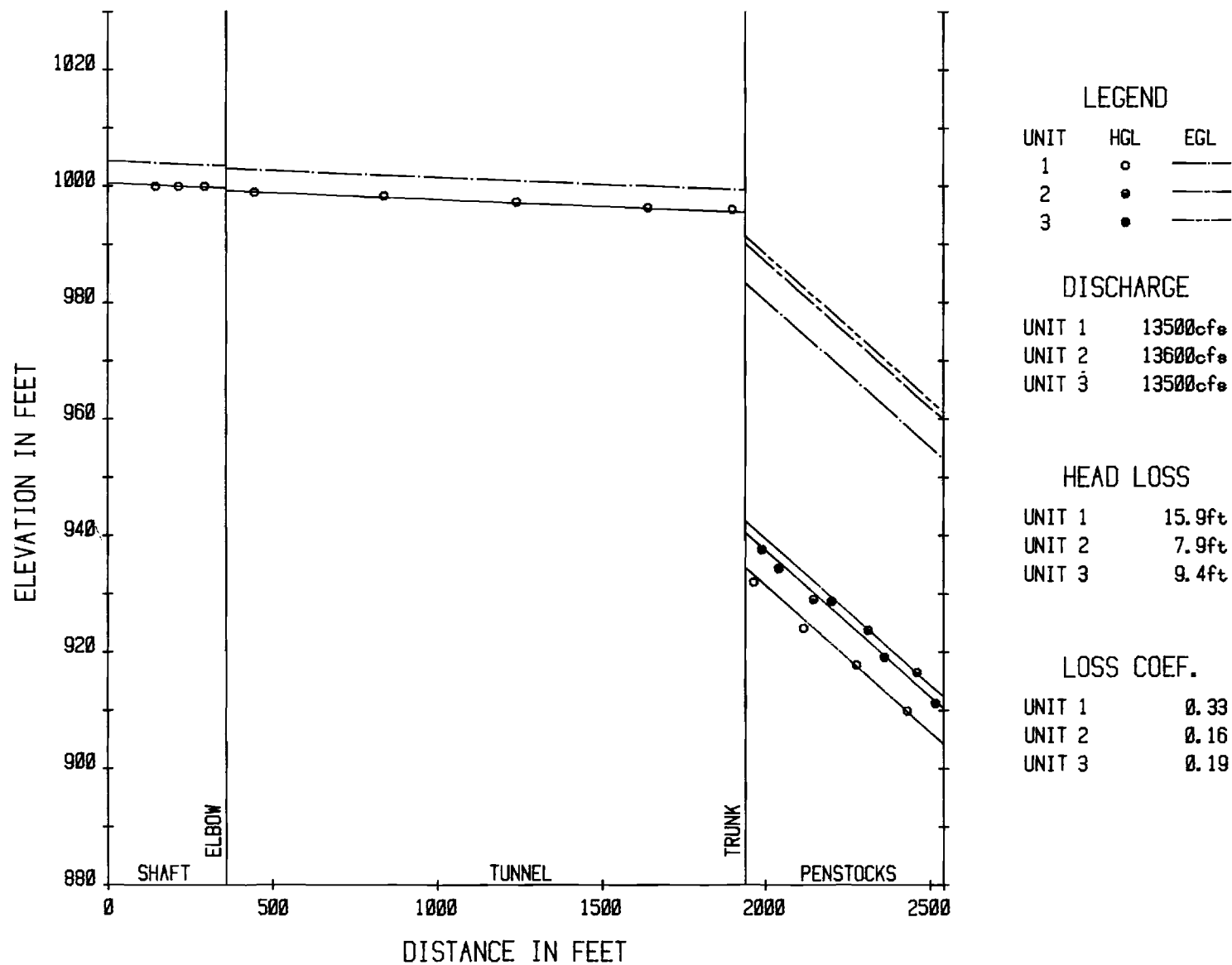


Exhibit 34. Hydraulic and Energy Grade Lines in Scheme B-2 for Single Unit Generating.

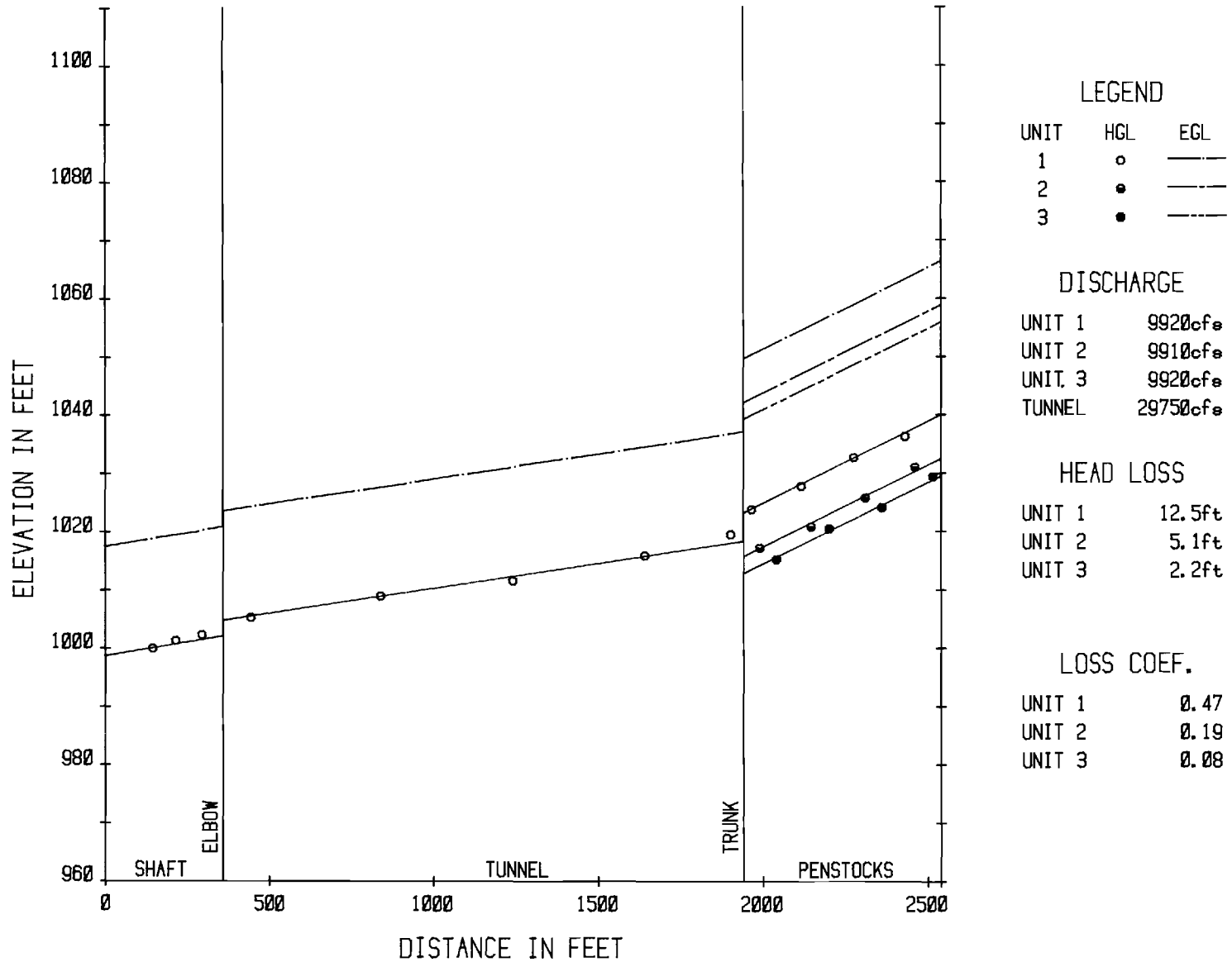


Exhibit 35. Hydraulic and Energy Grade Lines in Scheme B-2 for Three Units Pumping.

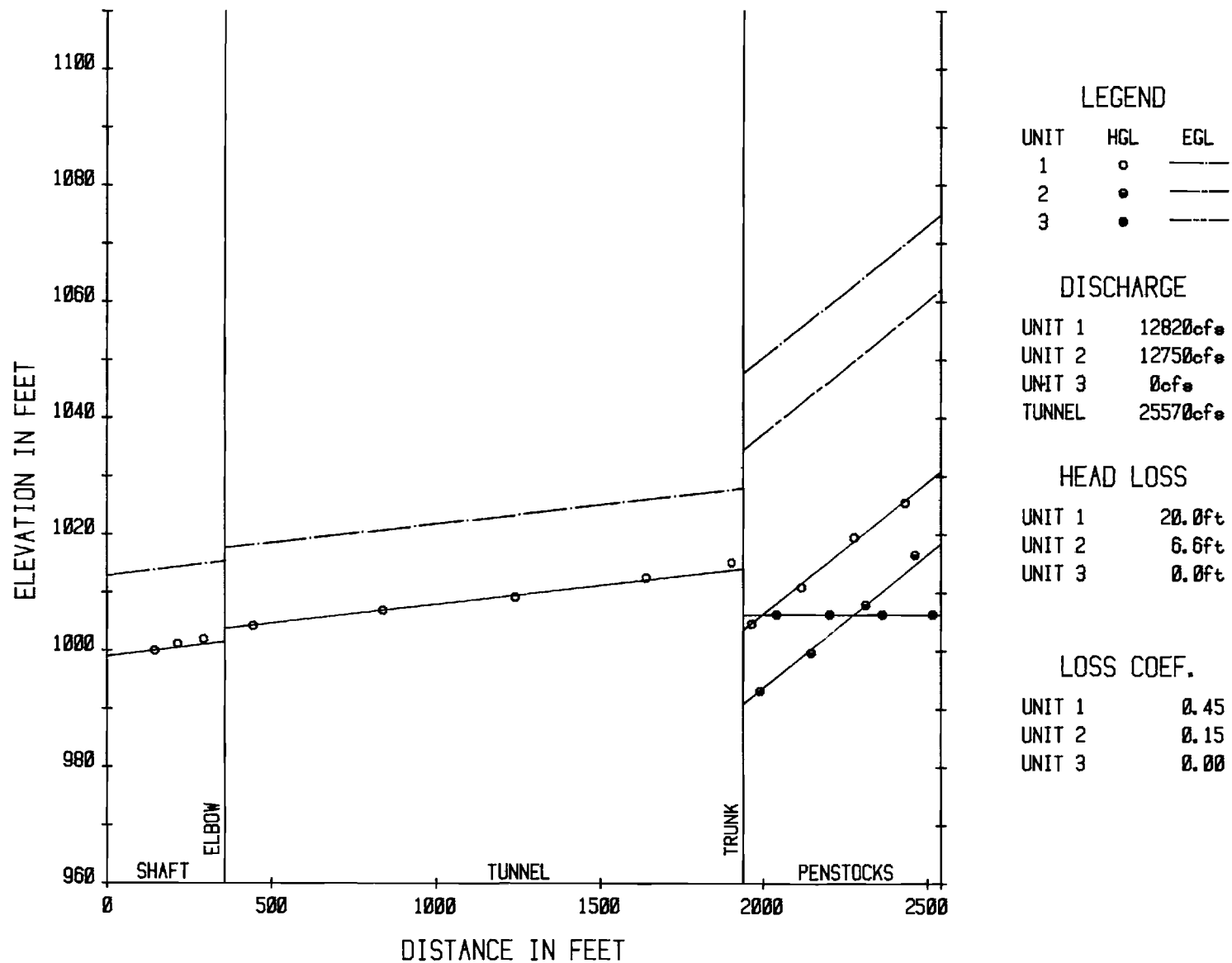


Exhibit 36. Hydraulic and Energy Grade Lines in Scheme B-2 for Units 1 and 2 Pumping.

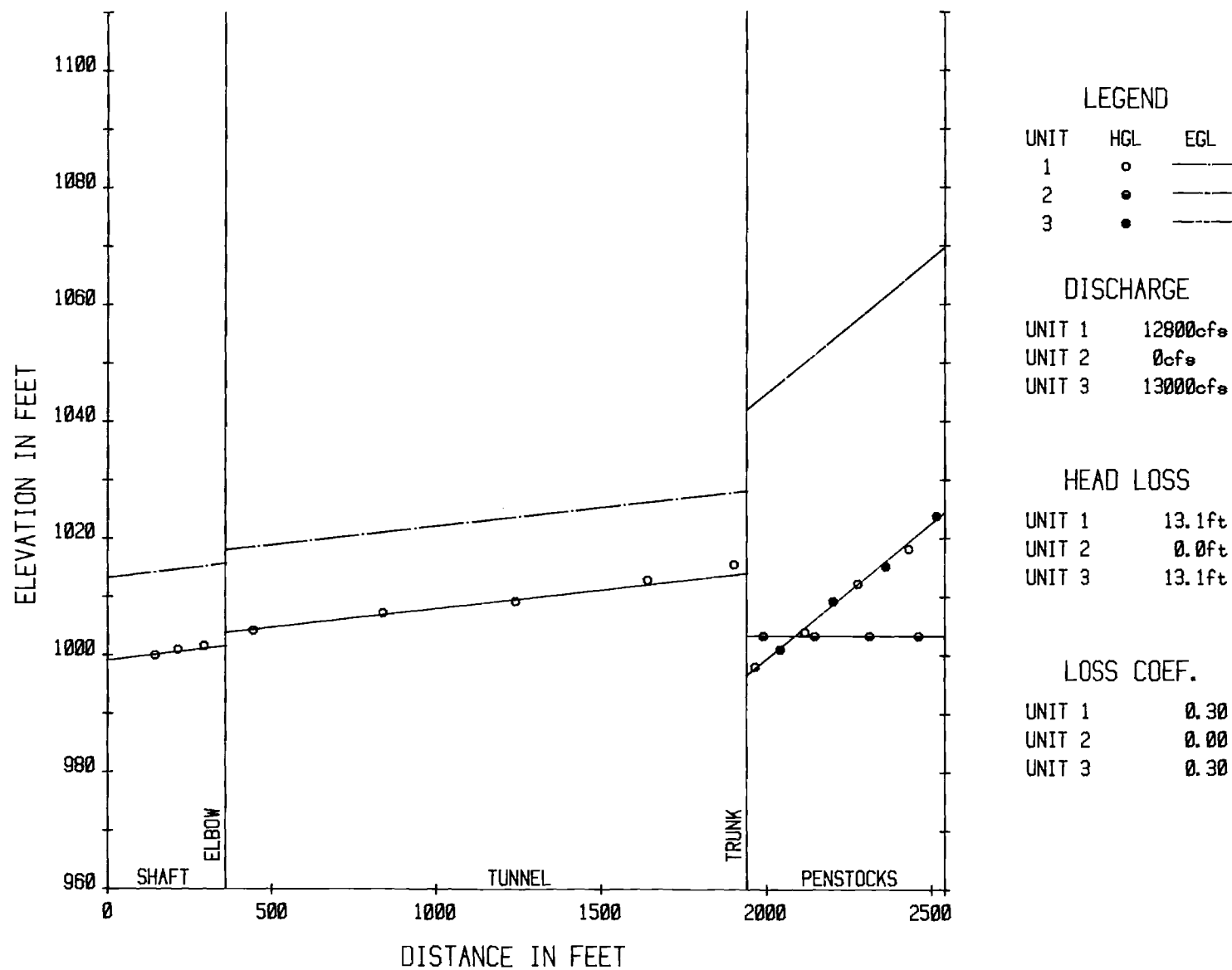


Exhibit 37. Hydraulic and Energy Grade Lines in Scheme B-2 for Units 1 and 3 Pumping.

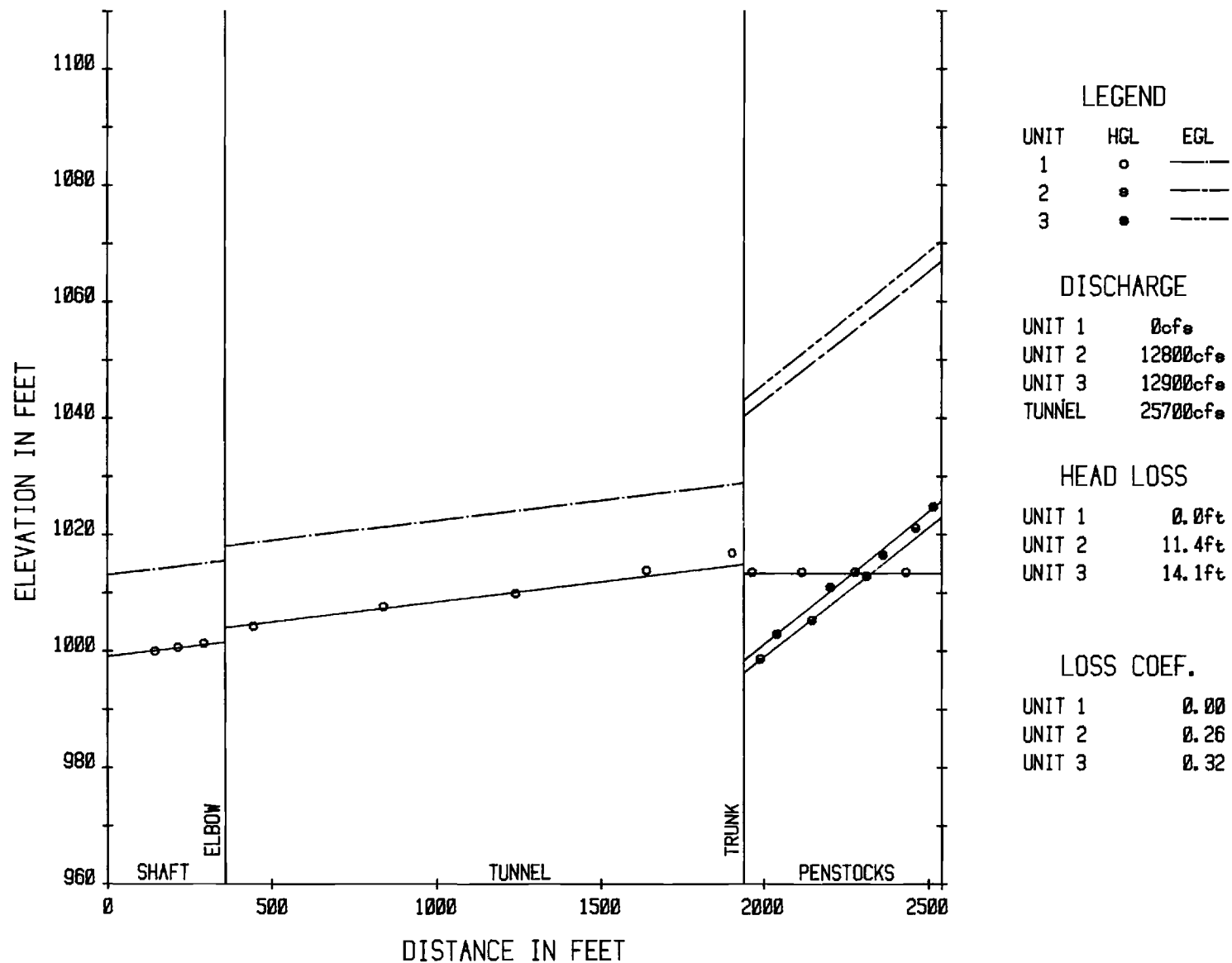


Exhibit 38. Hydraulic and Energy Grade Lines in Scheme B-2 for Units 2 and 3 Pumping.

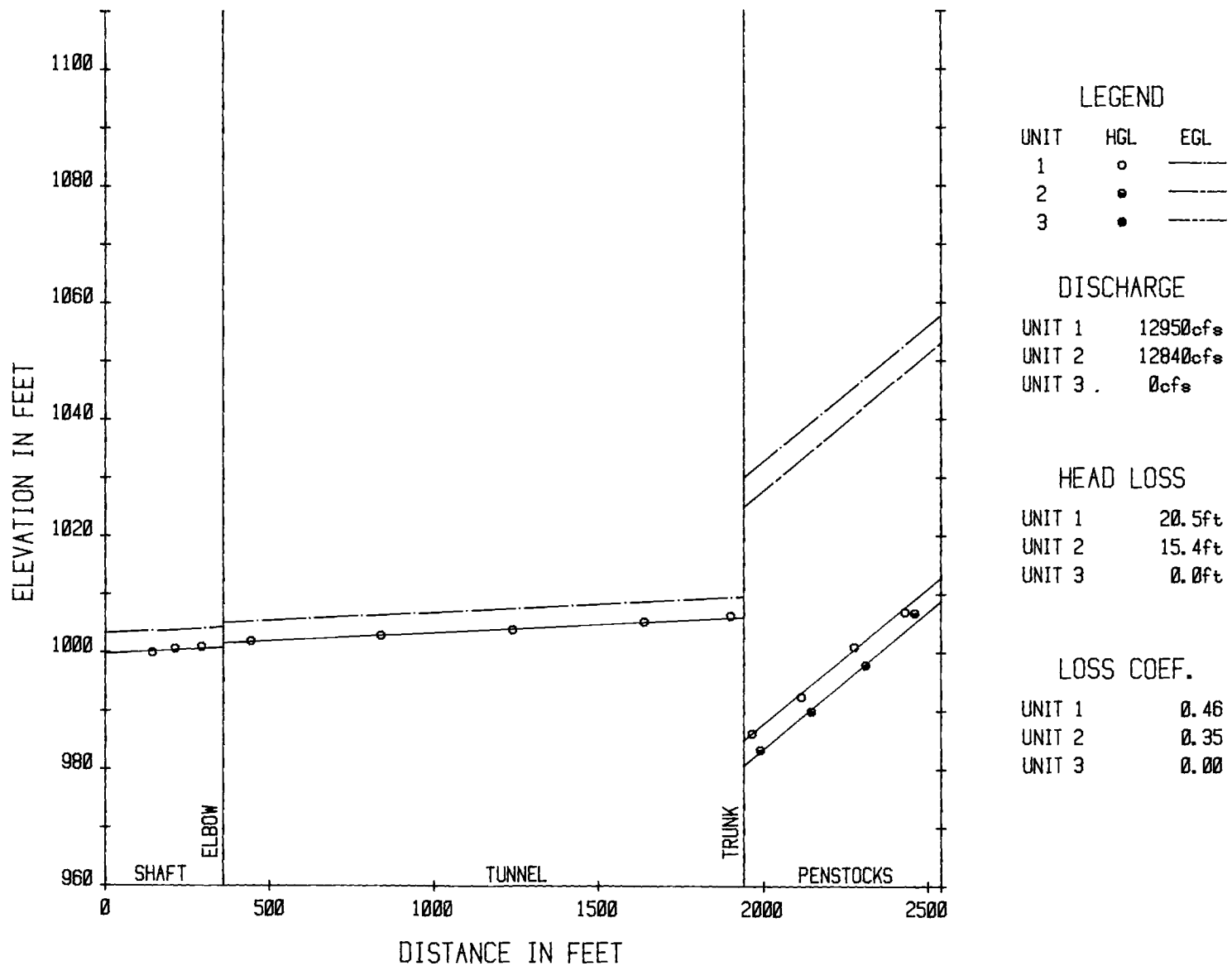


Exhibit 39a. Hydraulic and Energy Grade Lines in Scheme B-2 for Single Units 1 and 2 Pumping.

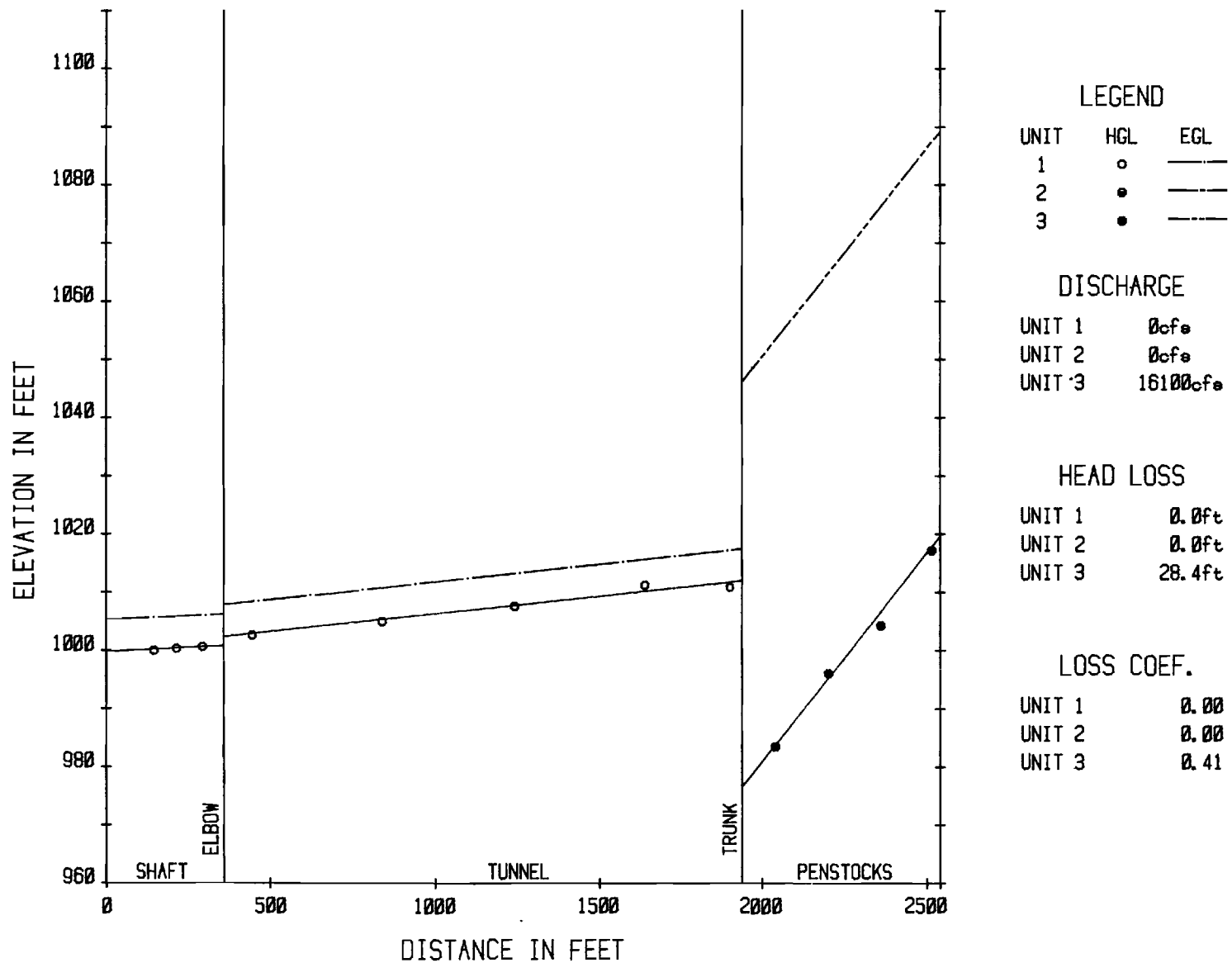


Exhibit 39b. Hydraulic and Energy Grade Lines in Scheme B-2 for Unit 3 Pumping.

TABLE 5
SUMMARY OF ACTUAL LOSS COEFFICIENTS
FOR B-2 SCHEME

<u>MODE</u>	K_{L_1} (<u>UNIT 1</u>)	K_{L_2} (<u>UNIT 2</u>)	K_{L_3} (<u>UNIT 3</u>)
Three Units Generating	0.57	0.24	0.07
Units 1 and 2 Generating	0.38	0.18	--
Units 1 and 3 Generating	0.41	--	0.08
Units 2 and 3 Generating	--	0.25	0.11
Single Unit Generating	0.33	0.16	0.19
Three Units Pumping	0.47	0.19	0.08
Units 1 and 2 Pumping	0.45	0.15	--
Units 1 and 3 Pumping	0.30	--	0.30
Units 2 and 3 Pumping	--	0.26	0.32
Single Unit Pumping	0.46	0.35	0.41

TABLE 6
SUMMARY OF
RELATIVE LOSS COEFFICIENTS
FOR B-2 SCHEME

<u>MODE</u>	K_{R_1} (<u>UNIT 1</u>)	K_{R_2} (<u>UNIT 2</u>)	K_{R_3} (<u>UNIT 3</u>)
Three Units Generating	0.57	0.26	0.15
Units 1 and 2 Generating	0.38	0.20	--
Units 1 and 3 Generating	0.41	--	0.16
Units 2 and 3 Generating	--	0.27	0.19
Single Unit Generating	0.33	0.18	0.27
Three Units Pumping	0.47	0.21	0.16
Units 1 and 2 Pumping	0.45	0.17	--
Units 1 and 3 Pumping	0.30	--	0.38
Units 2 and 3 Pumping	--	0.28	0.40
Single Unit Pumping	0.46	0.37	0.49

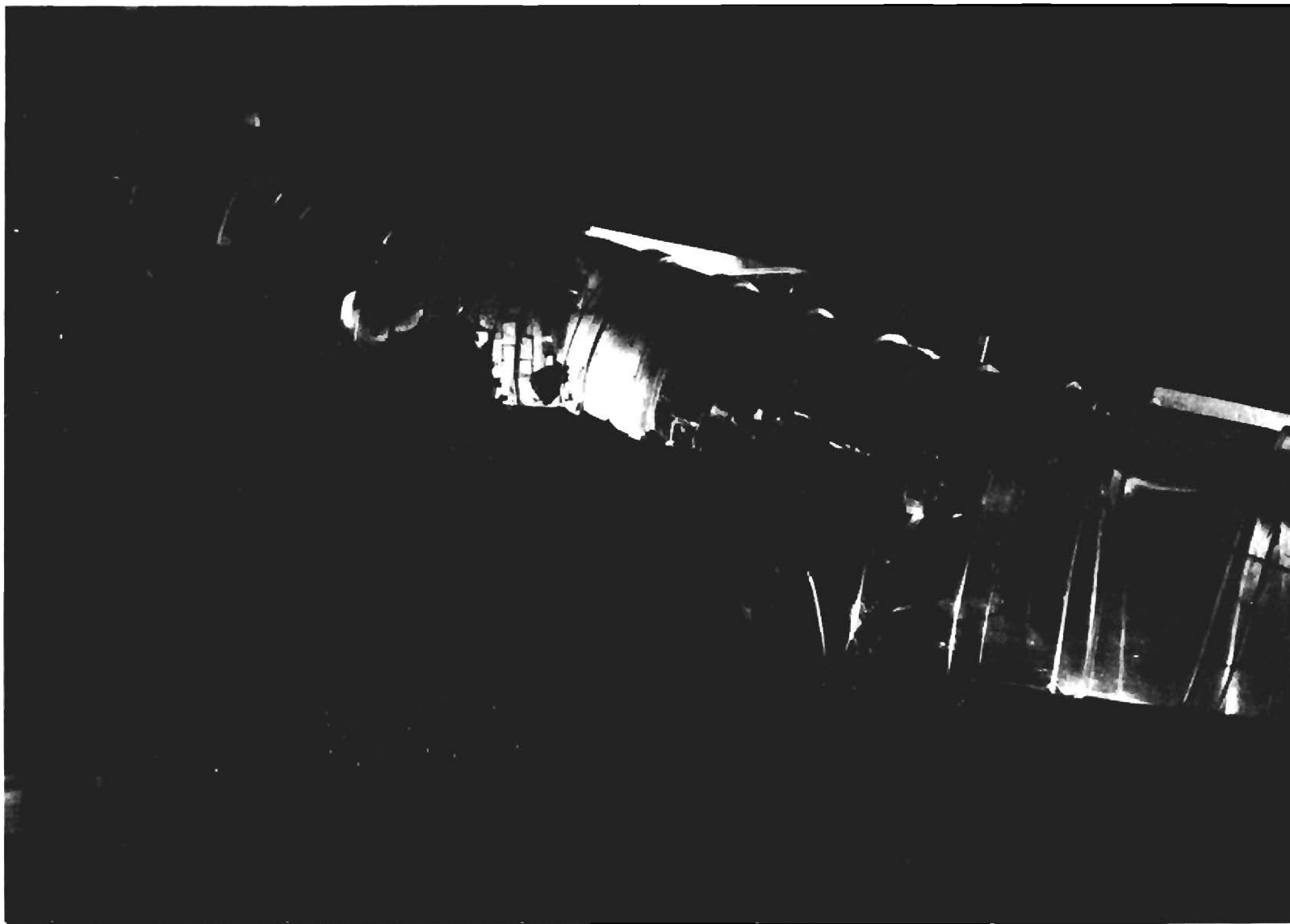


Exhibit 40. View of Tuft Pattern in Trunk of Scheme B-2 for Three Units Generating.

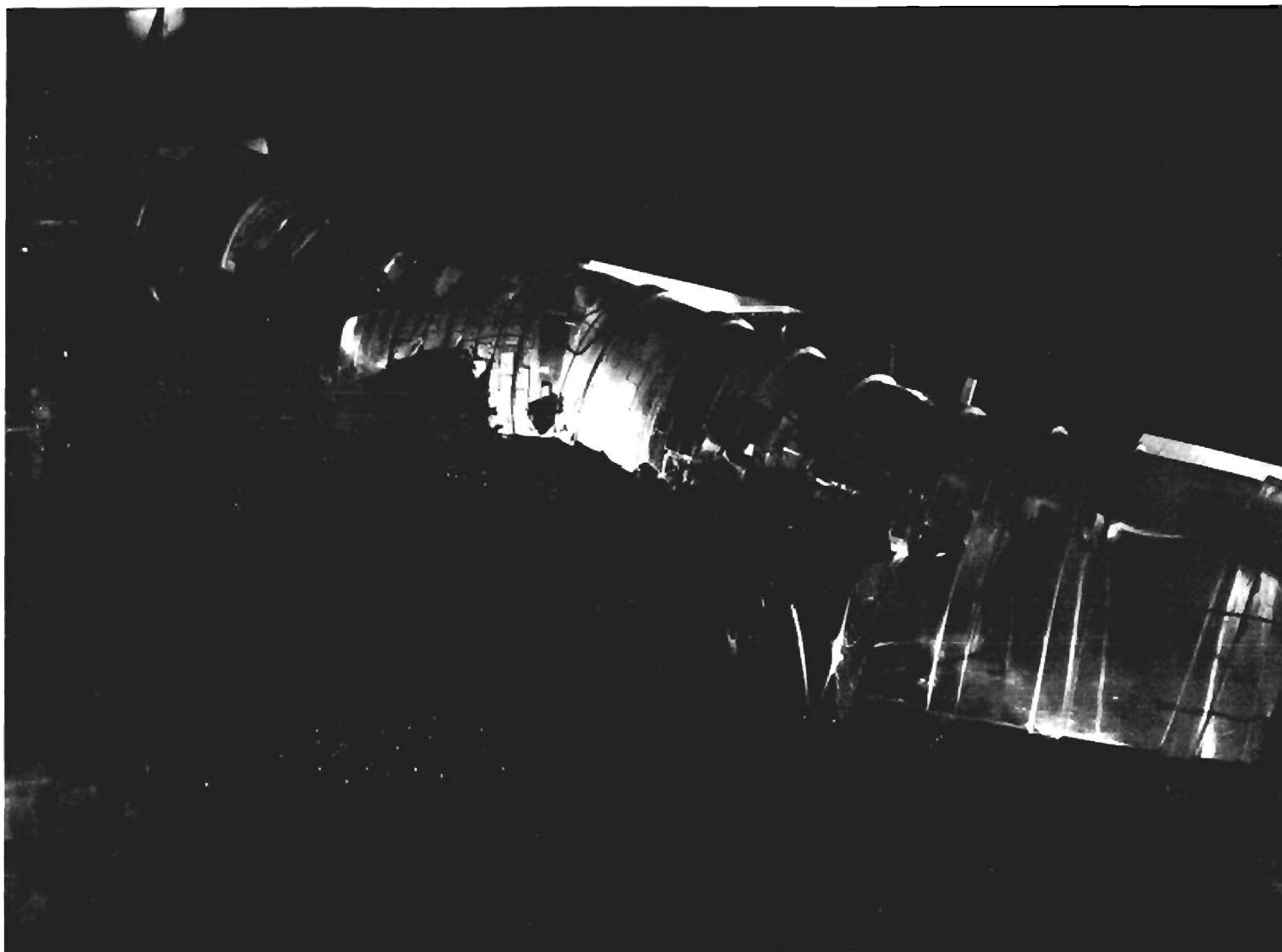


Exhibit 41. View of Tuft Pattern in Trunk of Scheme B-2 for Unit 3 Generating.

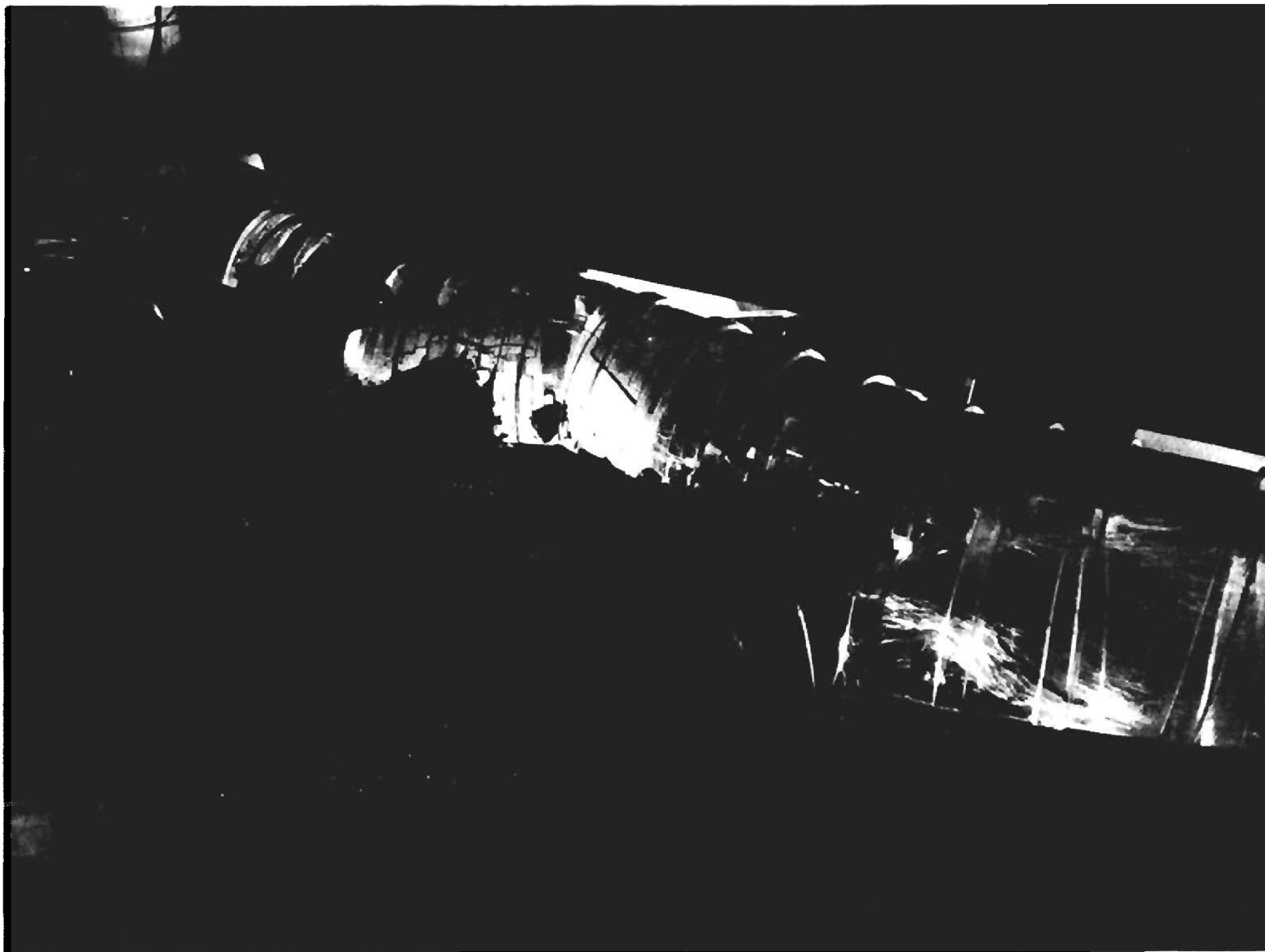


Exhibit 42. View of Tuft Pattern in Trunk of Scheme B-2 for
Three Units Pumping.

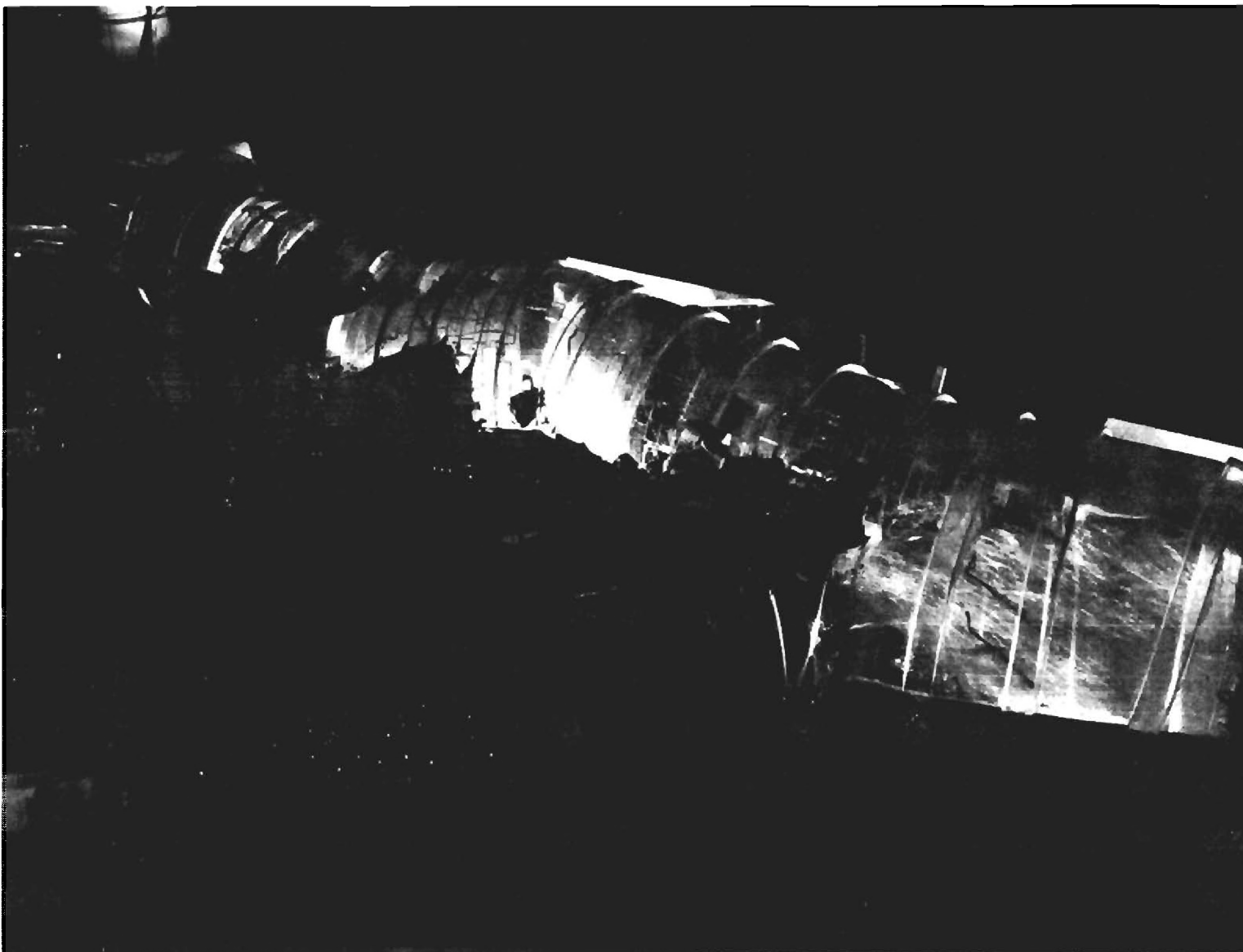


Exhibit 43. View of Tuft Pattern in Trunk of Scheme B-2 for Units 2 and 3 Pumping.

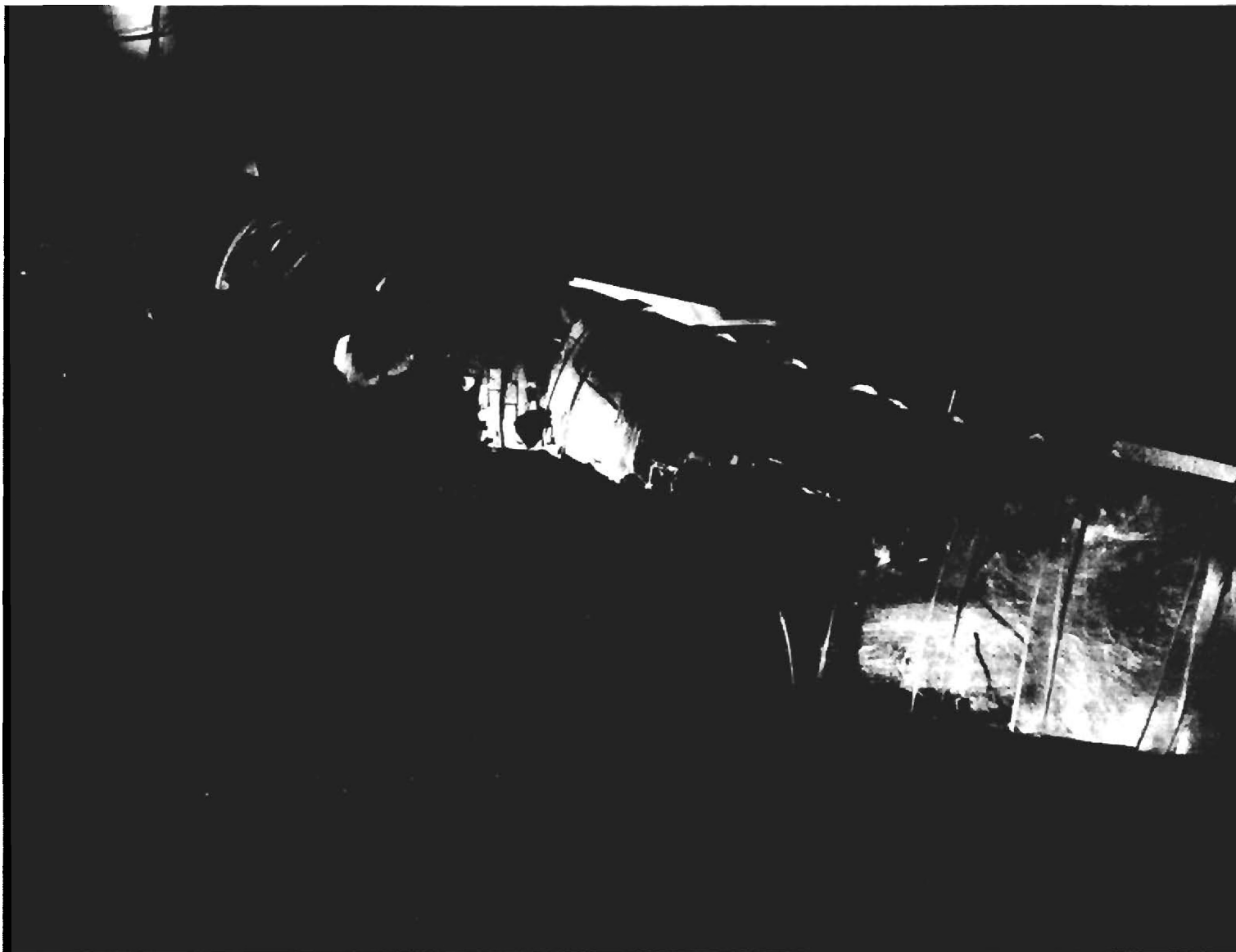


Exhibit 44. View of Tuft Pattern in Trunk of Scheme B-2 for Unit 3 pumping.

Table 7. Values of Relative Hydraulic Grade
Line in Trunk of B-2 Scheme.

TRUNK HYDRAULIC GRADE LINE SCHEME B-2

UNIT 1	UNIT 2	UNIT 3	PIEZOMETER NUMBER						
(cfs)	(cfs)	(cfs)	1	2	3	4	5	6	7
PUMPING MODE									
10030	9860	9970	1020.5	1018.2	1025.1	1030.0	1021.1	1021.1	1021.8
12770	12900	0	999.3	1006.3	1007.6	1015.5	1001.0	1001.0	1012.9
12770	0	13070	1002.6	1006.3	1000.0	1012.5	1013.9	1014.9	1017.2
0	12750	13040	1006.9	1008.3	1014.9	1032.3	1015.8	1016.2	1019.1
12800	0	0	988.8	1001.3	985.8	998.0	999.0	999.7	1003.3
0	12790	0	990.8	1001.7	997.4	1018.8	999.7	1000.0	1004.0
0	0	13000	1000.7	995.7	1000.7	1001.0	1001.3	1001.0	1023.1
GENERATING MODE									
0	0	12960	997.0	957.1	997.4	997.4	997.0	996.4	994.7
11070	11070	11070	969.0	974.3	964.4	976.2	970.6	972.3	974.3
13510	13530	0	952.2	993.4	950.2	967.0	957.1	964.4	981.5
13460	0	13440	992.4	961.1	948.5	987.2	985.5	984.8	981.9
0	13440	13440	952.8	961.7	992.7	987.8	985.5	985.2	982.2
0	0	13310	997.0	956.1	997.4	997.0	997.0	996.4	994.4
0	13490	0	954.8	997.7	994.4	991.1	988.1	989.8	994.4
13440	0	0	992.4	994.4	951.5	990.4	988.8	990.4	994.7

HYDRAULIC GRADE LINE ELEVATIONS ARE IN FEET

CHAPTER V

TEST RESULTS FOR SCHEME C-1

Principally for the purpose of providing a basis for comparison the straight pipe Scheme C-1 shown in Exhibit 1 was tested for head loss for the fourteen cases listed in Table 1.

Head-Loss Data

The hydraulic grade lines in the vertical shaft, tunnel, and penstocks are plotted on Exhibits 45-54 for Scheme C-1. In contrast to the corresponding plots for Schemes B-1 and B-2, the location of the piezometers in the penstocks are referenced to the D-Line of Exhibit 1 rather than to the junction with the trunk. Hence the head losses of Exhibits 45-54 are relative to the U-Line and D-Line, yielding relative loss coefficients. For purposes of comparison with the other schemes the actual loss coefficients have been computed and reported in Table 8, while Table 9 summarizes the relative loss coefficients printed on Exhibits 45-54.

As expected the head loss coefficients for the unstreamlined bifurcation model are much greater than for the two previous schemes.

Flow Patterns in Bifurcation Model

Although photographs were taken of the tuft orientation for all fourteen test cases, only several are reported here. Only in the pumping mode was photography of the air bubble patterns very successful.

Exhibit 55 illustrates the condition of three units generating. In this single case Scheme C-1 performed nearly as well as Modified Scheme B-1. In the pumping mode the turbulence created by the sudden expansion was very severe as shown by Exhibit 56 for three units pumping and Exhibit 57 for only Unit 3 pumping. In the latter case the turbulence can be seen to

persist through the elbow in the tunnel.

No measurements were made of the pressure distribution in the trunk of Scheme C-1.

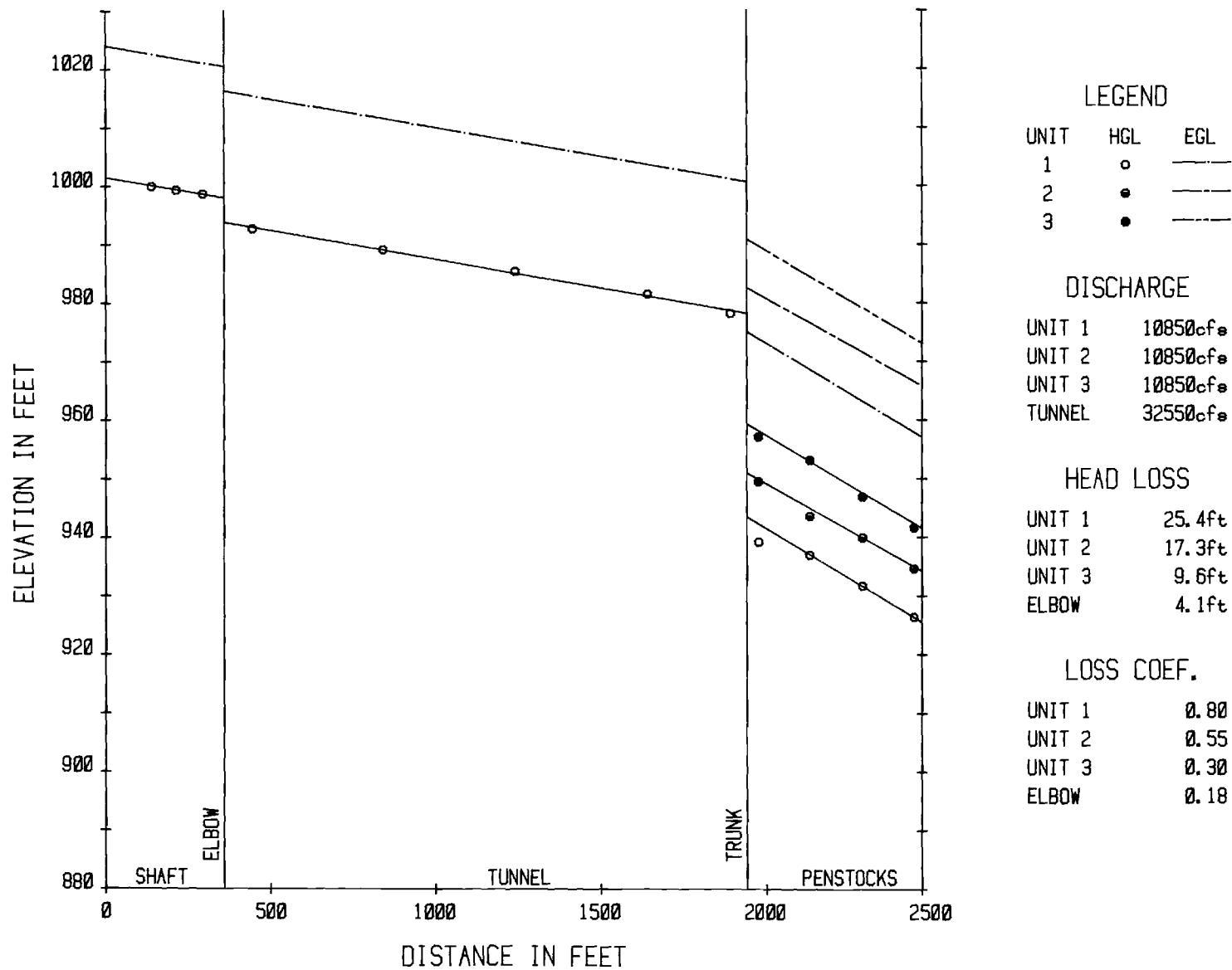
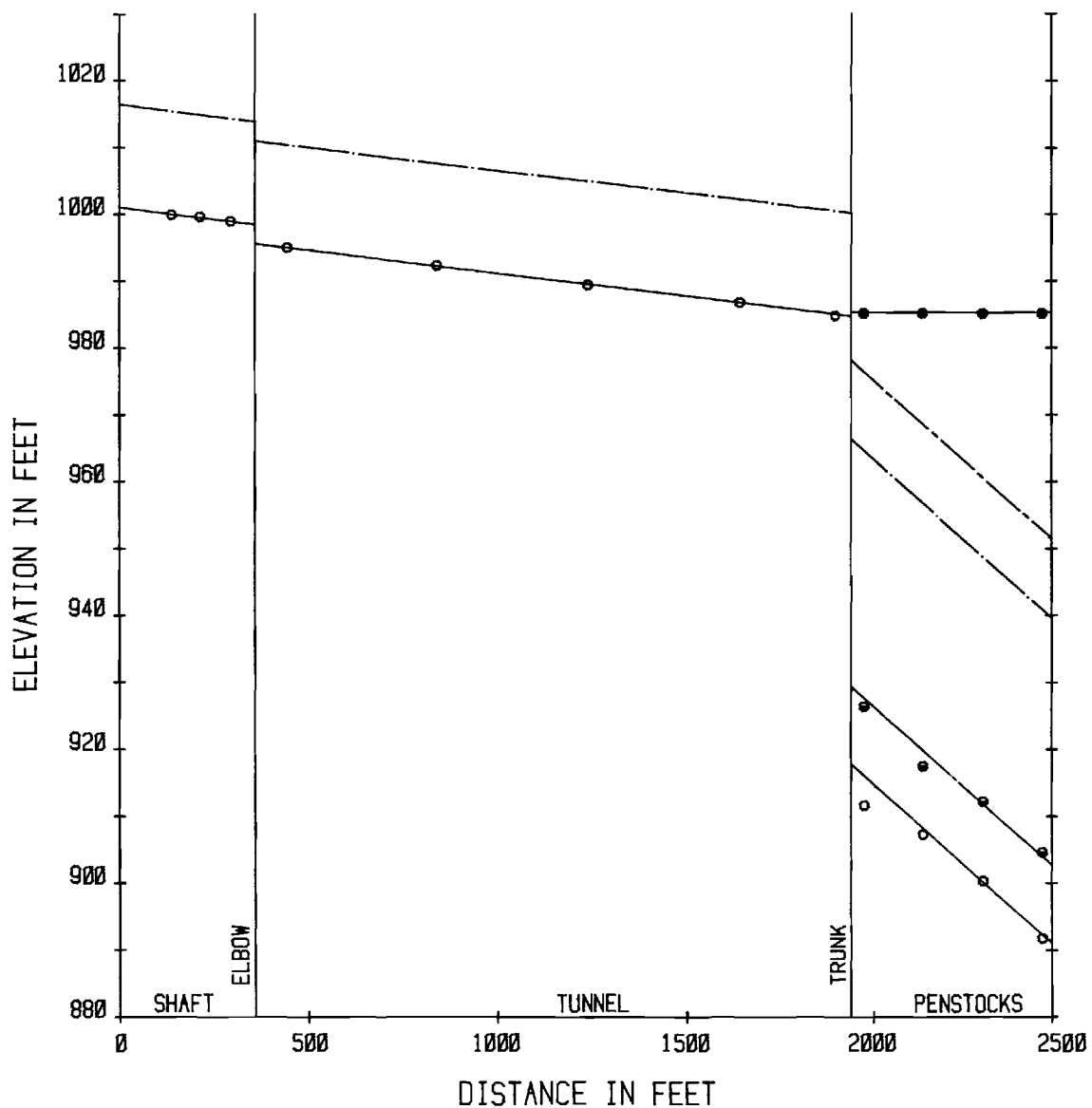


Exhibit 45. Hydraulic and Energy Grade Lines in Scheme C-1 for Three Units Generating.



LEGEND

UNIT	HGL	EGL
1	○	—
2	●	—
3	●	—

DISCHARGE

UNIT 1	13460cfs
UNIT 2	13490cfs
UNIT 3	0cfs
TUNNEL	26950cfs

HEAD LOSS

UNIT 1	33.6ft
UNIT 2	21.7ft
UNIT 3	0.0ft
ELBOW	2.8ft

LOSS COEF.

UNIT 1	0.69
UNIT 2	0.45
UNIT 3	0.00
ELBOW	0.18

Exhibit 46. Hydraulic and Energy Grade Lines in Schem C-1 for Units 1 and 2 Generating.

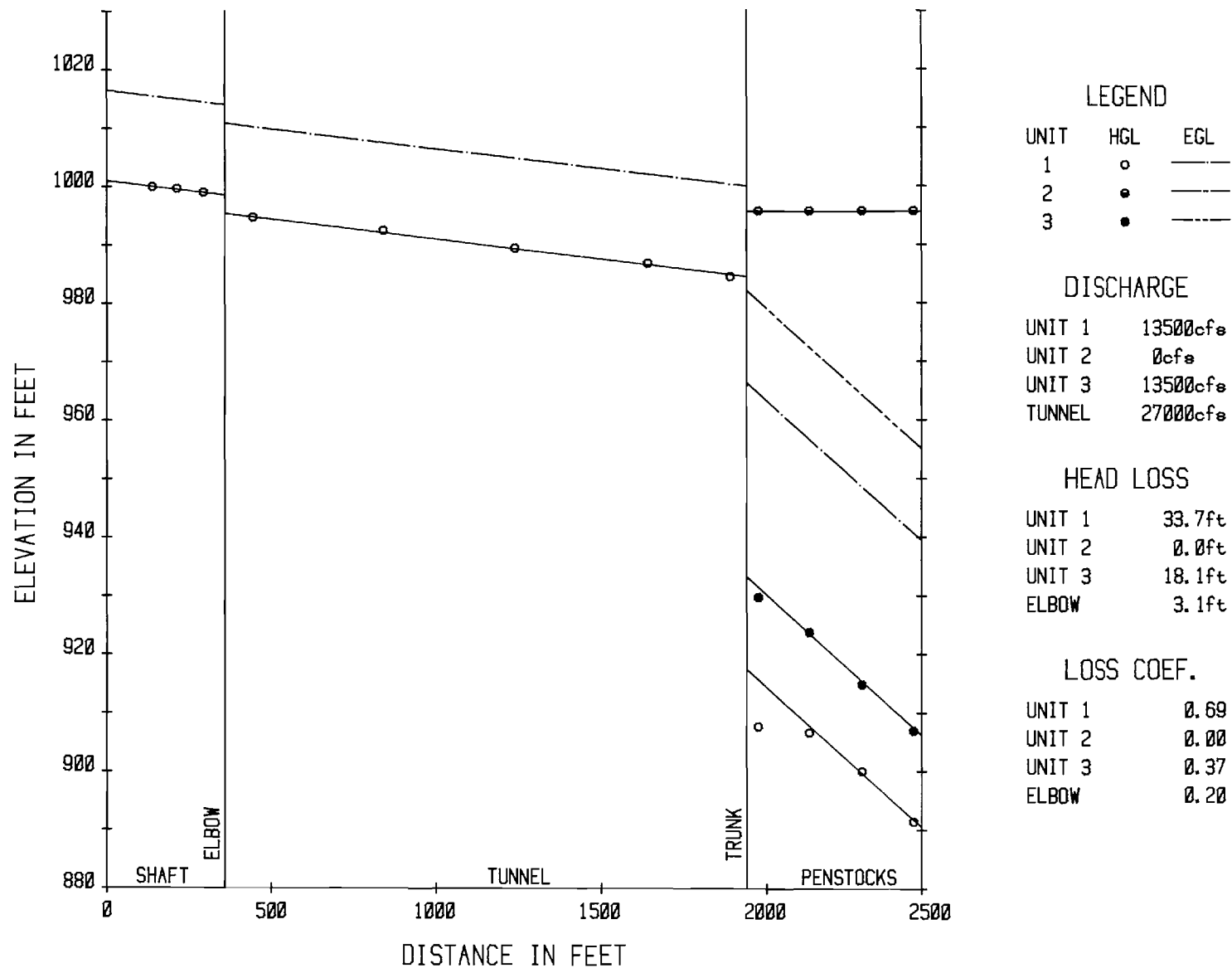


Exhibit 47. Hydraulic and Energy Grade Lines in Scheme C-1 for Units 1 and 3 Generating.

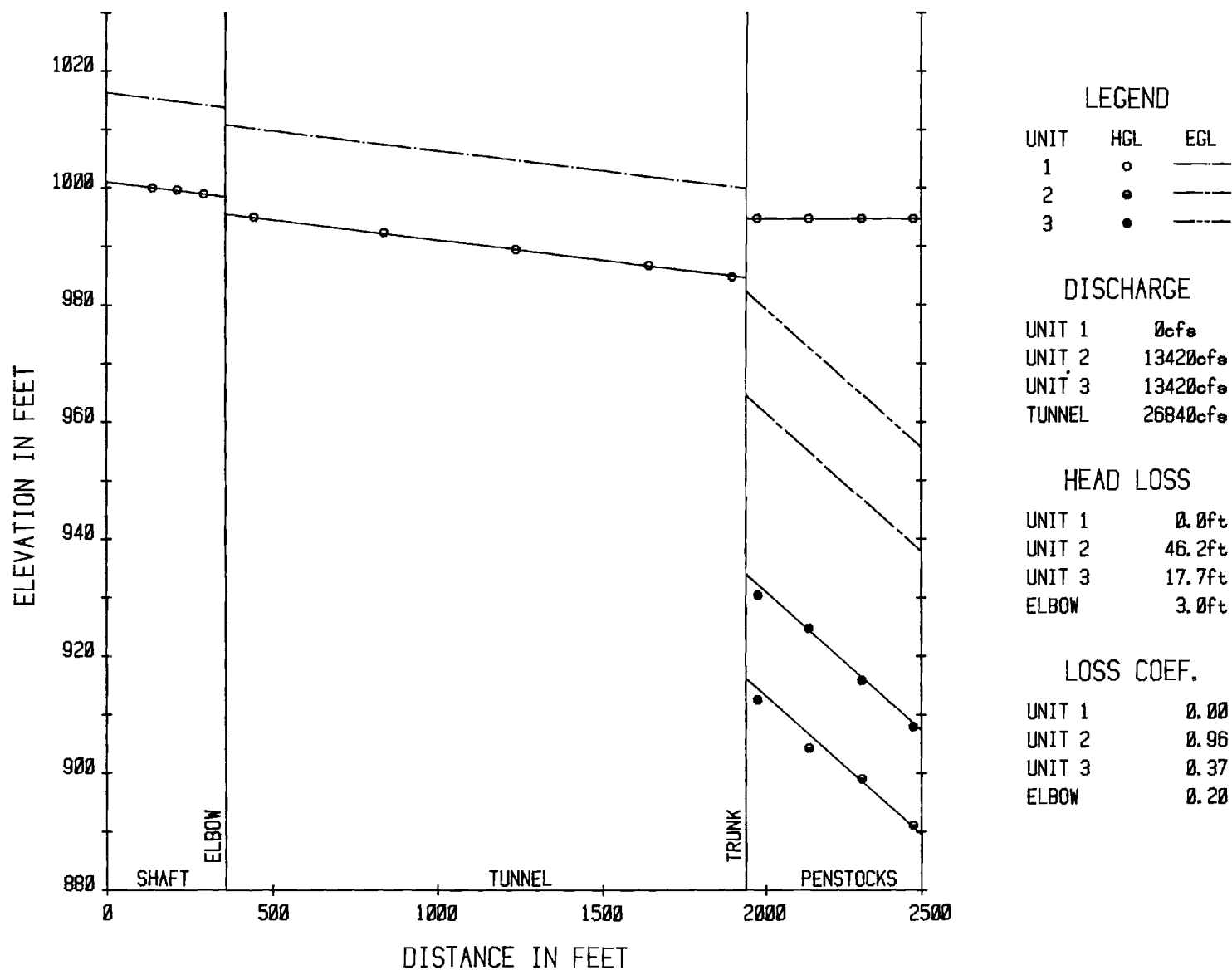


Exhibit 48. Hydraulic and Energy Grade Lines in Scheme C-1 for Units 2 and 3 Generating.

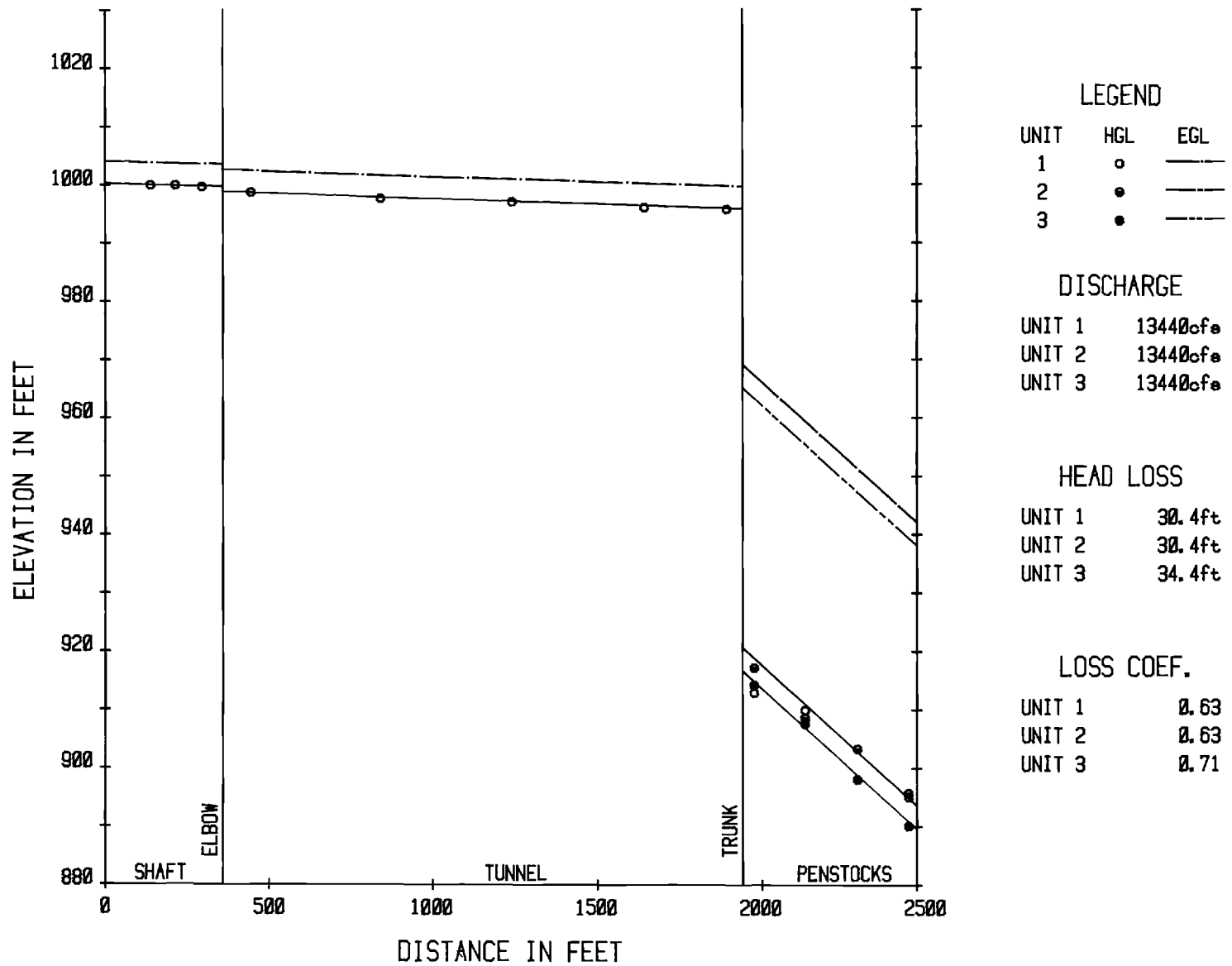


Exhibit 49. Hydraulic and Energy Grade Lines in Scheme C-1 for Single Unit Generating.

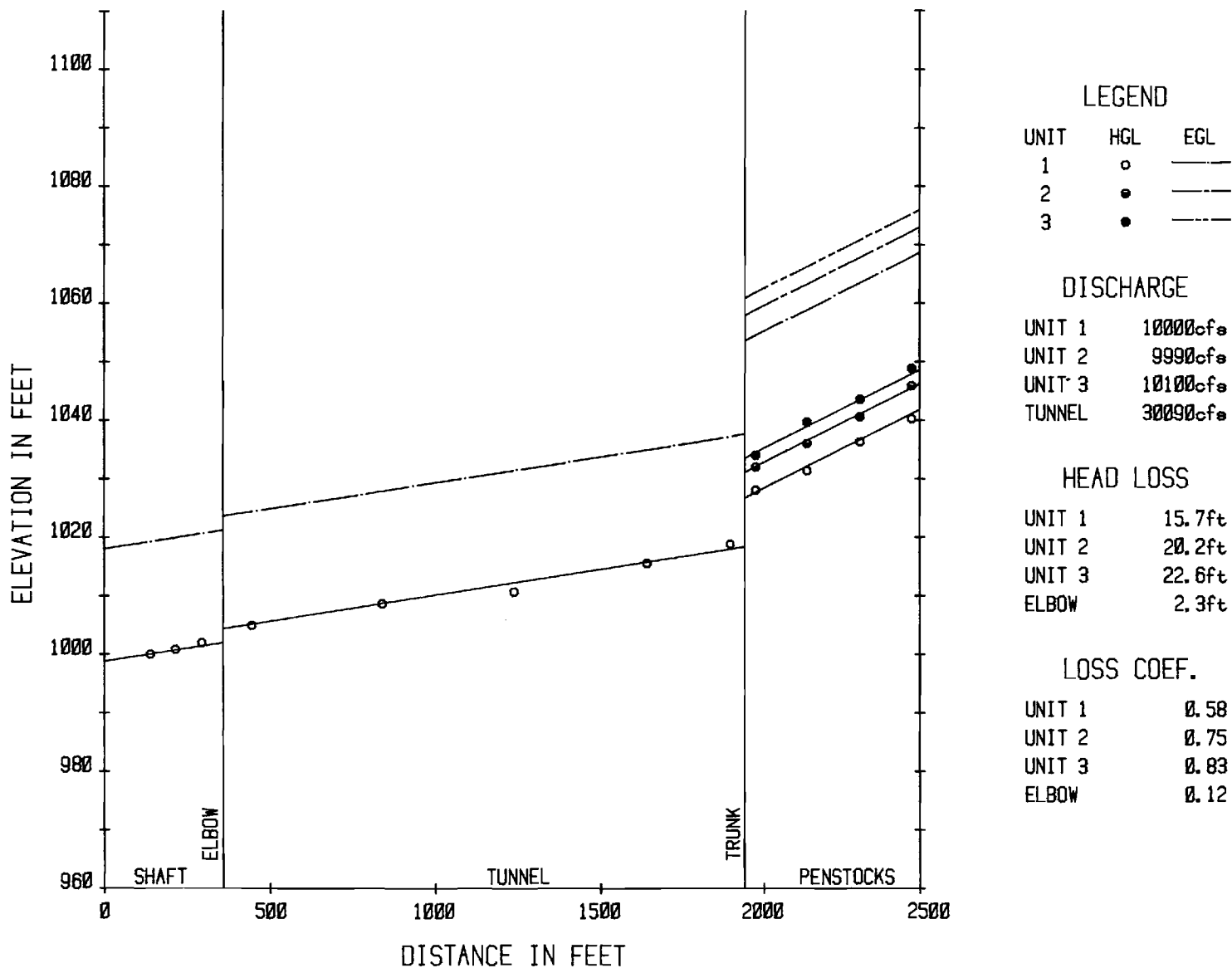


Exhibit 50. Hydraulic and Energy Grade Lines in Scheme C-1 for Three Units Pumping.

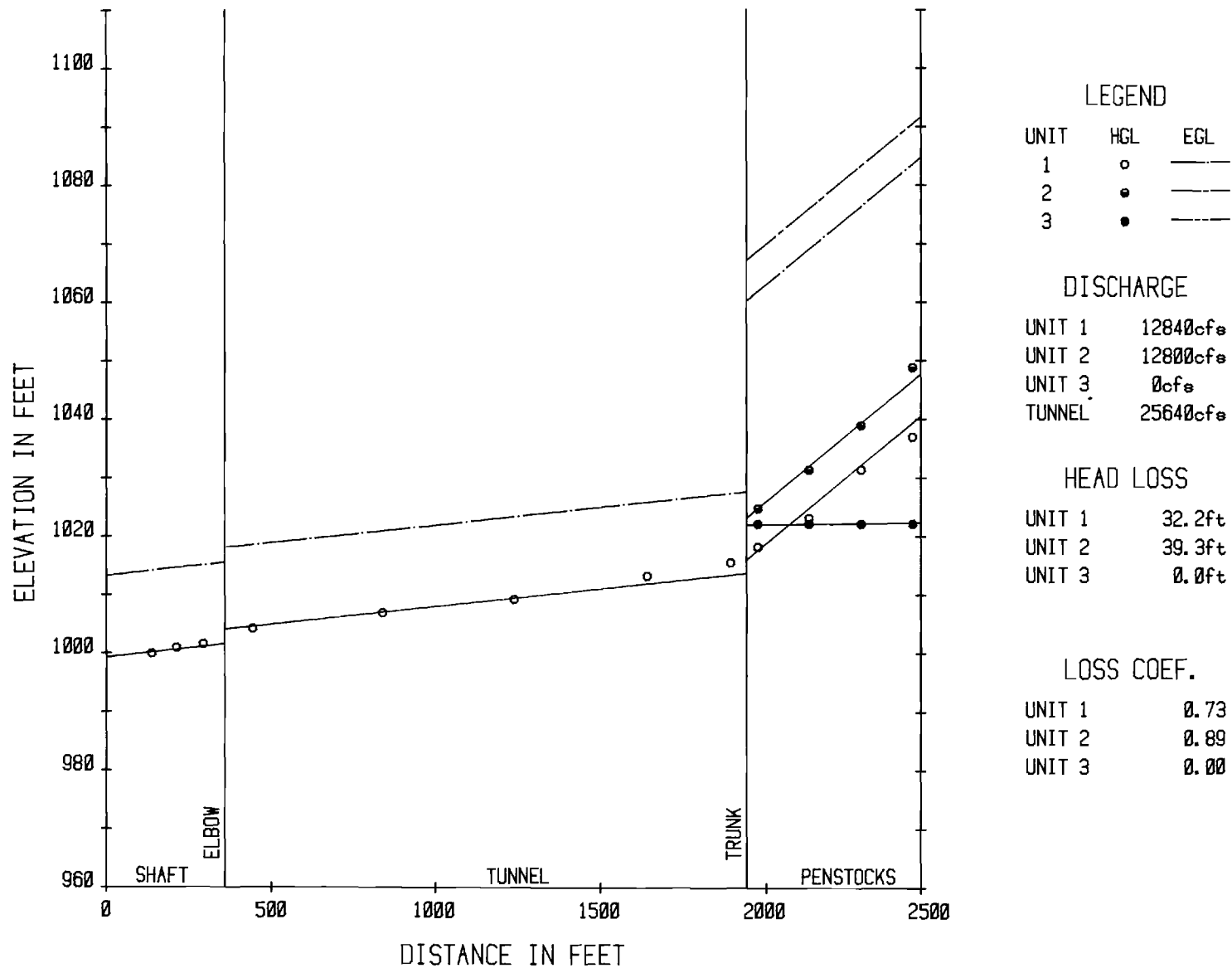


Exhibit 51. Hydraulic and Energy Grade Lines in Scheme C-1 for Units 1 and 2 Pumping.

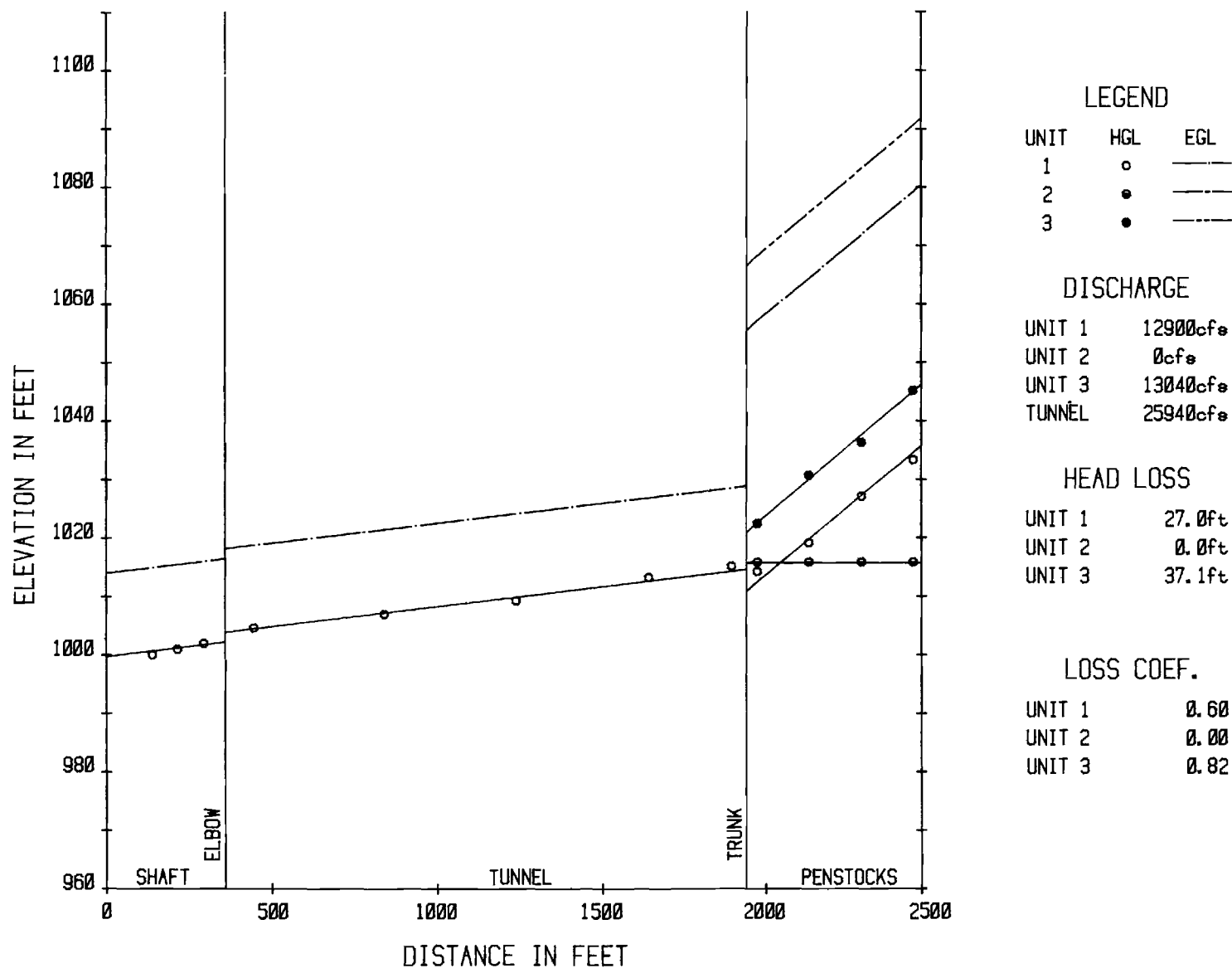


Exhibit 52. Hydraulic and Energy Grade Lines in Scheme C-1 for Units 1 and 3 Pumping.

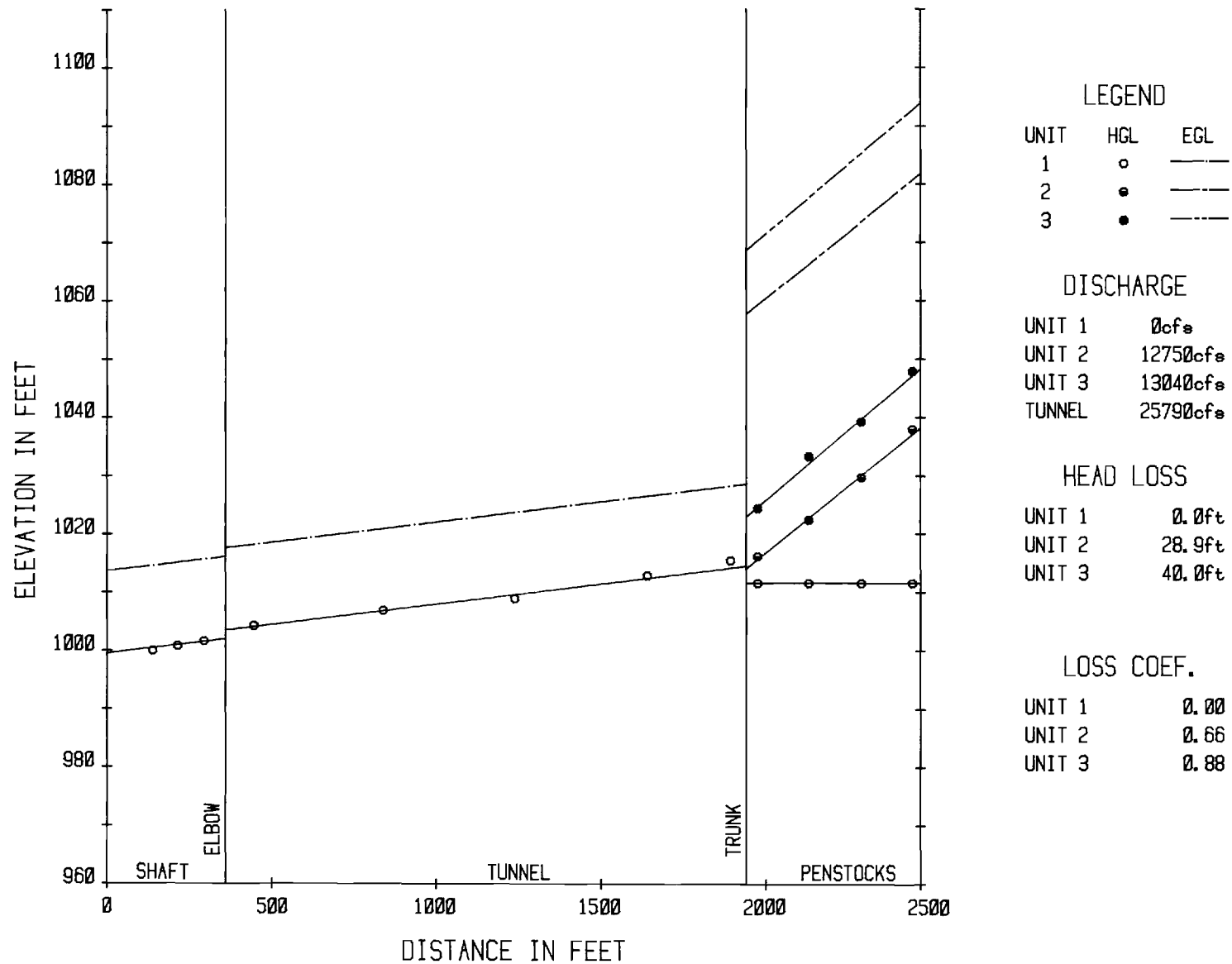


Exhibit 53. Hydraulic and Energy Grade Lines in Scheme C-1 for Units 2 and 3 Pumping.

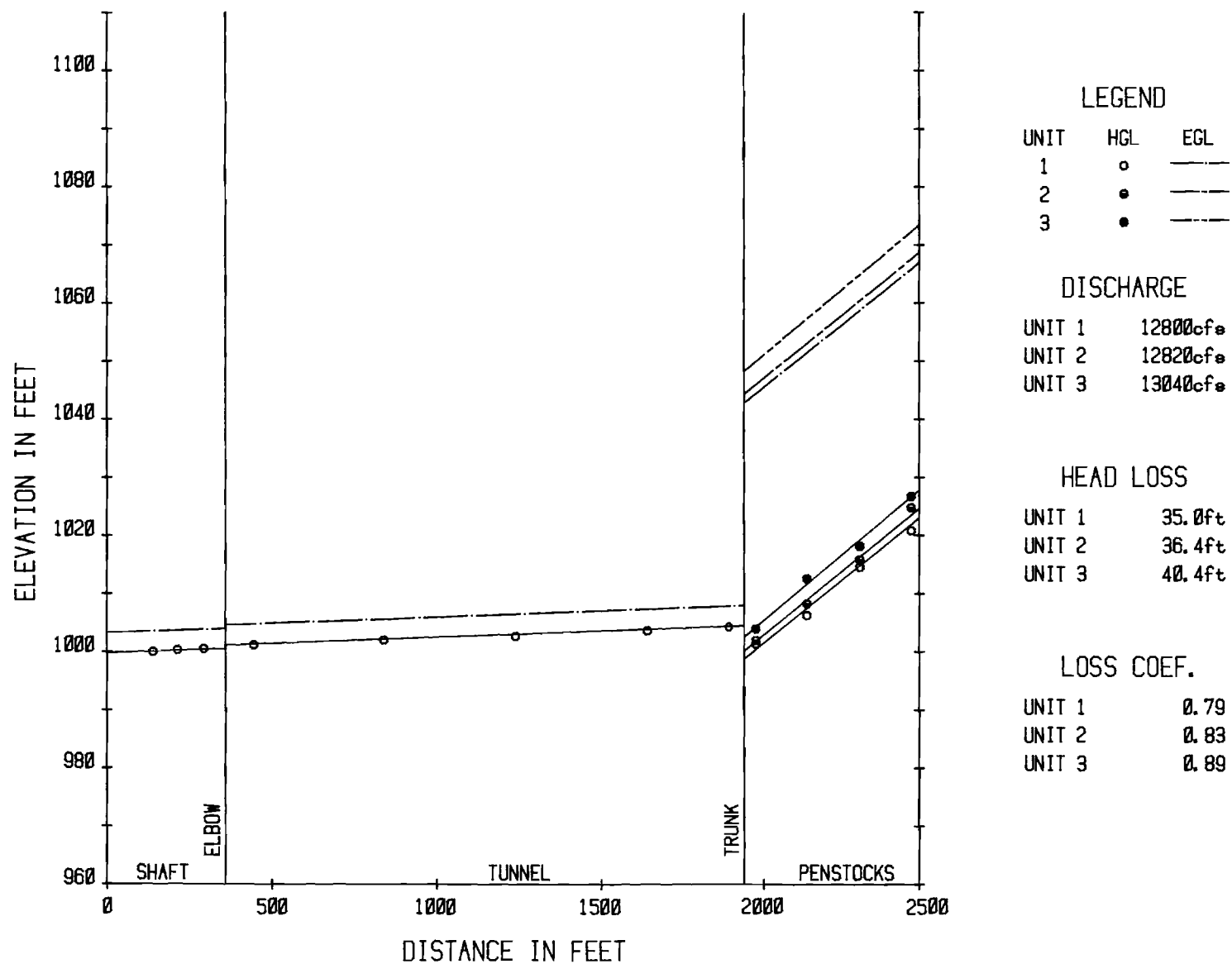


Exhibit 54. Hydraulic and Energy Grade Lines in Scheme C-1 for Single Unit Pumping.

TABLE 8
SUMMARY OF
ACTUAL LOSS COEFFICIENTS
FOR C-1 SCHEME

<u>MODE</u>	K_{L1} (<u>UNIT 1</u>)	K_{L2} (<u>UNIT 2</u>)	K_{L3} (<u>UNIT 3</u>)
Three Units Generating	0.80	0.49	0.18
Units 1 and 2 Generating	0.69	0.39	-
Units 1 and 3 Generating	0.69	-	0.25
Units 2 and 2 Generating	-	0.90	0.25
Single Unit Generating	0.63	0.57	0.59
Three Units Pumping	0.58	0.69	0.71
Units 1 and 2 Pumping	0.73	0.83	-
Units 1 and 3 Pumping	0.60	-	0.70
Units 2 and 3 Pumping	-	0.60	0.76
Single Unit Pumping	0.79	0.77	0.77

TABLE 9
SUMMARY OF
RELATIVE LOSS COEFFICIENTS
FOR C-1 SCHEME

<u>MODE</u>	K_{R_1} (<u>UNIT 1</u>)	K_{R_2} (<u>UNIT 2</u>)	K_{R_3} (<u>UNIT 3</u>)
Three Units Generating	0.80	0.55	0.30
Units 1 and 2 Generating	0.69	0.45	-
Units 1 and 3 Generating	0.69	-	0.37
Units 2 and 3 Generating	-	0.96	0.37
Single Unit Generating	0.63	0.63	0.71
Three Units Pumping	0.58	0.75	0.83
Units 1 and 2 Pumping	0.73	0.89	-
Units 1 and 3 Pumping	0.60	-	0.82
Units 2 and 3 Pumping	-	0.66	0.88
Single Unit Pumping	0.79	0.83	0.89



Exhibit 55. View of Tuft Pattern in Trunk of Scheme C-1 for Three Units Generating.



Exhibit 56. View of Tuft Pattern in Trunk of Scheme C-1 for Three Units Pumping.



Exhibit 57. View of Tuft Pattern in Trunk of Scheme C-1 for Unit 3 Pumping.

CHAPTER VI

TEST RESULTS FOR SCHEME A-1

As shown by Exhibit 1 the final scheme tested, Scheme A-1, differed by the absence of the elbow at the transition from the tunnel to the trunk, as well as the manner of bifurcating from trunk to penstocks. This scheme was also tested for the fourteen cases listed in Table 1. In an attempt to prevent structural failure of the model, the trunk was reinforced by bands prior to installation. This modification has an adverse effect on documentation of flow patterns because of the light scattering effect of the structural bands.

Head-Loss Data

Using the piezometer locations indicated on Exhibit 6, the hydraulic grade lines of all fourteen test cases are plotted on Exhibits 58-67. As with Schemes B-1 and B-2 the head loss coefficients listed on the exhibits are actual ones, not relative. Tables 10 and 11 are included to summarize the actual and relative loss coefficients for Scheme A-1, respectively. The results will be compared with the other three schemes in the next chapter.

Flow Patterns in Bifurcation Model

Exhibits 68-74 show that the flow pattern in the generating mode of operation is fairly smooth. Dead zones apparently only occur in the penstocks of the units that are not operating.

Because of the relatively gradual transition in the deceleration regions between penstock and trunk the flow pattern for three units pumping shows an improvement over Schemes B-1 and B-2, especially in the case of Scheme B-1. Exhibits 76-78 illustrate the flow patterns in the

trunk for the three respective combinations of two units pumping. For single unit operation Exhibits 79-81 show that the flow is highly turbulent in the trunk because of the sudden deceleration. There is no marked improvement of Scheme A-1 over Schemes B-1 and B-2 for single unit pumping except in the case of Unit 3.

Pressure Distribution in Trunk

The locations of the eight piezometer taps used to measure the pressure distribution in the trunk of Scheme A-1 are depicted on Exhibit 9. The results in prototype units referenced to the 1000 ft value assigned to piezometer number 0 are listed in Table 12. Values for piezometer number 4 are not reported because it was discovered that it malfunctioned during the testing. The differences in pressure through the trunk are generally smaller for Scheme A-1 than for Schemes B-1 and B-2 because of better flow patterns.

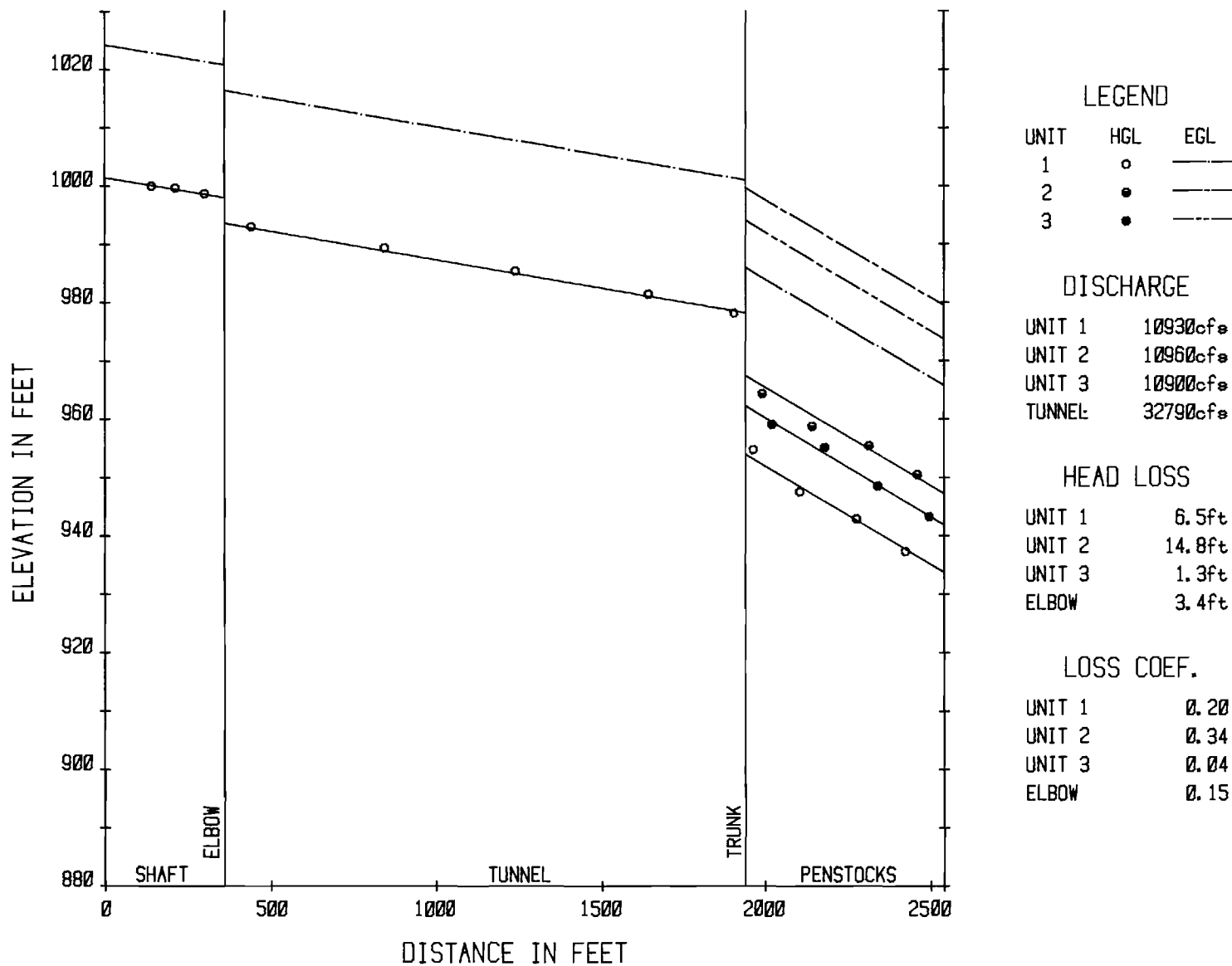


Exhibit 58. Hydraulic and Energy Grade Lines in Scheme A-1 for Three Units Generating.

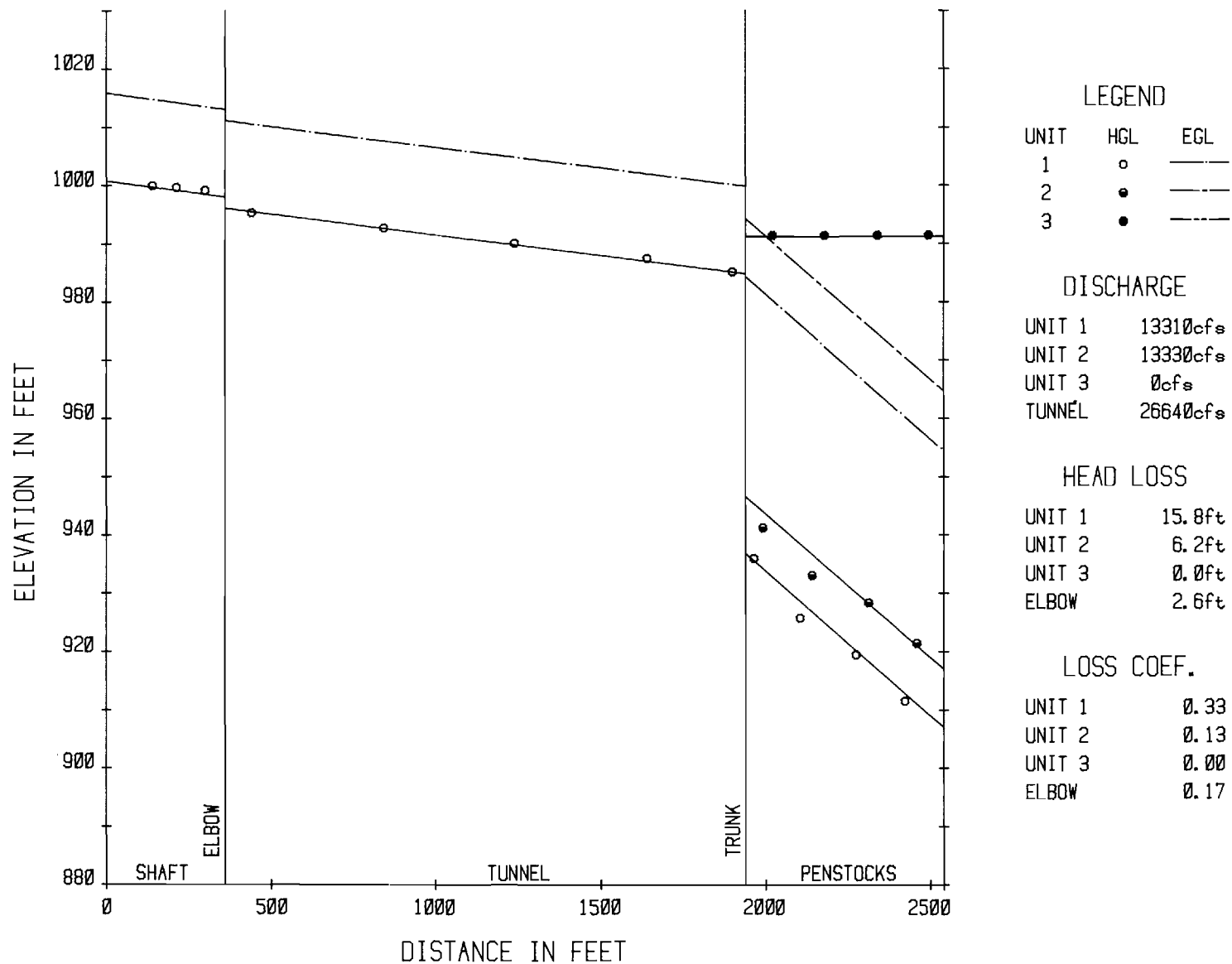


Exhibit 59. Hydraulic and Energy Grade Lines in Scheme A-1 for Units 1 and 2 Generating.

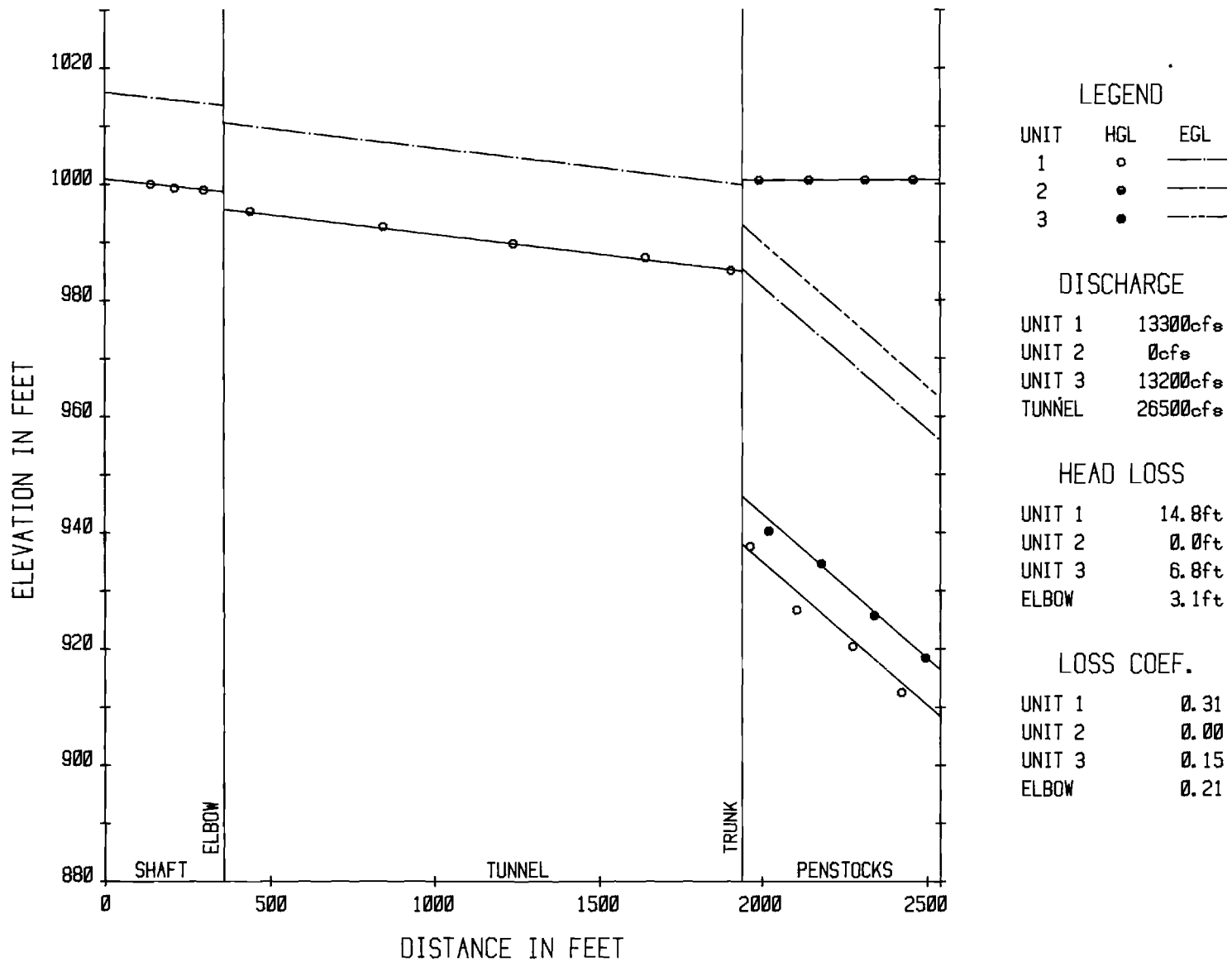


Exhibit 60. Hydraulic and Energy Grade Lines in Scheme A-1 for Units 1 and 3 Generating.

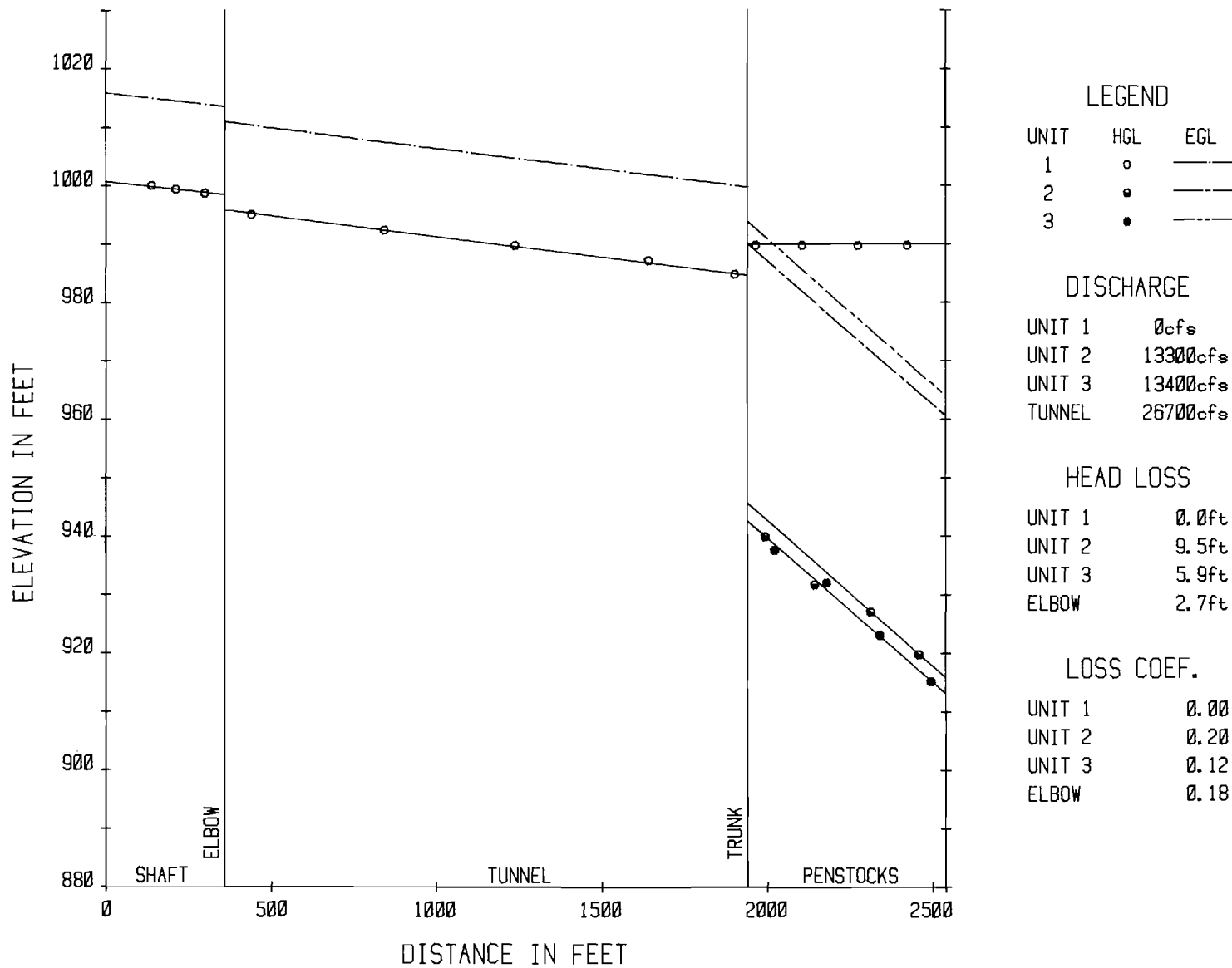


Exhibit 61. Hydraulic and Energy Grade Lines in Scheme A-1 for Units 2 and 3 Generating.

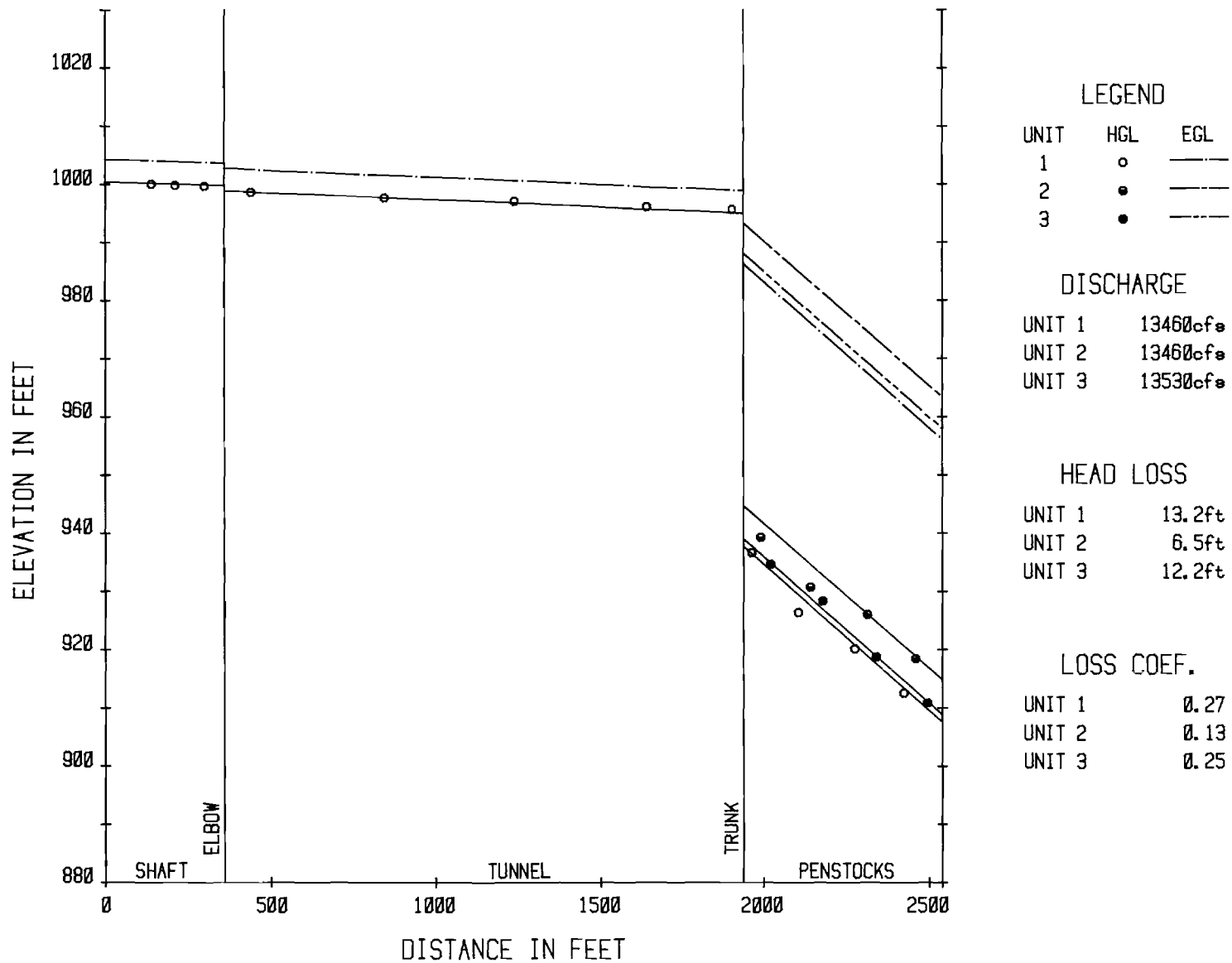


Exhibit 62. Hydraulic and Energy Grade Lines in Scheme A-1 for Single Unit Generating.

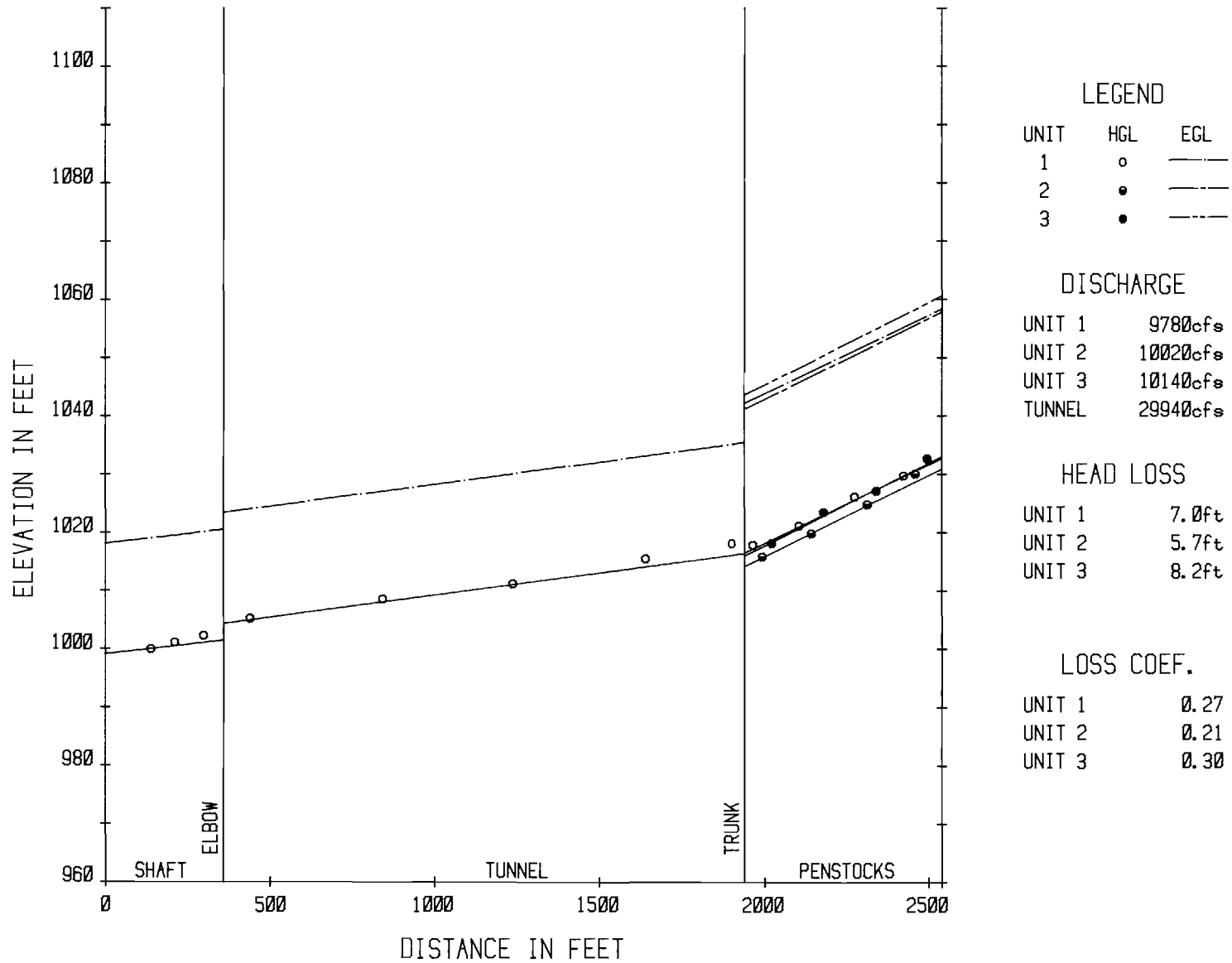


Exhibit 63. Hydraulic and Energy Grade Lines in Scheme A-1 for Three Units Pumping.

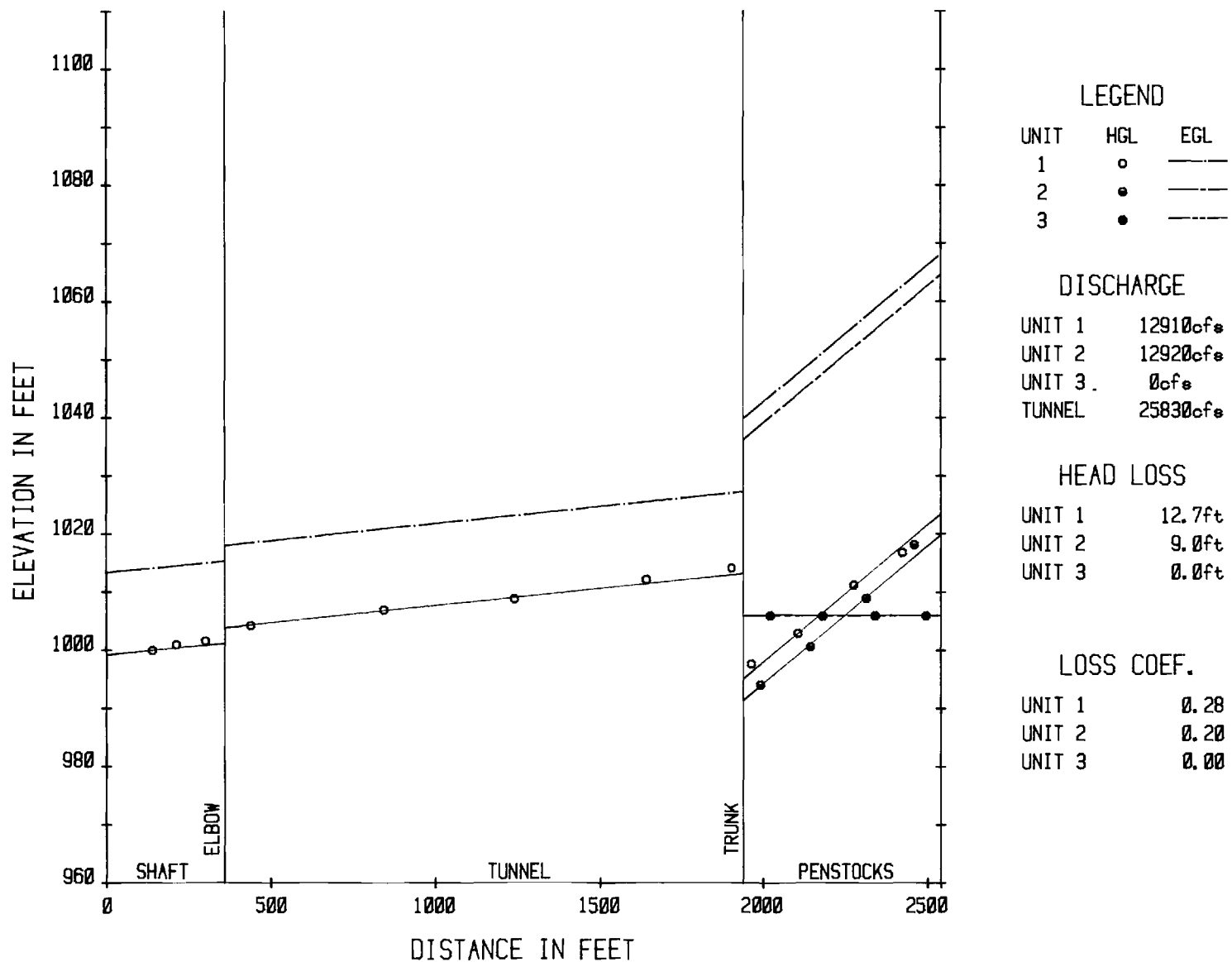


Exhibit 64. Hydraulic and Energy Grade Lines in Scheme A-1 for Units 1 and 2 Pumping.

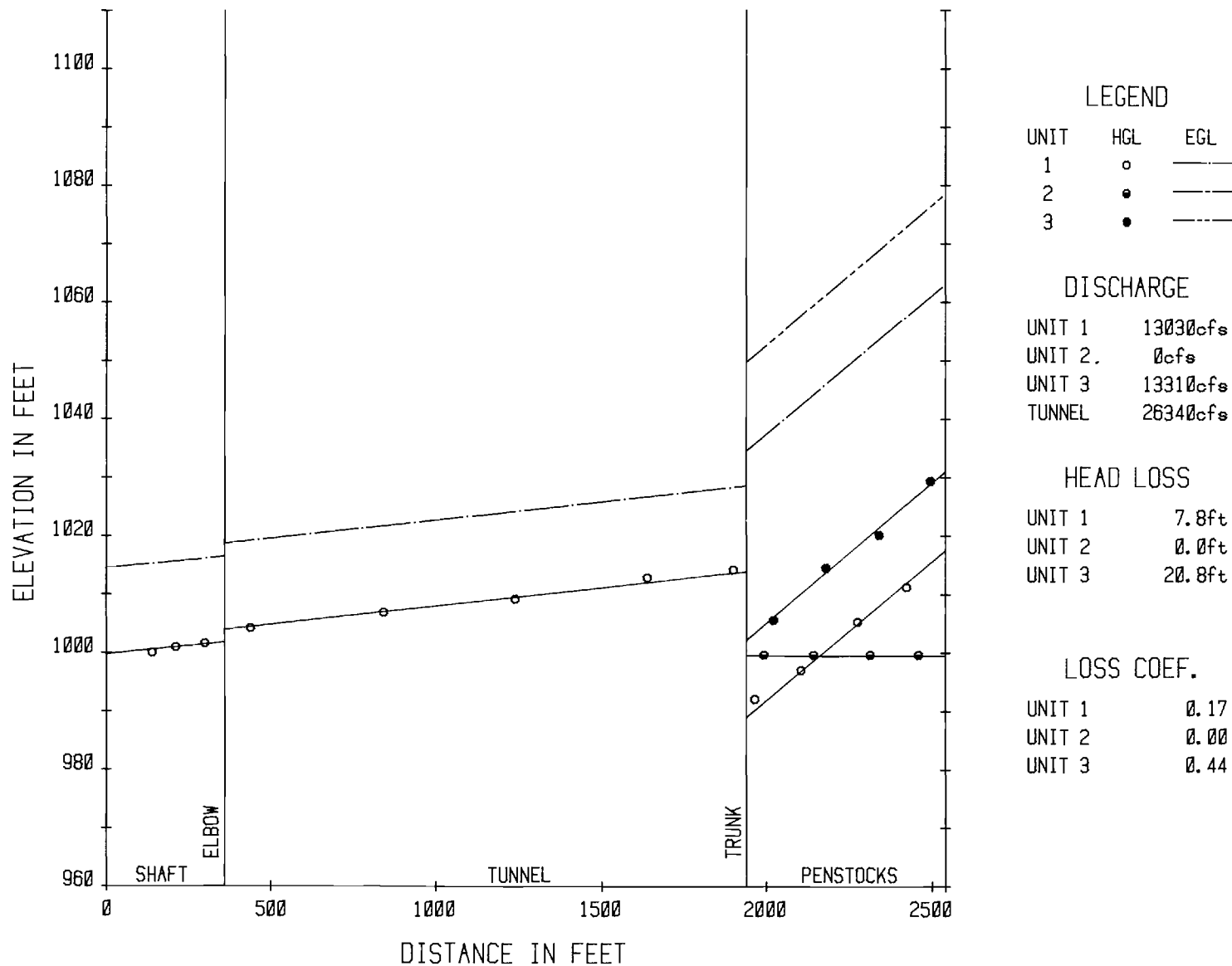


Exhibit 65. Hydraulic and Energy Grade Lines in Scheme A-1 for Units 1 and 3 Pumping.

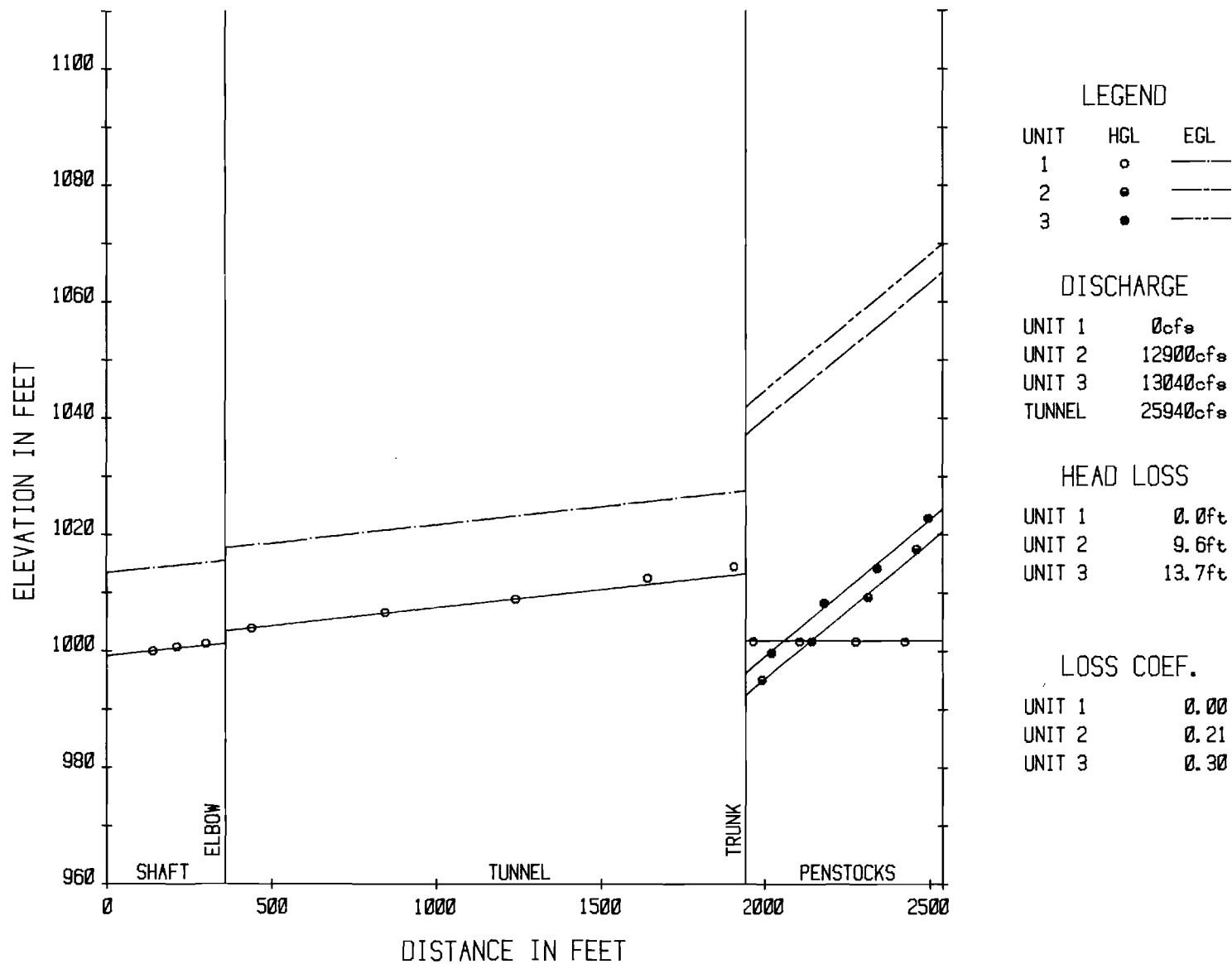


Exhibit 66. Hydraulic and Energy Grade Lines in Scheme A-1 for Units 2 and 3 Pumping.

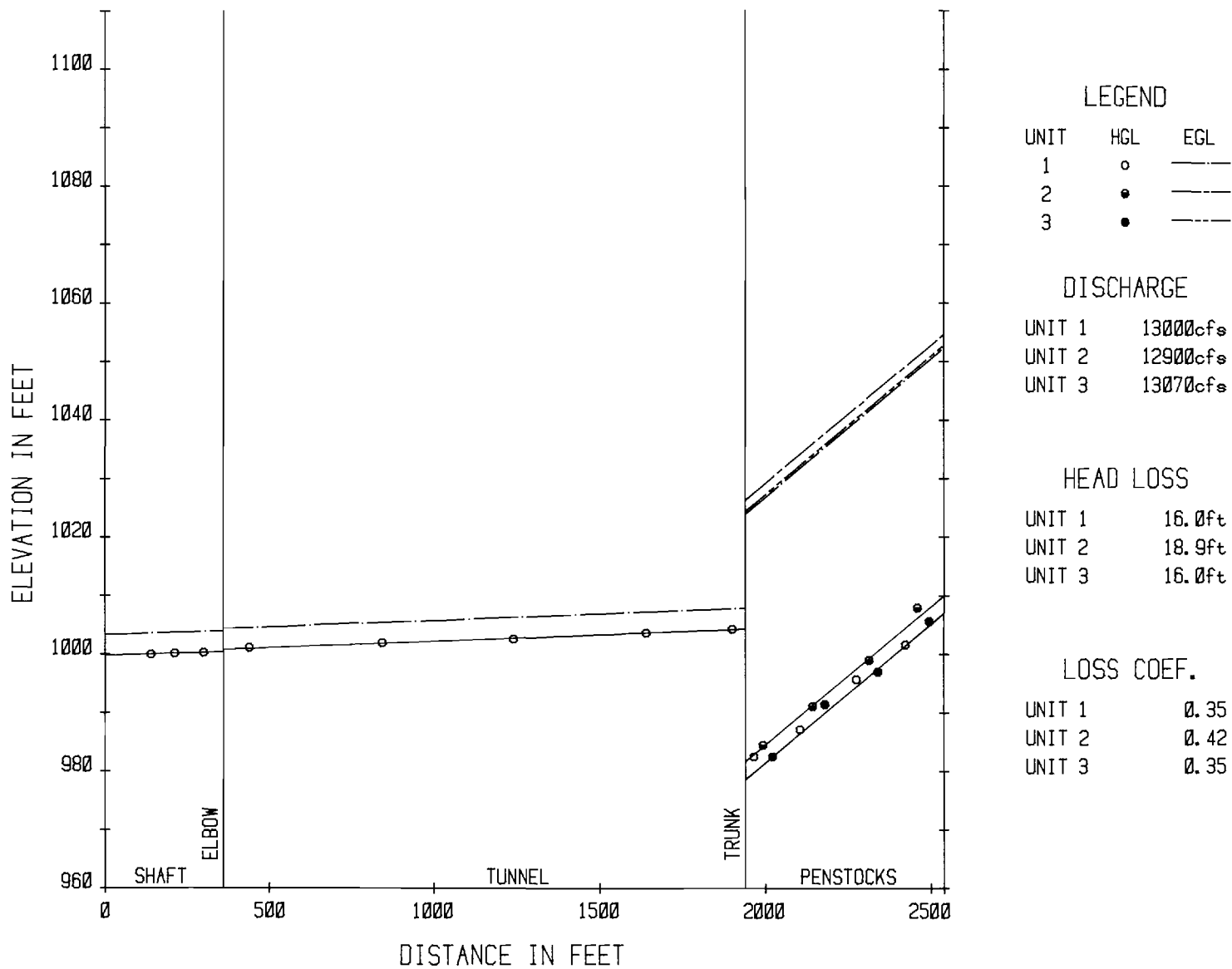


Exhibit 67. Hydraulic and Energy Grade Lines in Scheme A-1 for Single Unit Pumping.

TABLE 10
SUMMARY OF ACTUAL LOSS COEFFICIENTS
FOR A-1 SCHEME

<u>MODE</u>	K_{L_1} (<u>UNIT 1</u>)	K_{L_2} (<u>UNIT 2</u>)	K_{L_3} (<u>UNIT 3</u>)
Three Units Generating	0.20	0.34	0.04
Units 1 and 2 Generating	0.33	0.13	--
Units 1 and 3 Generating	0.31	--	0.15
Units 2 and 3 Generating	--	0.20	0.12
Single Unit Generating	0.27	0.13	0.25
Three Units Pumping	0.27	0.21	0.30
Units 1 and 2 Pumping	0.28	0.20	--
Units 1 and 3 Pumping	0.17	--	0.44
Units 2 and 3 Pumping	--	0.21	0.30
Single Unit Pumping	0.35	0.42	0.35

TABLE 11
SUMMARY OF
RELATIVE LOSS COEFFICIENTS
FOR A-1 SCHEME

<u>MODE</u>	K_{R_1} (<u>UNIT 1</u>)	K_{R_2} (<u>UNIT 2</u>)	K_{R_3} (<u>UNIT 3</u>)
Three Units Generating	0.20	0.36	0.11
Units 1 and 2 Generating	0.33	0.15	--
Units 1 and 3 Generating	0.31	--	0.22
Units 2 and 3 Generating	--	0.22	0.19
Single Unit Generating	0.27	0.15	0.32
Three Units Pumping	0.27	0.23	0.37
Units 1 and 2 Pumping	0.28	0.22	--
Units 1 and 3 Pumping	0.17	--	0.51
Units 2 and 3 Pumping	--	0.23	0.37
Single Unit Pumping	0.35	0.44	0.42

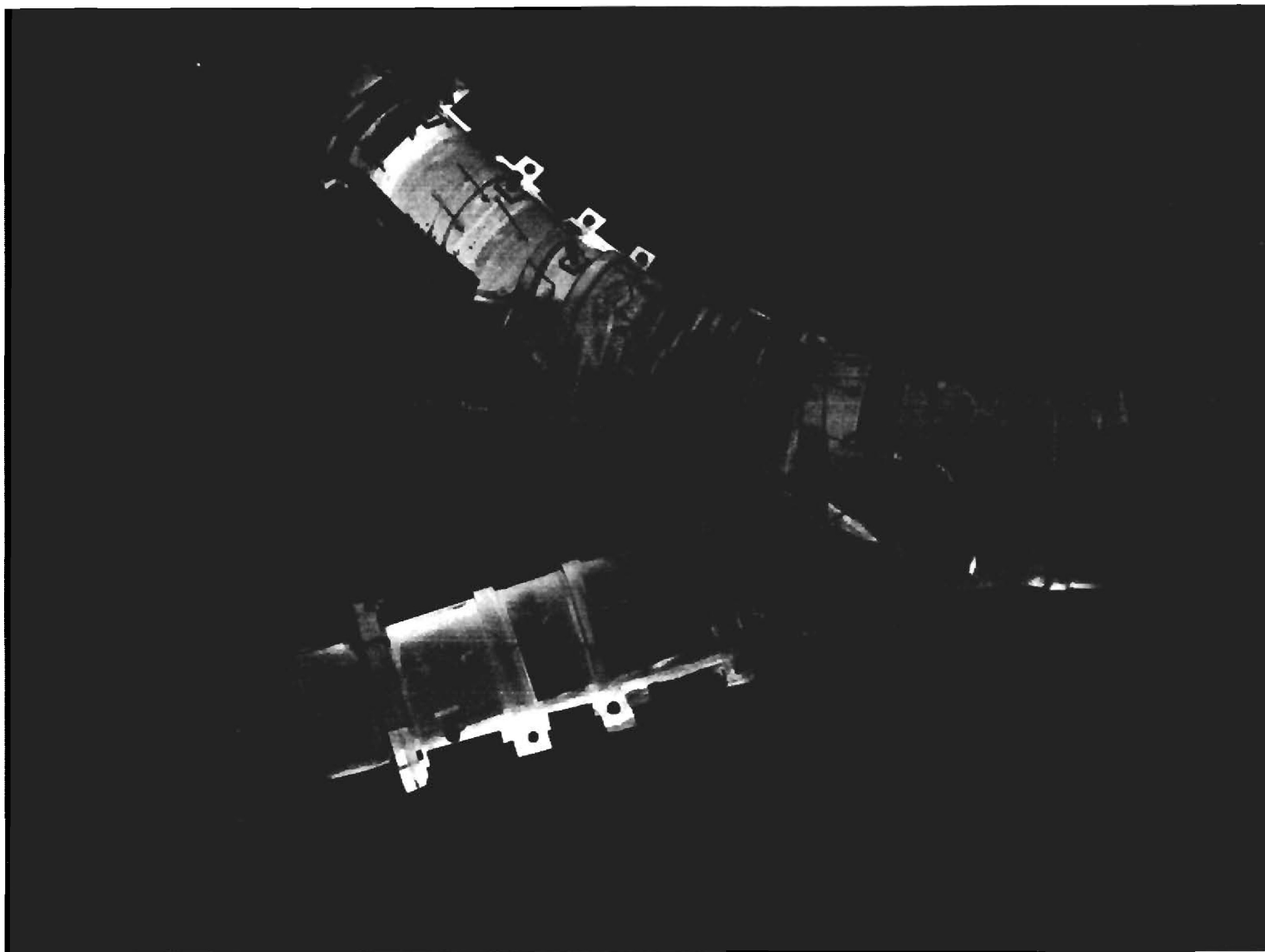


Exhibit 68. View of Tuft Pattern in Trunk of Scheme A-1 for Three Units Generating.

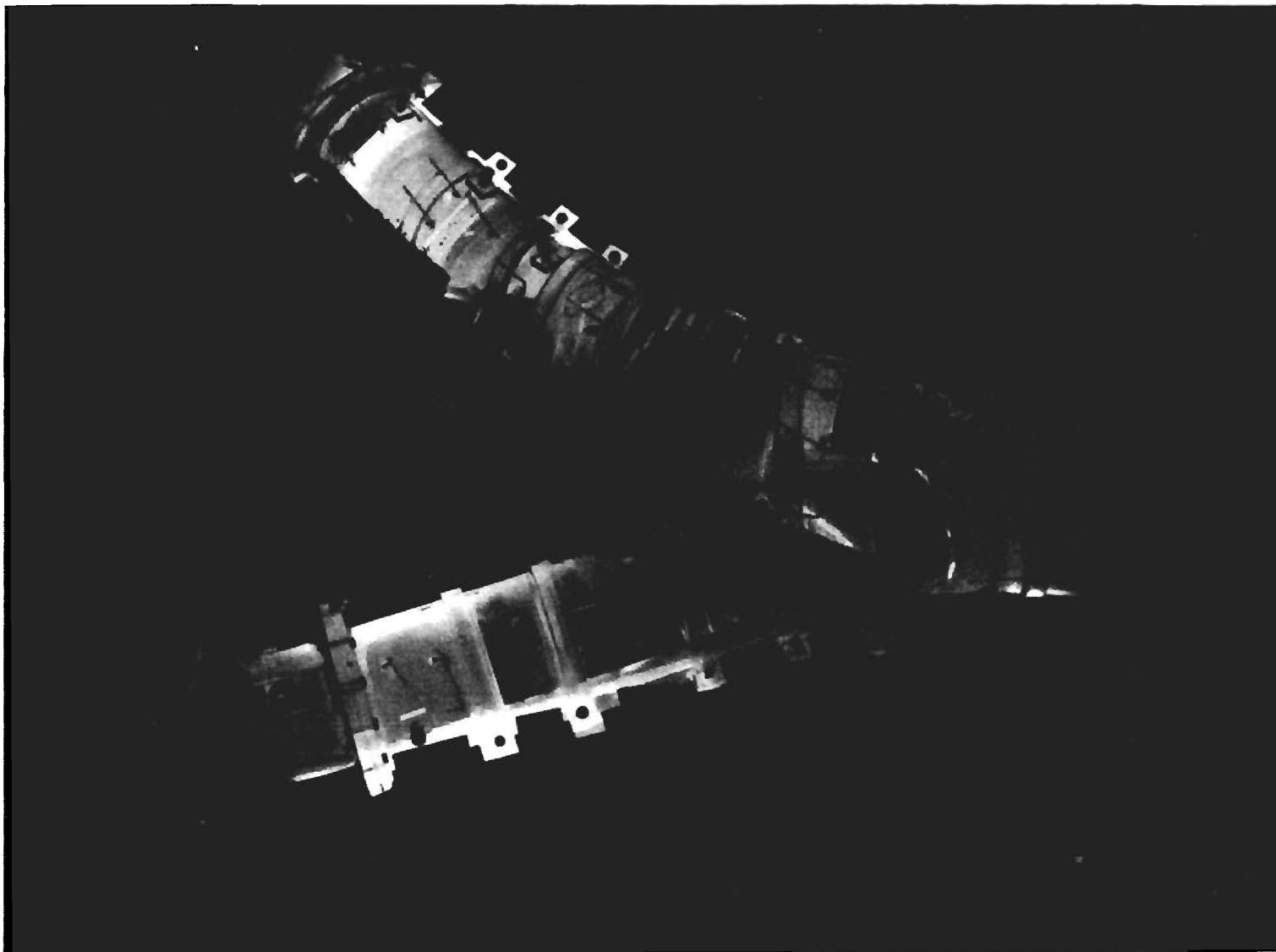


Exhibit 69. View of Tuft Pattern in Trunk of Scheme A-1 for Units 1 and 2 Generating.

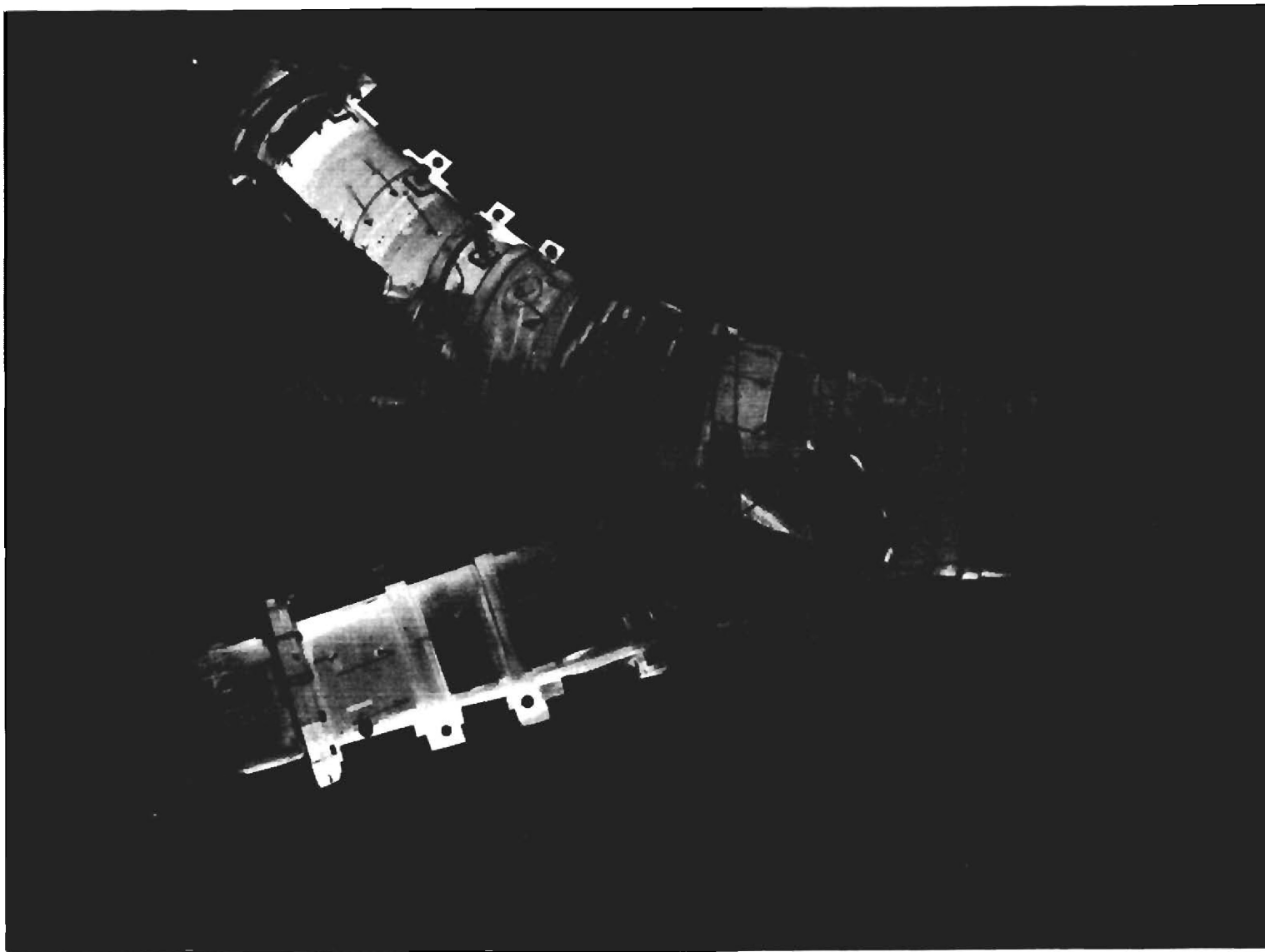


Exhibit 70. View of Tuft Pattern in Trunk of Scheme A-1 for Units 1 and 3 Generating.

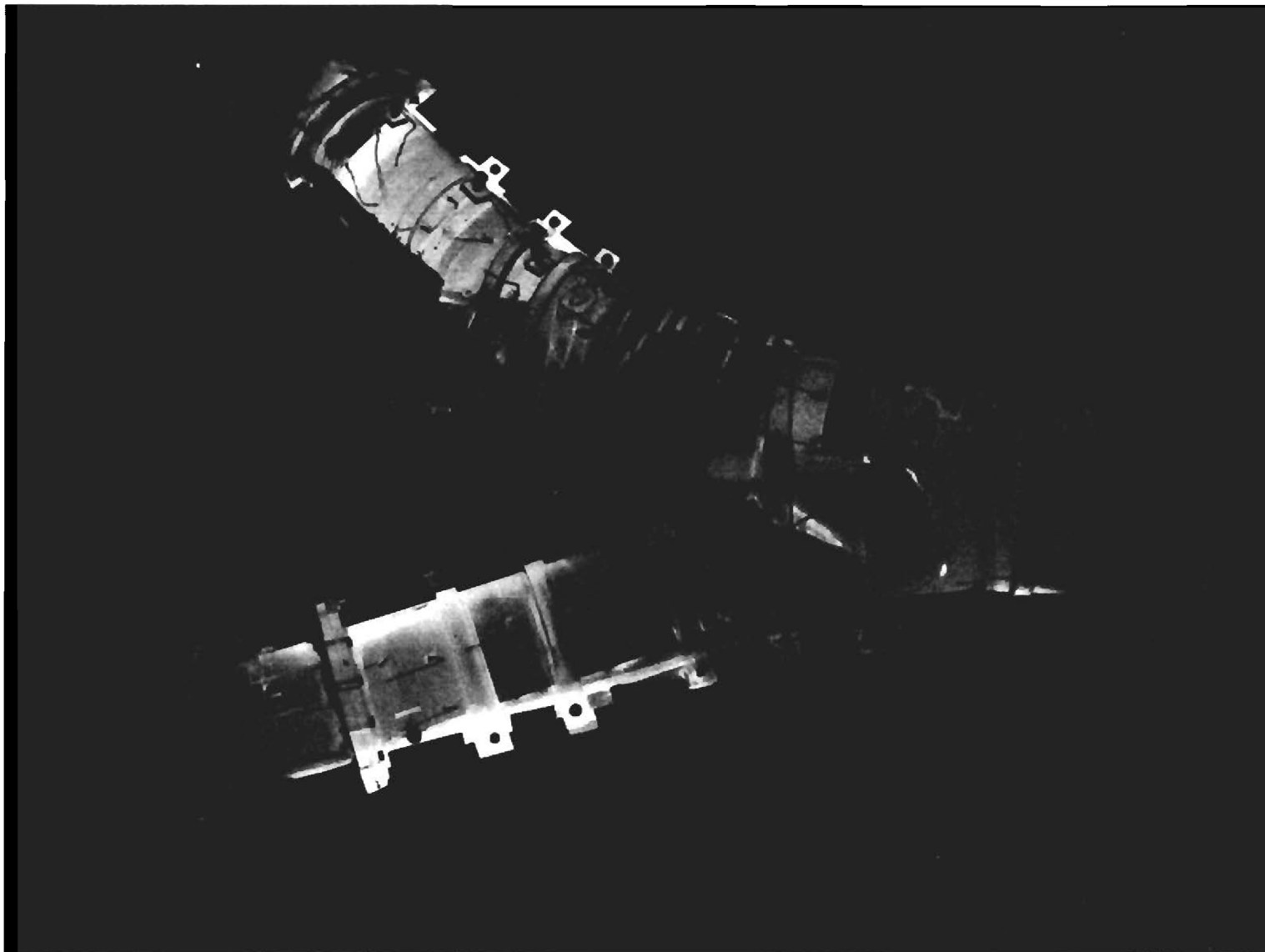


Exhibit 71. View of Tuft Pattern in Trunk of Scheme A-1 for Units 2 and 3 Generating.

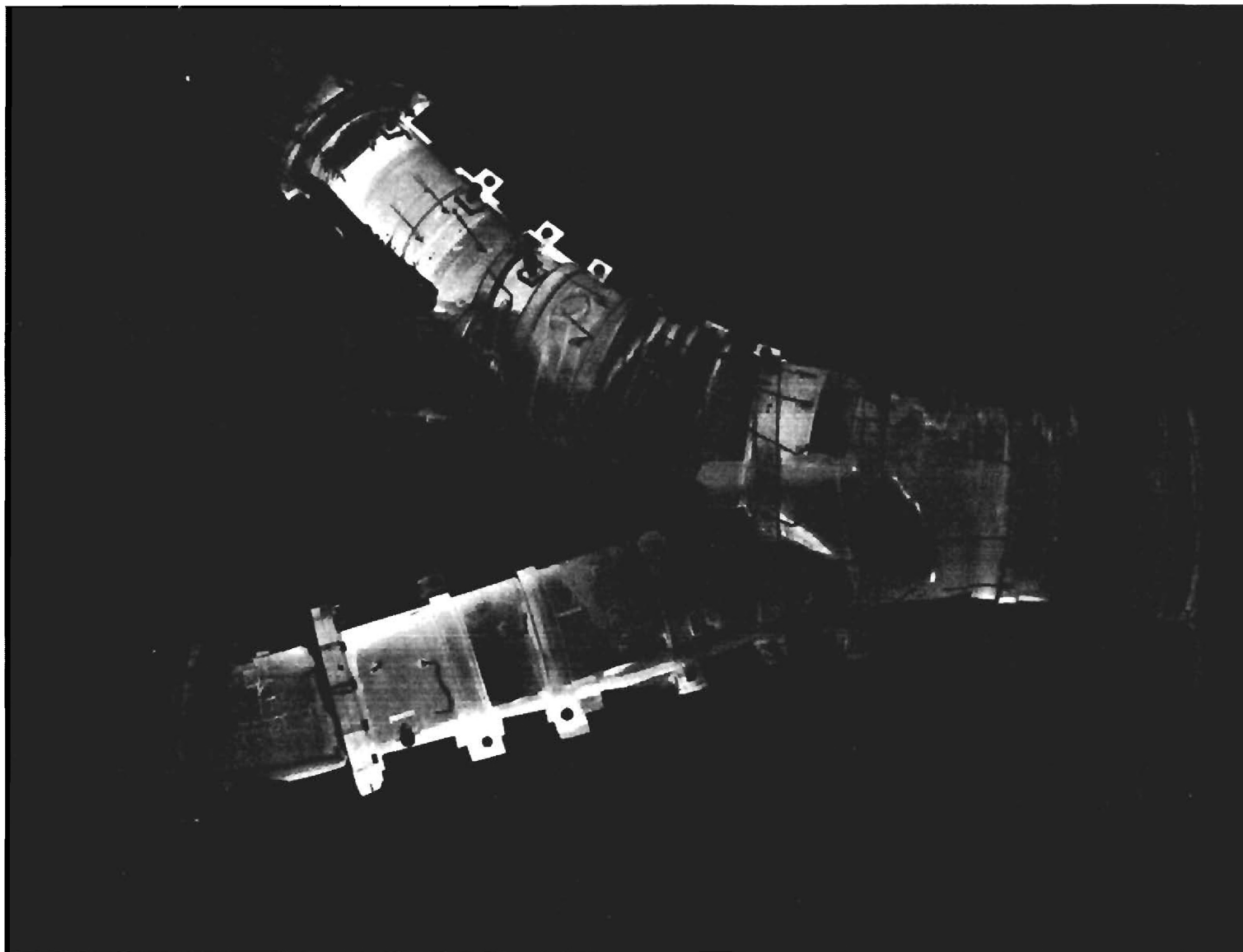


Exhibit 72. View of Tuft Pattern in Trunk of Scheme A-1 for Unit 1 Generating.

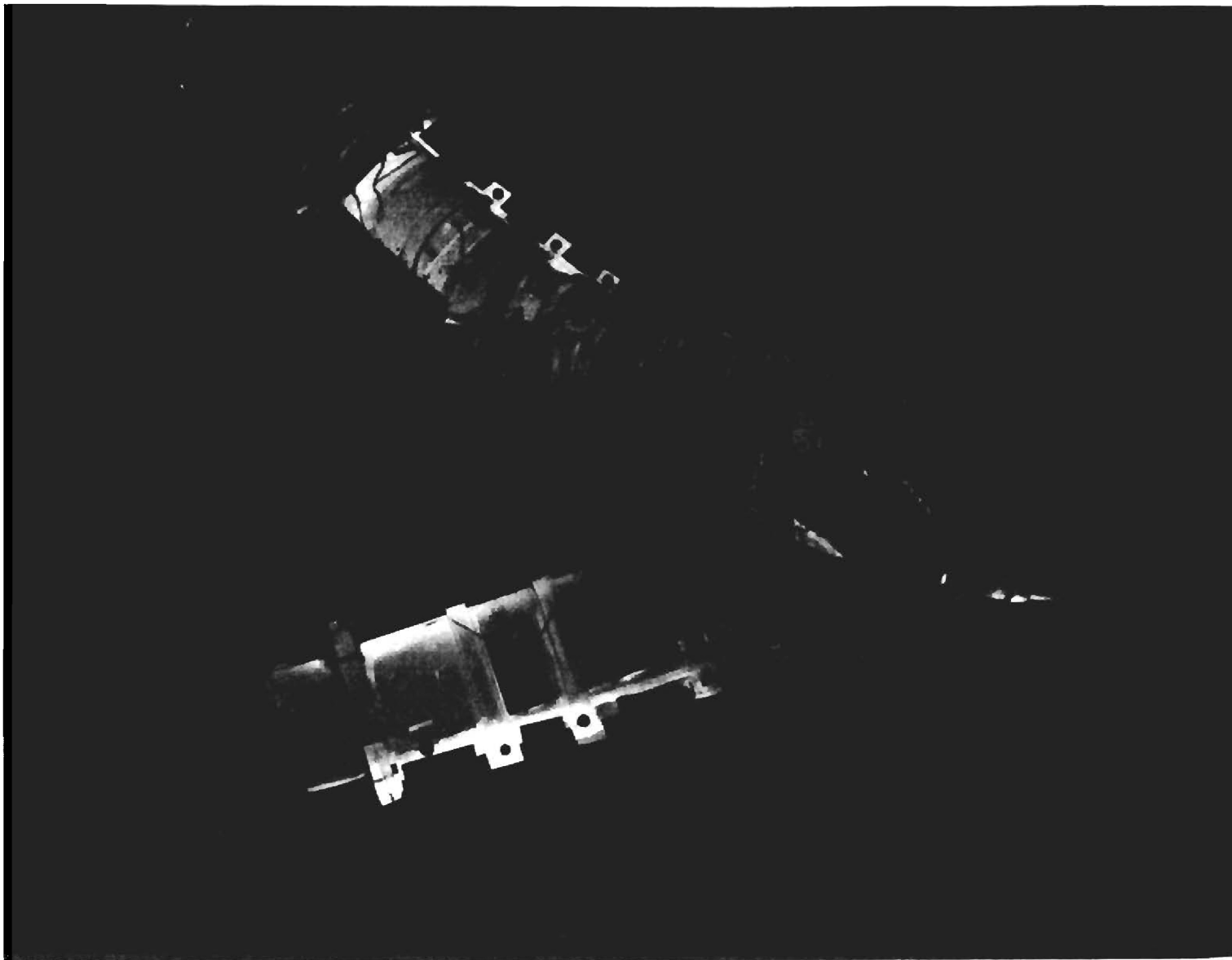


Exhibit 73. View of Tuft Pattern in Trunk of Scheme A-1 for
Unit 2 Generating.

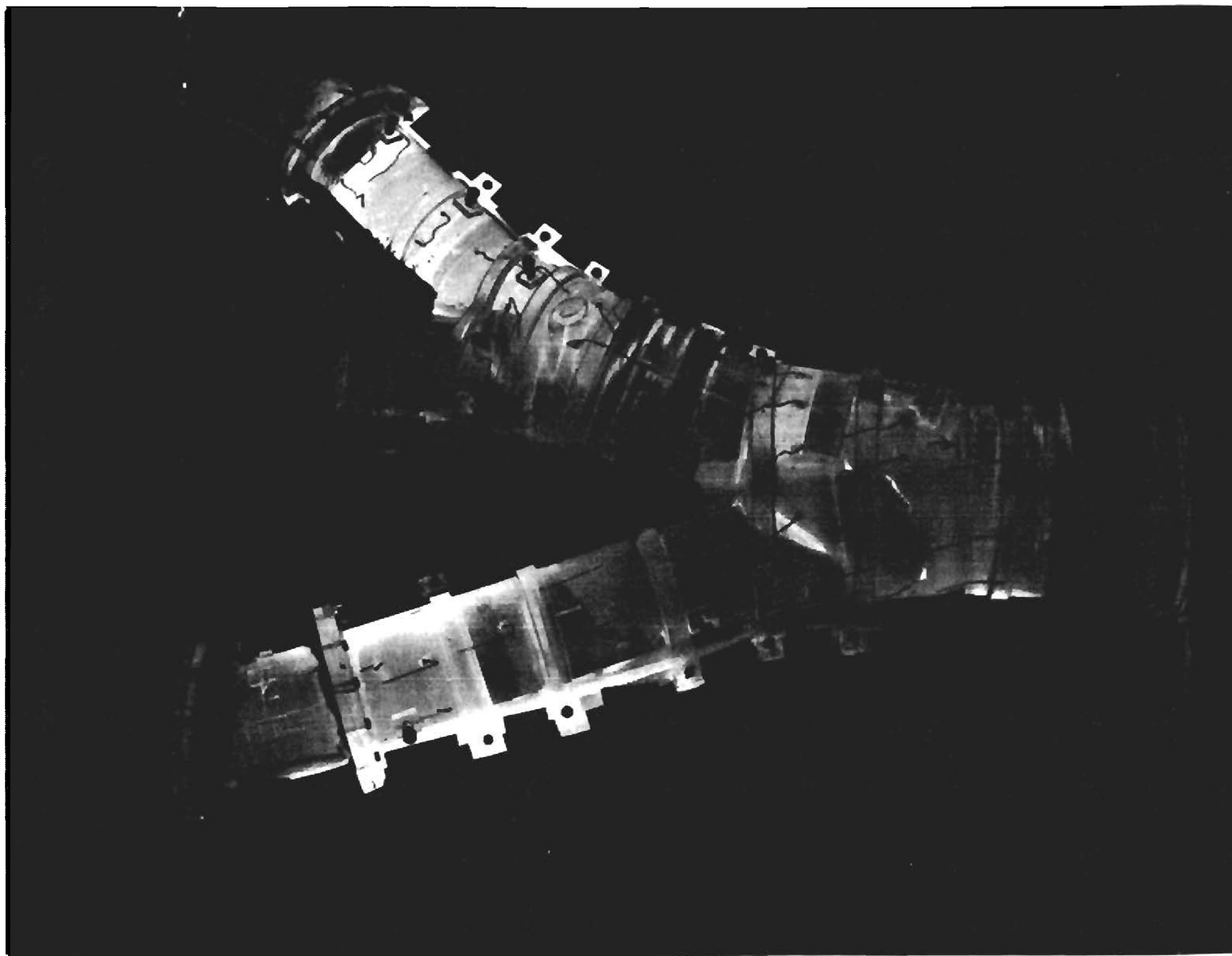


Exhibit 74. View of Tuft Pattern in Trunk of Scheme A-1 for Unit 3 Generating.

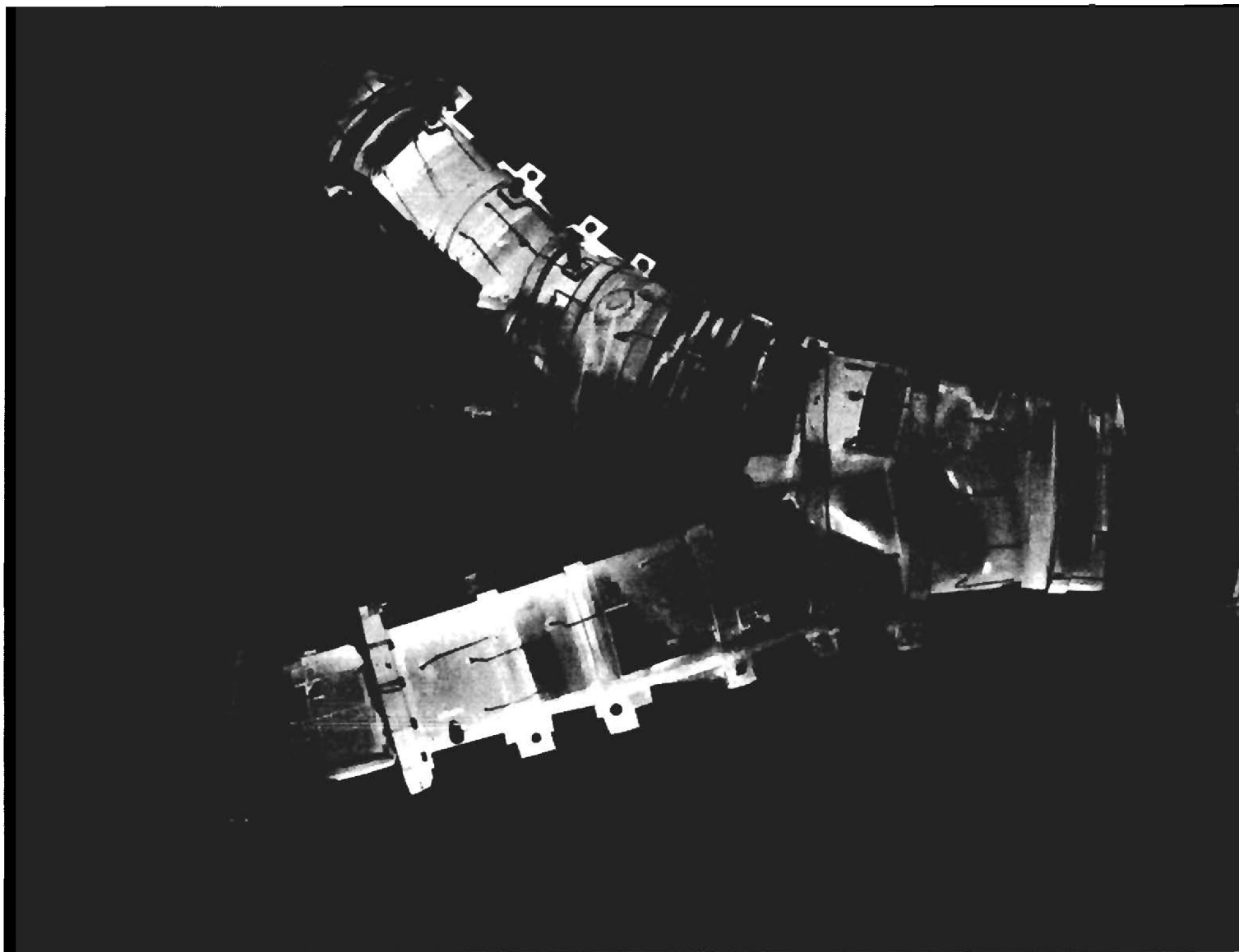


Exhibit 75. View of Tuft Pattern in Trunk of Scheme A-1 for Three Units Pumping.

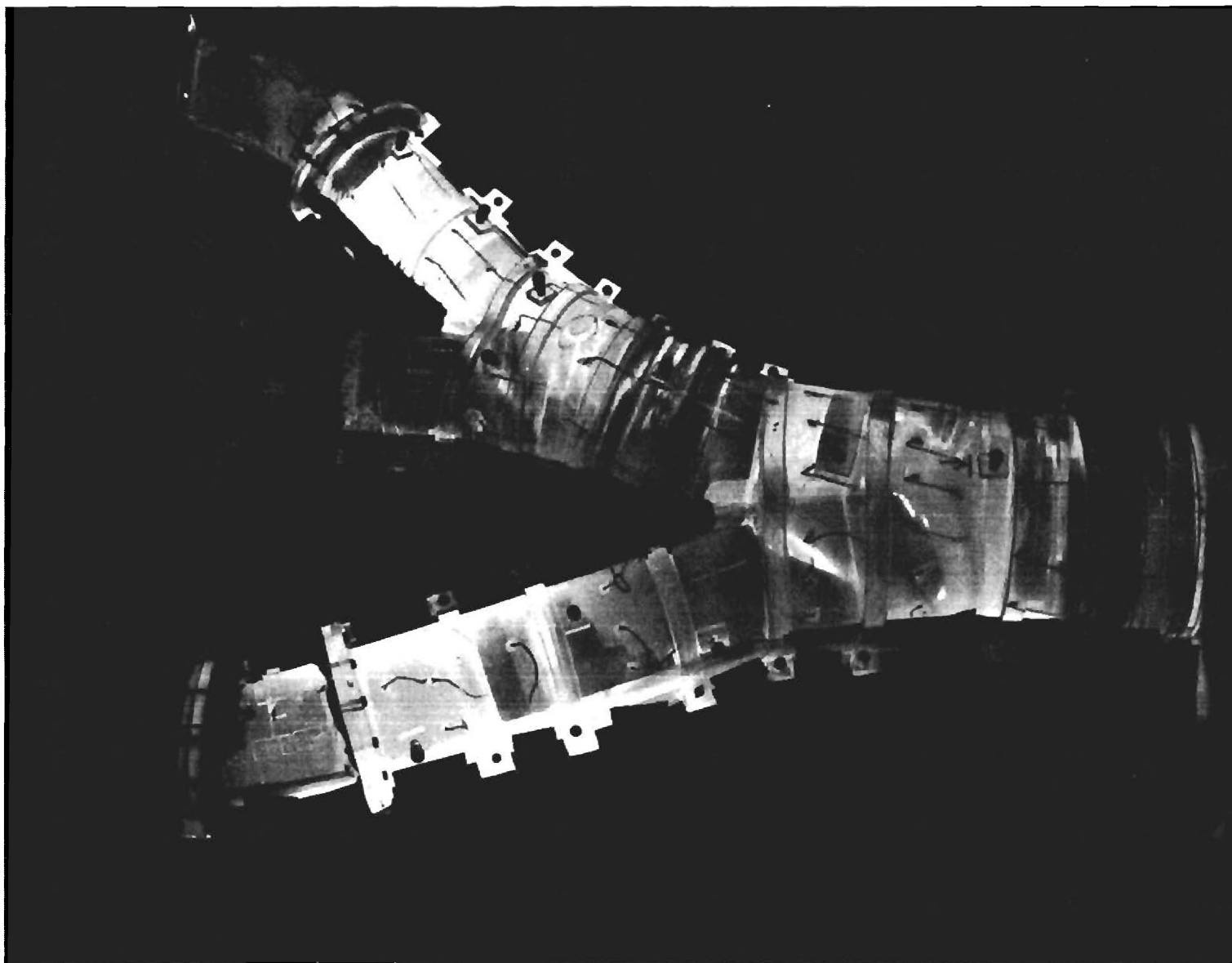


Exhibit 76. View of Tuft Pattern in Trunk of Scheme A-1 for Units 1 and 2 Pumping.

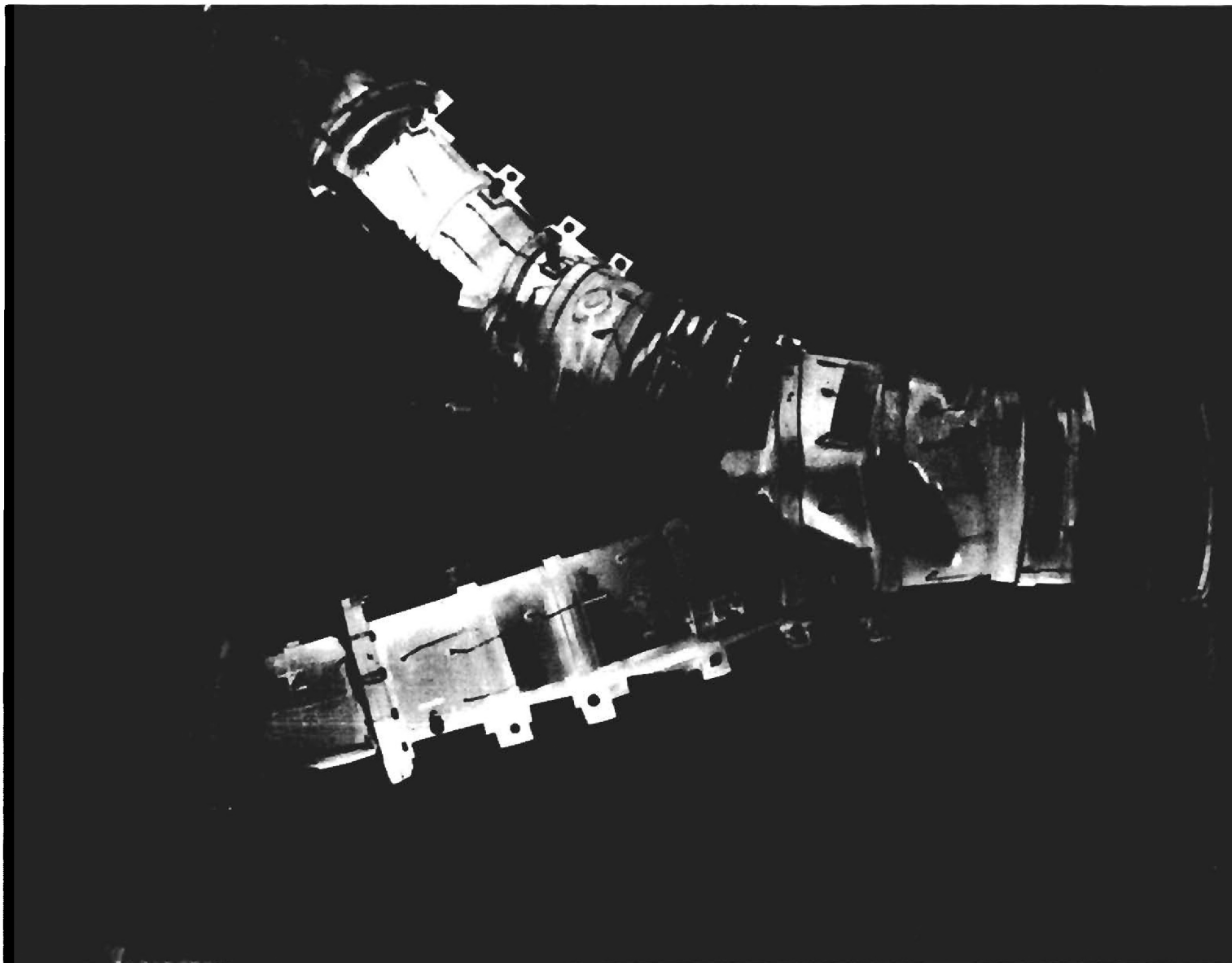


Exhibit 77. View of Tuft Pattern in Trunk of Scheme A-1 for Units 1 and 3 Pumping.

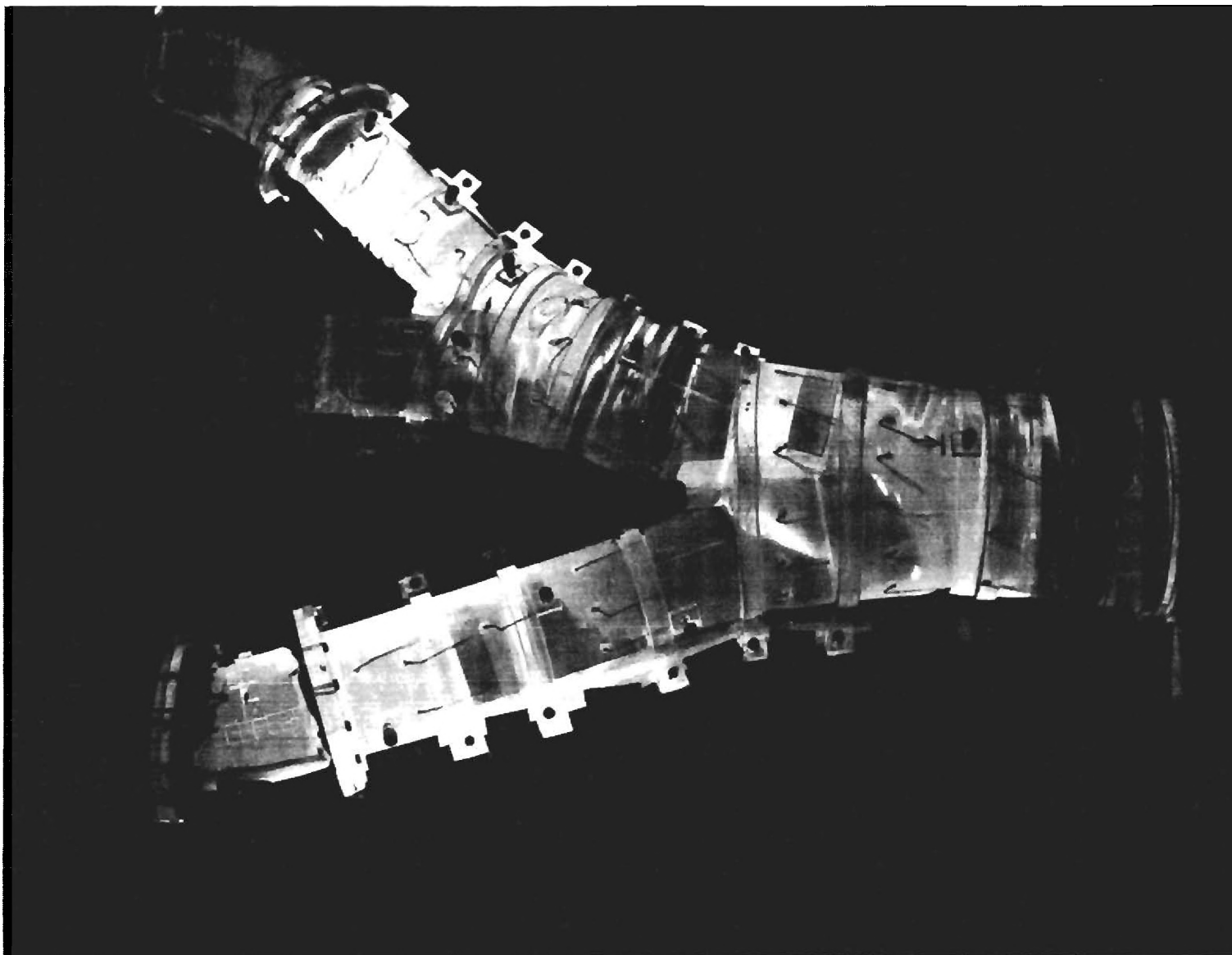


Exhibit 78. View of Tuft Pattern in Trunk of Scheme A-1 for Units 2 and 3 Pumping.

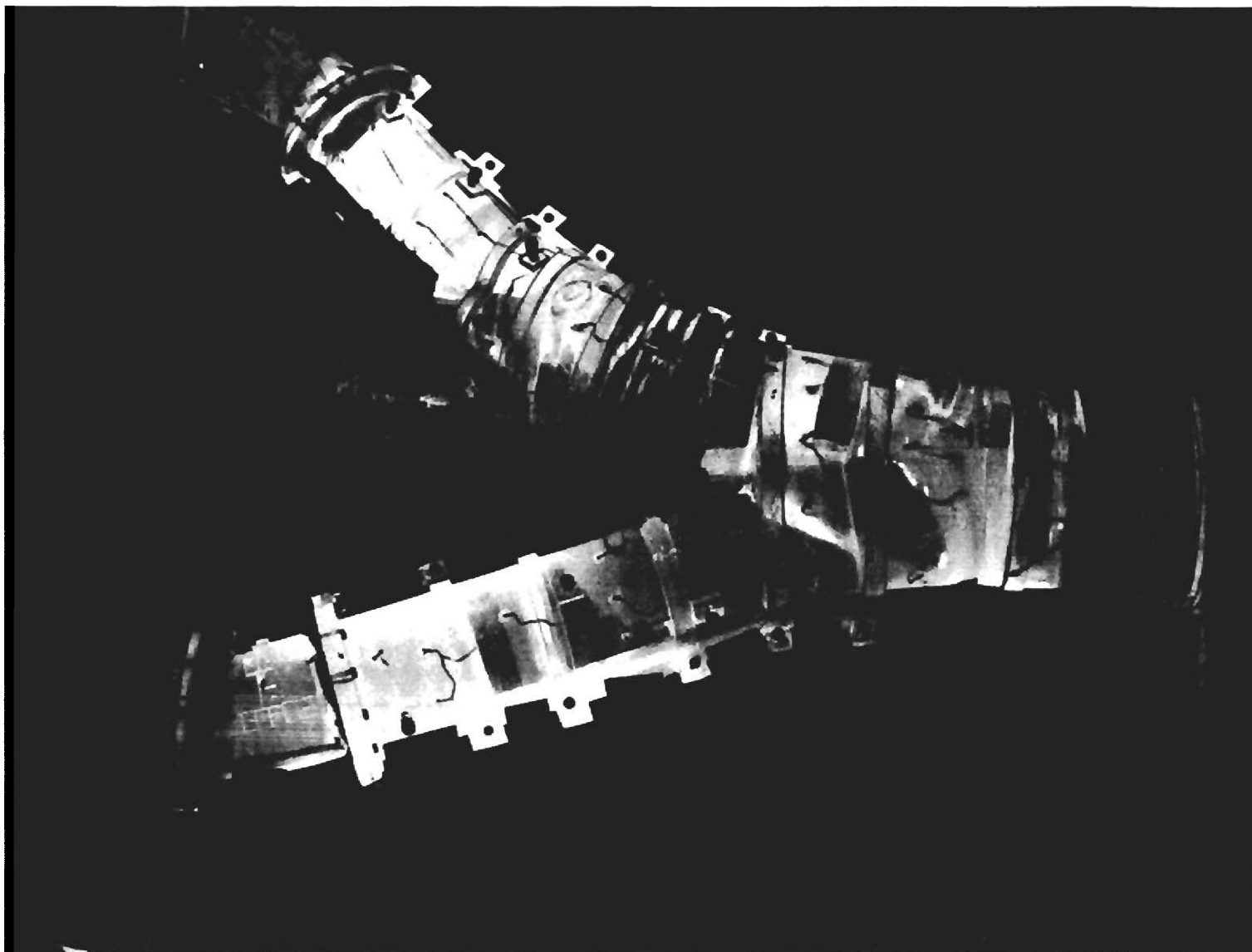


Exhibit 79. View of Tuft Pattern in Trunk of Scheme A-1 for Unit 1 Pumping.

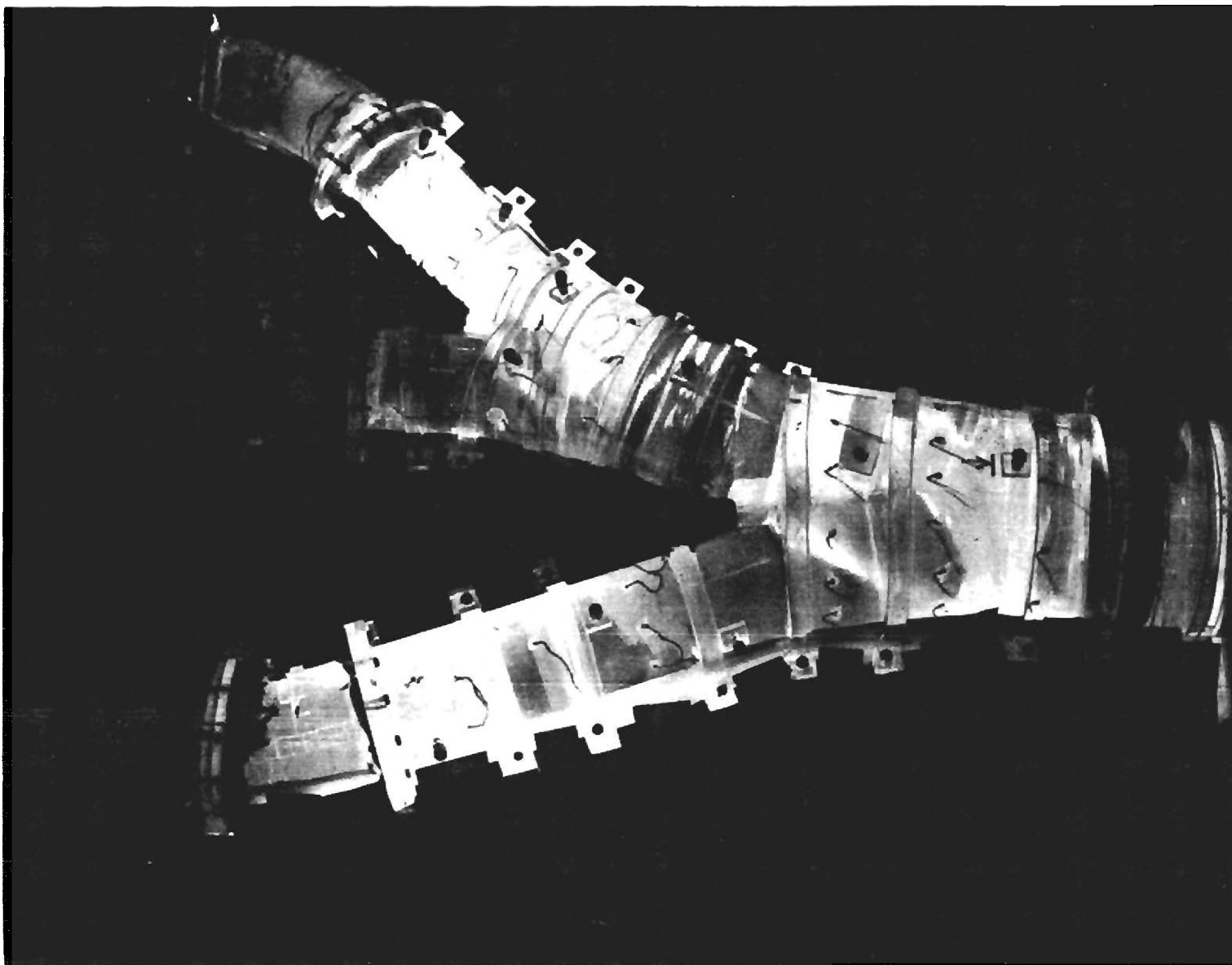


Exhibit 80. View of Tuft Pattern in Trunk of Scheme A-1 for Unit 2 Pumping.

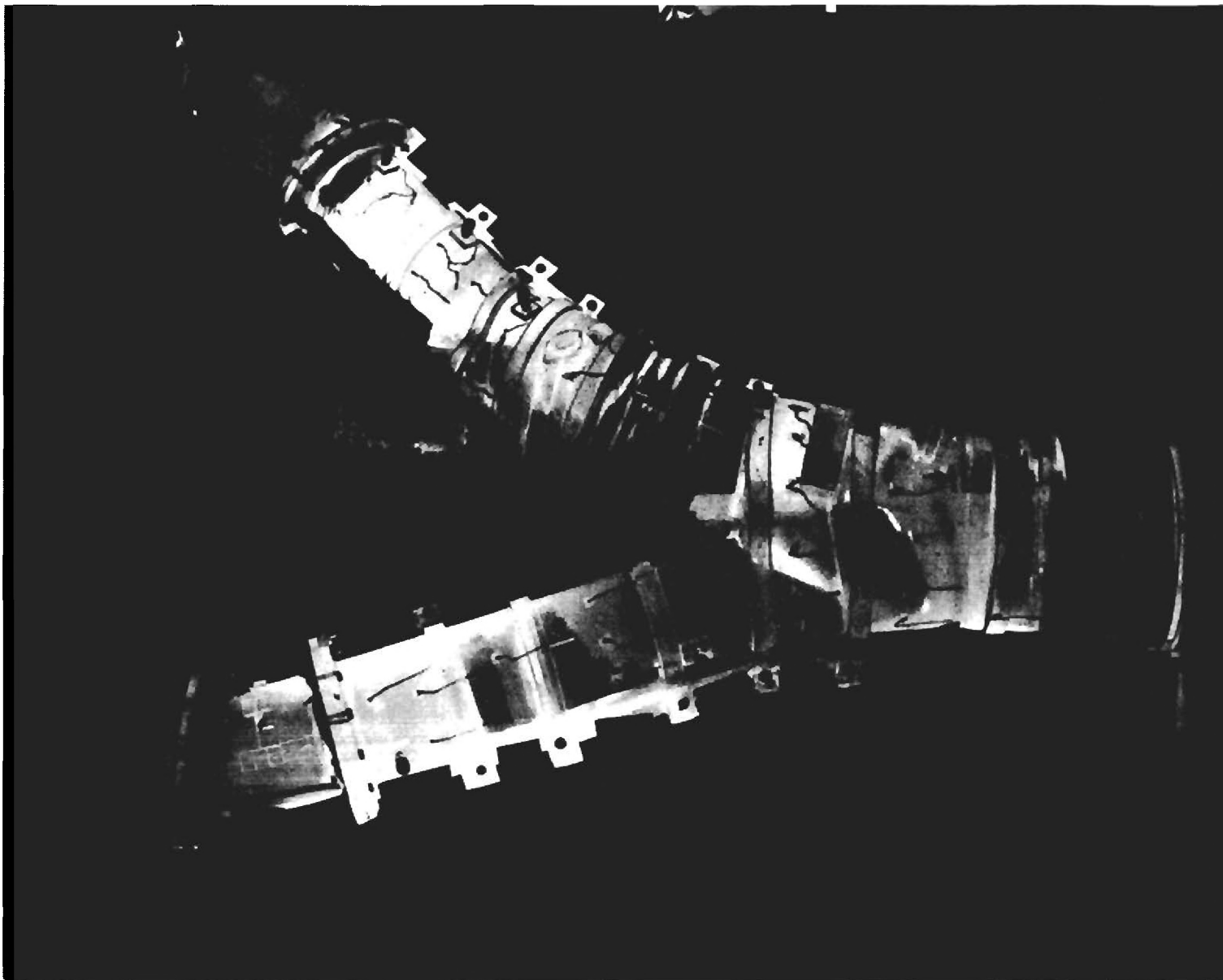


Exhibit 81. View of Tuft Pattern in Trunk Scheme A-1 for Unit 3 Pumping.

Table 12. Values of Relative Hydraulic Grade
Line in Trunk of A-1 Scheme.

TRUNK HYDRAULIC GRADE LINE SCHEME A-1

UNIT 1	UNIT 2	UNIT 3	PIEZOMETER NUMBER						
(cfs)	(cfs)	(cfs)	1	2	3	5	6	7	8
PUMPING MODE									
9750	9690	10010	1021.8	1015.5	1020.1	1022.1	1018.8	1022.4	1021.5
12710	12820	0	1004.6	993.4	1002.0	1005.9	1000.7	1006.3	1013.2
12770	0	13170	999.0	1000.3	999.7	1011.6	1008.3	1013.2	1014.5
0	12750	13240	1002.0	999.0	1004.6	1006.6	1008.6	1010.2	1014.5
0	0	13170	989.8	989.8	989.8	989.8	989.8	989.4	991.4
0	12790	0	991.4	987.1	994.1	996.4	998.0	997.0	1000.0
12880	0	0	987.8	988.8	988.1	1001.7	997.4	1001.0	1004.0
GENERATING MODE									
13260	0	0	960.4	995.4	994.7	998.0	990.4	996.0	996.4
0	13330	0	993.4	955.1	985.2	997.4	989.8	995.1	995.7
0	0	13440	997.4	997.4	997.4	953.1	997.0	996.7	995.7
0	13440	13420	990.4	954.8	984.5	955.8	988.1	988.1	985.5
13420	13420	0	956.8	950.5	968.0	991.4	963.0	983.2	985.5
13490	0	13530	957.1	998.7	996.7	953.8	988.5	987.5	985.2
10930	10960	10980	969.3	971.3	981.9	969.0	975.3	981.2	979.5

HYDRAULIC GRADE LINE ELEVATIONS ARE IN FEET

CHAPTER VII

COMPARISON OF FOUR SCHEMES

Each of the four schemes was tested under the fourteen test cases listed in Table 1. For all of the schemes head loss coefficients were determined from the direct measurement of piezometric head in the straight legs of the comprehensive model, and flow patterns in the trunk and penstocks were observed. In addition, with the exception of Case C-1 the pressure distribution in the trunks of the bifurcation models was measured. The most useful comparison of the various schemes is that of head loss coefficients. In general the comparison of flow patterns from scheme to scheme for the same operating condition would result in virtually the same conclusion, that is, one scheme is deemed better than the other.

Table 13 has been prepared to allow for the comparison of the relative loss coefficients for the various schemes. For multiple unit operation the values of the loss coefficients from Tables 3, 6, 9, and 11 are averaged to yield a single value for the particular condition. For Modified Scheme B-1 the values reported in Table 13 for some of the generating modes will not check with those on Table 3 because there were some additional tests that are not listed in the latter table.

In the 14 test cases Scheme A-1 was best 9 times; Scheme B-2, 3 times, Modified B-1 once, with Schemes A-1 and B-2 tied once. In the 3-unit generating mode Scheme B-2 head loss was 50 percent greater and Modified B-1 125 percent greater than Scheme A-1. In the 3-unit pumping mode Scheme B-2 head loss was 3 percent less than and Scheme Modified B-1 45 percent greater than Scheme A-1. Overall Scheme A-1 was the best scheme.

The flow patterns observed in Scheme A-1 always appeared to have less

turbulence and be more streamlined than in Scheme B-2, which itself showed a considerable improvement over Modified Scheme B-1.

From a hydraulic flow pattern standpoint Scheme A-1 was the best of the four schemes tested. The improvement was principally a result of (1) more gradual transitions from penstocks to trunks and (2) the absence of the elbow, and (3) the manner in which the flow was divided off the trunk to the penstocks, and vice versa.

TABLE 13
COMPARISON OF PERFORMANCE OF SCHEMES
A-1, B-1, B-2, AND C-1
BASED ON RELATIVE LOSS COEFFICIENTS K_R

<u>MODE</u>	<u>A-1</u>	<u>MODIFIED B-1</u>	<u>B-2</u>	<u>C-1</u>	Least Head Loss Scheme
Three Units Generating	0.22	0.50	0.33	0.55	A-1
Units 1 and 2 Generating	0.24	0.38	0.29	0.57	A-1
Units 1 and 3 Generating	0.27	0.42	0.29	0.53	A-1
Units 2 and 3 Generating	0.21	0.42	0.23	0.67	A-1
Unit 1 Generating	0.27	0.34	0.33	0.63	A-1
Unit 2 Generating	0.15	0.30	0.18	0.63	A-1
Unit 3 Generating	0.32	0.50	0.27	0.71	B-2
Three Units Pumping	0.29	0.42	0.28	0.72	B-2
Units 1 and 2 Pumping	0.25	0.34	0.31	0.81	A-1
Units 1 and 3 Pumping	0.34	0.36	0.34	0.71	(A-1) (B-2)
Units 2 and 3 Pumping	0.30	0.46	0.34	0.77	A-1
Unit 1 Pumping	0.35	0.31	0.46	0.79	B-1
Unit 2 Pumping	0.44	0.48	0.37	0.83	B-2
Unit 3 Pumping	0.42	0.74	0.49	0.89	A-1

CHAPTER VIII

PERFORMANCE OF ELBOW BETWEEN VERTICAL SHAFT AND TUNNEL

For each test of the four schemes investigated the complete set of values of the HGL in the vertical shaft and the tunnel allowed for the determination of the elbow loss coefficient K_L defined by Eq. (4). Because of the difficulty in assessing the head loss H_L for the smaller flows only data for two-unit and three-unit operation is considered. Furthermore, the nonlinear variation of the HGL in the vertical shaft for data taken in the pumping mode (see Exhibits 15-18, 35-38, 50-53, and 75-78) precluded the determination of reliable values of K_L with flow in that direction. The nonuniform flow downstream of the elbow did not have adequate time to develop in the relatively short vertical shaft when flow was in the pumping mode. In contrast the straightening vanes in the upper elbow enhanced flow development in the shaft when operation was in the generating mode. Moreover, in the generating mode flow development in the tunnel was greatly augmented by the much longer conduit.

Elbow loss coefficients for the pumping mode will not be considered in the analysis or discussion because of the reasons just cited.

For flow in the generating mode the elbow loss coefficients are as follows:

<u>Units Operating</u>	K_L Scheme				<u>Average</u>
	<u>Modified B-1</u>	<u>B-2</u>	<u>C-1</u>	<u>A-1</u>	
1 and 2	0.14	0.20	0.18	0.17	0.17
1 and 3	0.19	0.17	0.20	0.21	0.19
2 and 3	0.17	0.16	0.20	0.18	0.18
1, 2, and 3	<u>0.15</u>	<u>0.17</u>	<u>0.18</u>	<u>0.15</u>	<u>0.16</u>
Average	0.16	0.18	0.19	0.18	0.18

The overall average value of K_L is 0.18, compared with a value of 0.12 used in the actual design of the units. The standard deviation of the data listed above is 0.02. Previous laboratory investigations at the University of Munich by Hofmann and Wasielewski and in Japan by Ito⁻, who thoroughly summarized the German work, consistently yielded values of $K_L = 0.19$ for 90° elbows with a ratio of radius of curvature to pipe diameter $r/D = 3.3$. The maximum Reynolds number attained in the Japanese test program was approximately 325,000, corresponding to a range of 200,000 to 270,000 for the model study, for which the ratio of radius of curvature to tunnel diameter $r/D = 95/33 = 2.88$.

The results of the three laboratory investigations suggest that $K_L = 0.18$ to 0.19 for 90° elbows, for which $r/D \sim 3$ and the model Reynolds number is approximately 250,000. Even for the much greater prototype Reynolds number of approximately 58,000,000 the elbow loss coefficient would not be expected to be as low as 0.12.

CHAPTER IX

CONCLUSIONS AND RECOMMENDATIONS

Based upon the numerous tests conducted for the four schemes the average head-loss coefficient for the long-radius elbow at the base of the vertical shaft was found to be 0.18.

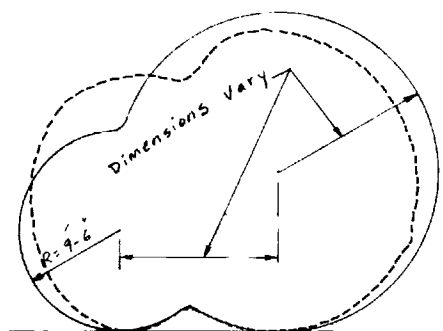
Based upon head-loss measurements and flow visualization in the trunk of the bifurcation portion of the model Scheme A-1 was overall the best scheme tested. The flow patterns observed in Scheme A-1 always appeared to possess less turbulence than in the other schemes, which in descending order of performance were B-1, Modified B-1, and C-1. It is believed that Scheme A-1 outperformed the others because of (1) more gradual transitions between trunk and penstocks, (2) the absence of the elbow, and (3) the manner in which the flow was divided from trunk to penstocks.

On the basis of the extensive model study results, Scheme A-1 is recommended as having the lowest overall hydraulic losses and the best hydraulic performance.

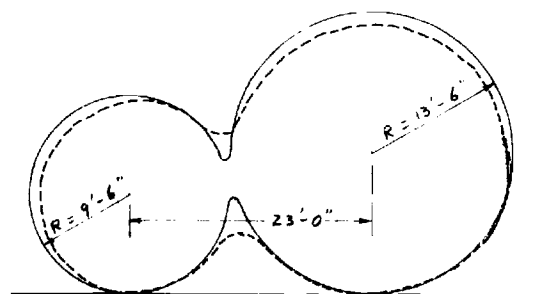
APPENDIX

The detailed design drawings of Schemes B-1 Modified, B-2, and A-1 are shown in Exhibits 82, 83, and 84, respectively. For purposes of comparison scaled-up cross sections of the as built model are also indicated on the exhibits. The greatest deviation between design and model construction occurred for Scheme B-1 Modified, as mentioned previously in the text.

Exhibit 82. Design Drawings and Model Cross Sections
for Modified Scheme B-1.



SECTION A-A



SECTION B-B

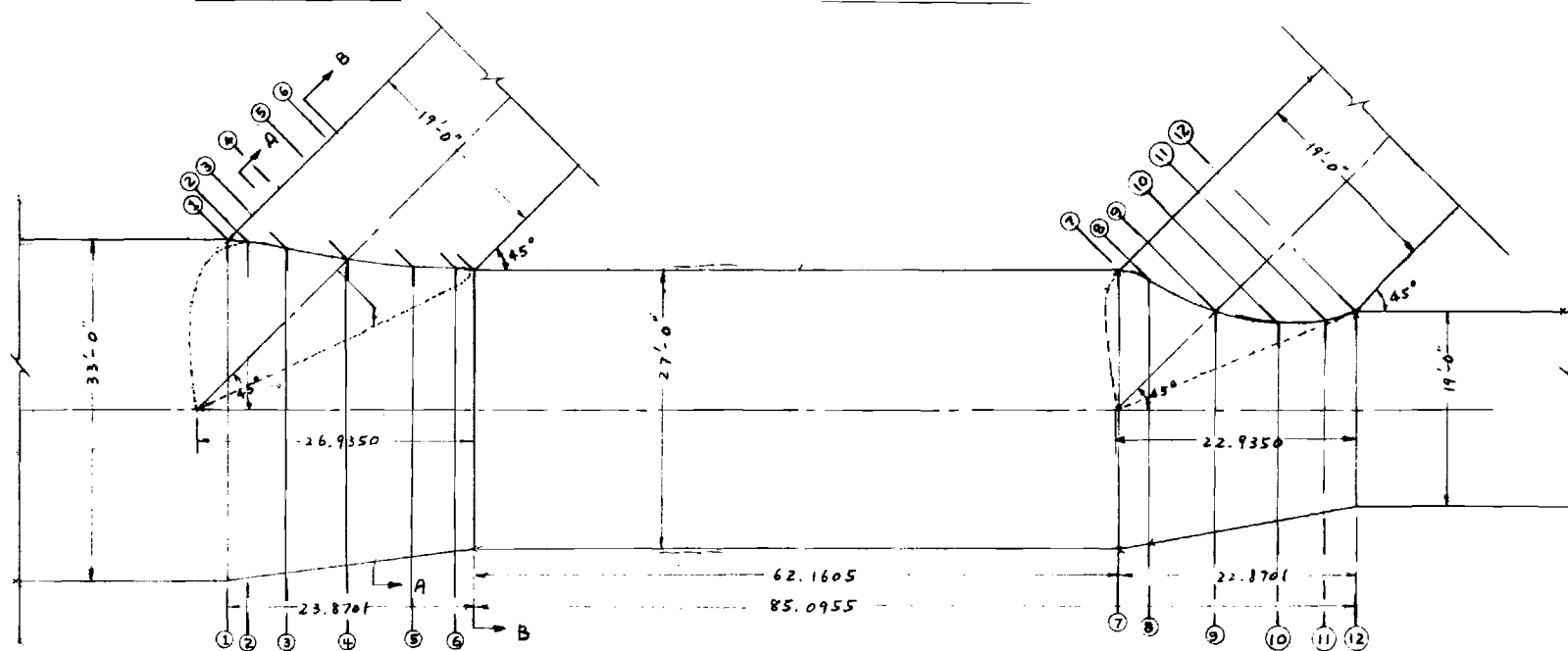


Exhibit 82.(Contd.) Design Drawings and Model Cross Sections
for Modified Scheme B-1.

— DESIGN
- - - MODEL AS BUILT

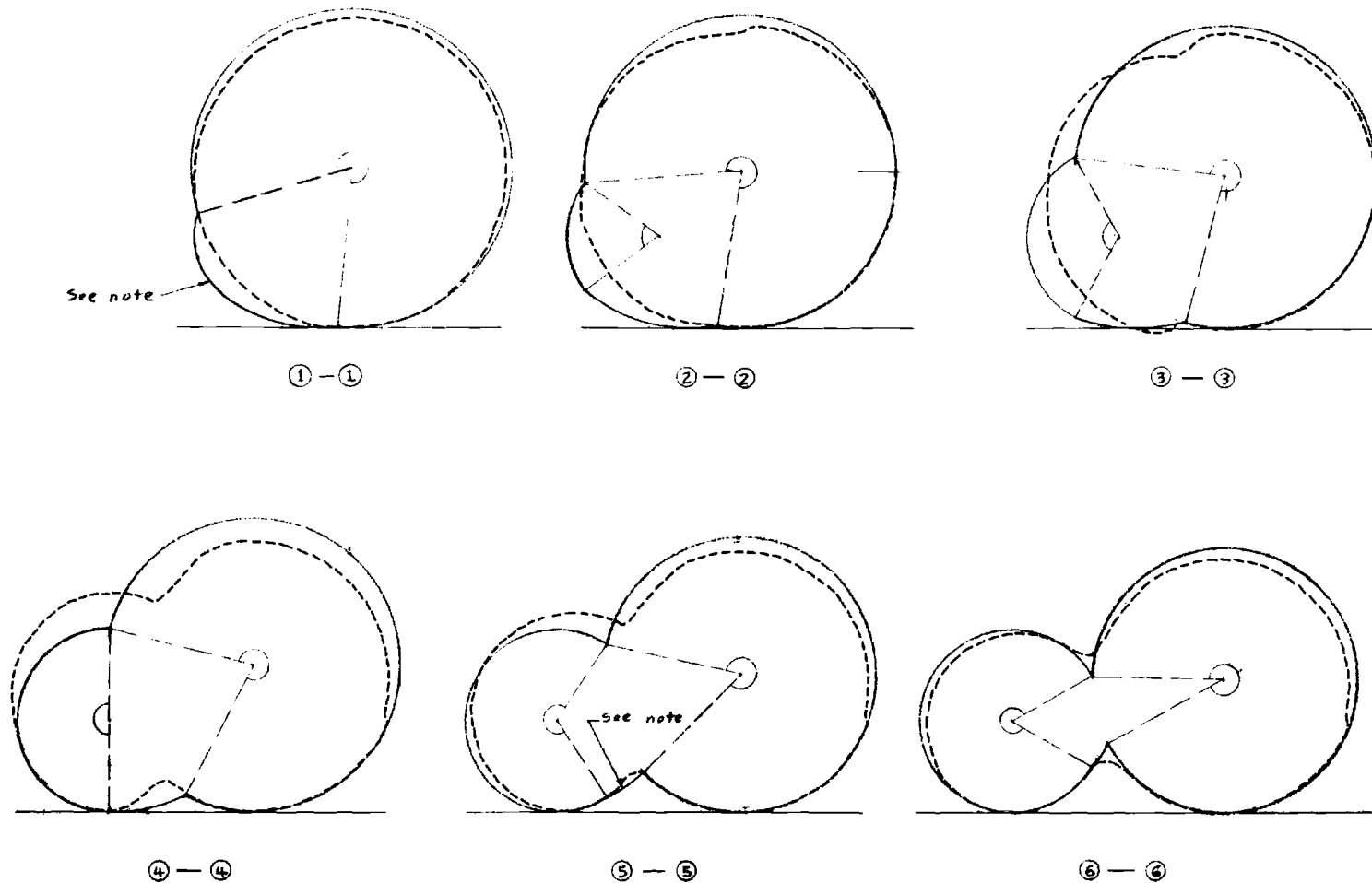
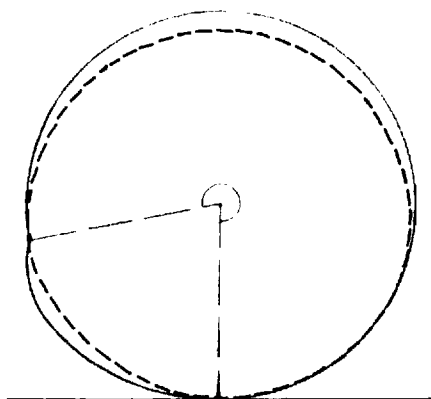
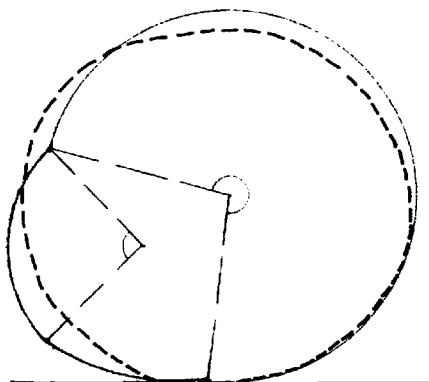


Exhibit 82.(Contd.) Design Drawings and Model Cross Sections
for Modified Scheme B-1.

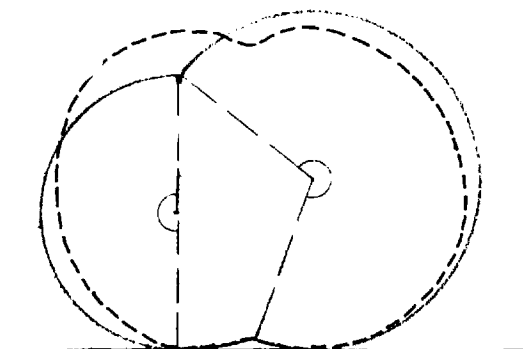
—— DESIGN
- - - - MODEL AS BUILT



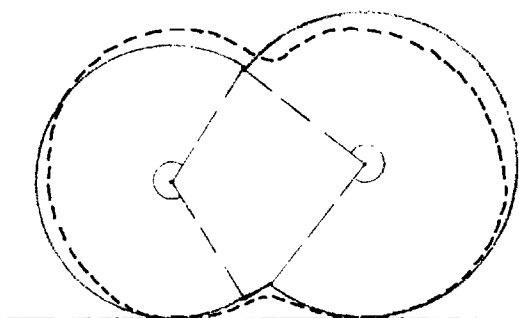
⑦ — ⑦



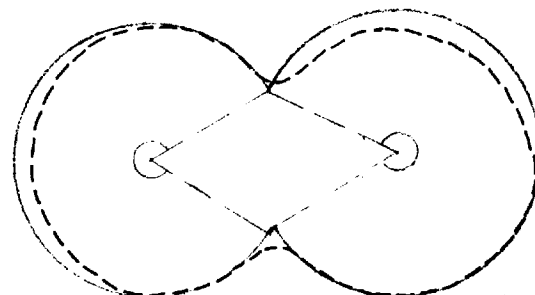
⑧ — ⑧



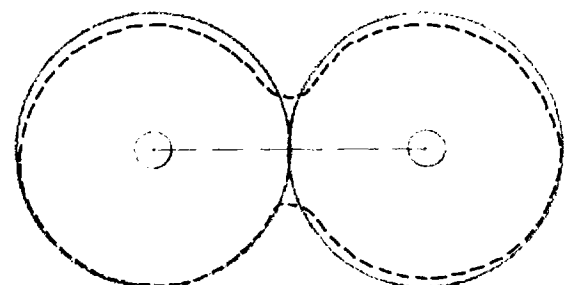
⑨ — ⑨



⑩ — ⑩



⑪ — ⑪



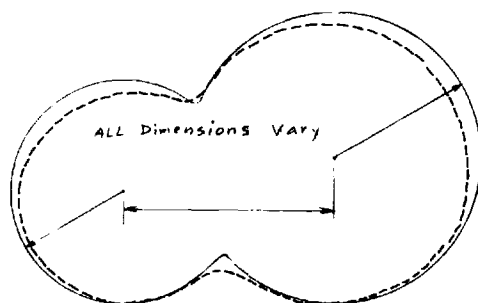
⑫ — ⑫

Exhibit 82.(Contd.) Design Drawings and Model Cross Sections
for Modified Scheme B-1.

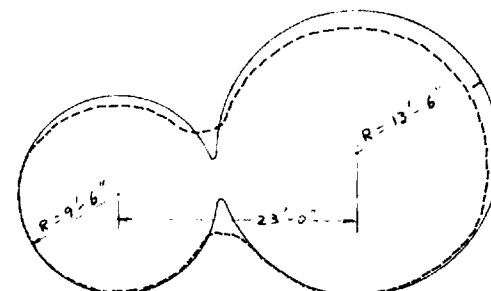
—— DESIGN
---- MODEL AS BUILT

Exhibit 83. Design Drawings and Model Cross Sections
for Scheme B-2.

SECTION A - A



SECTION B-B



SECTION C-C

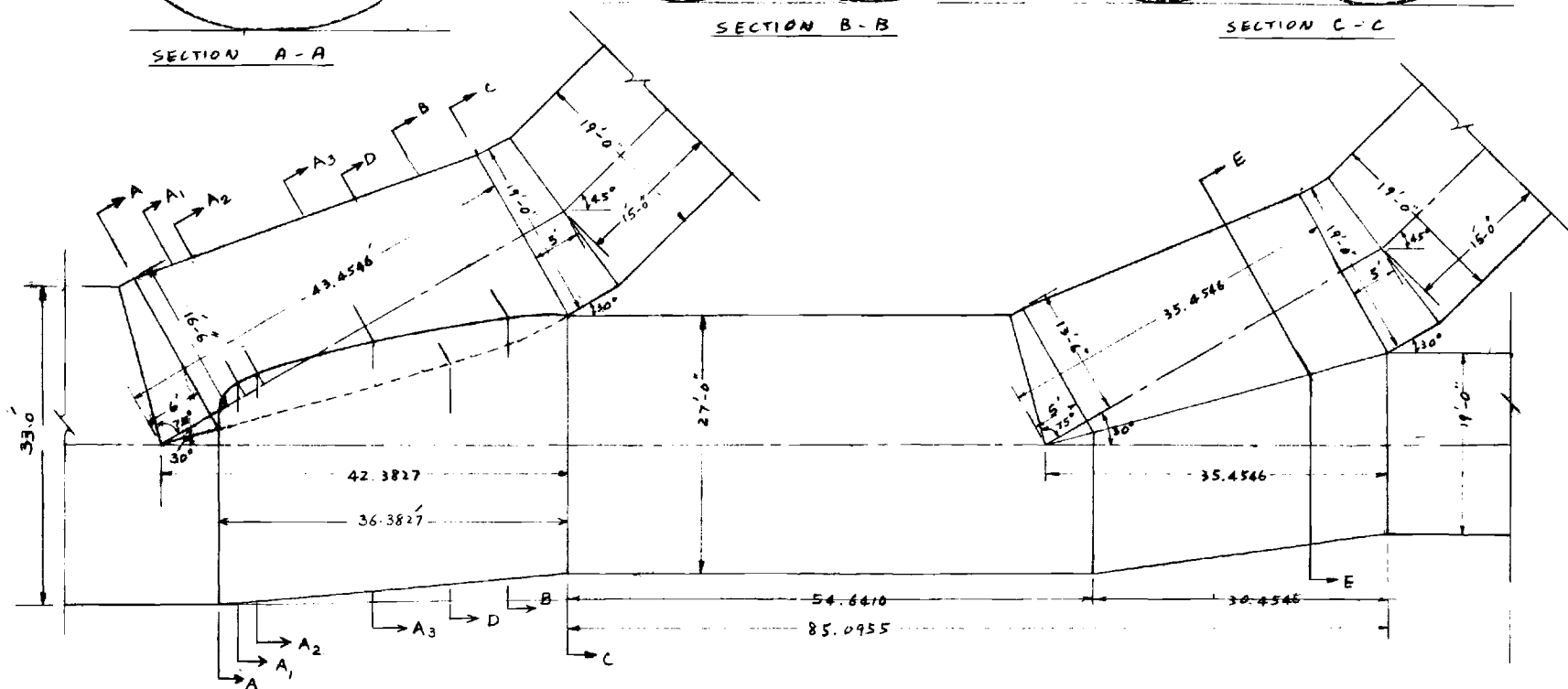
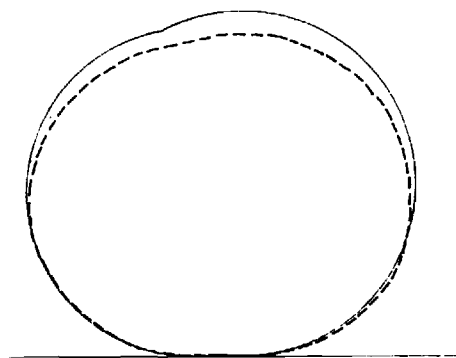
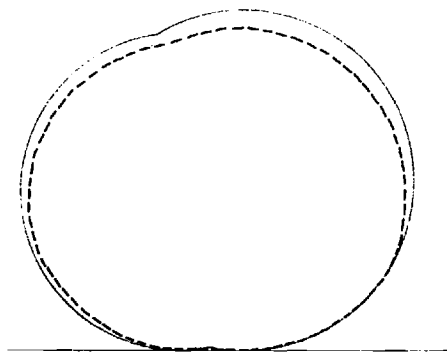
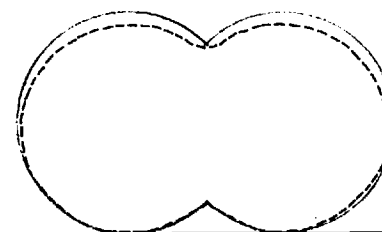
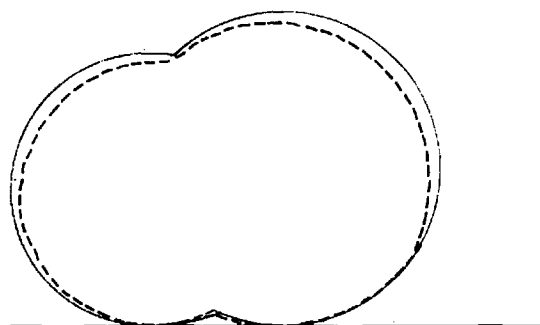
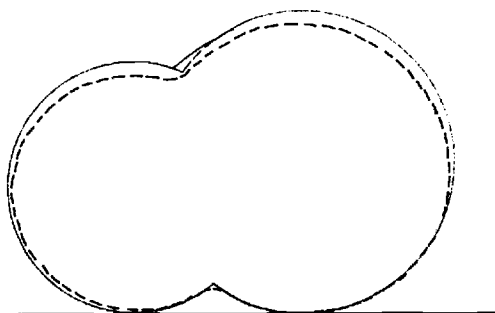


Exhibit 83.(Contd.) Design Drawings and Model Cross Sections
for Scheme B-2.

——— DESIGN
 - - - - - MODEL AS BUILT

SECTION A₁-A₁SECTION A₂-A₂

SECTION E-E

SECTION A₃-A₃

SECTION D-D

Exhibit 83.(Contd.) Design Drawings and Model Cross Sections
for Scheme B-2.

—— DESIGN
---- MODEL AS BUILT

Exhibit 84. Design Drawings and Model Cross
Sections for Scheme A-1.

_____ DESIGN
 - - - - - MODEL AS BUILT

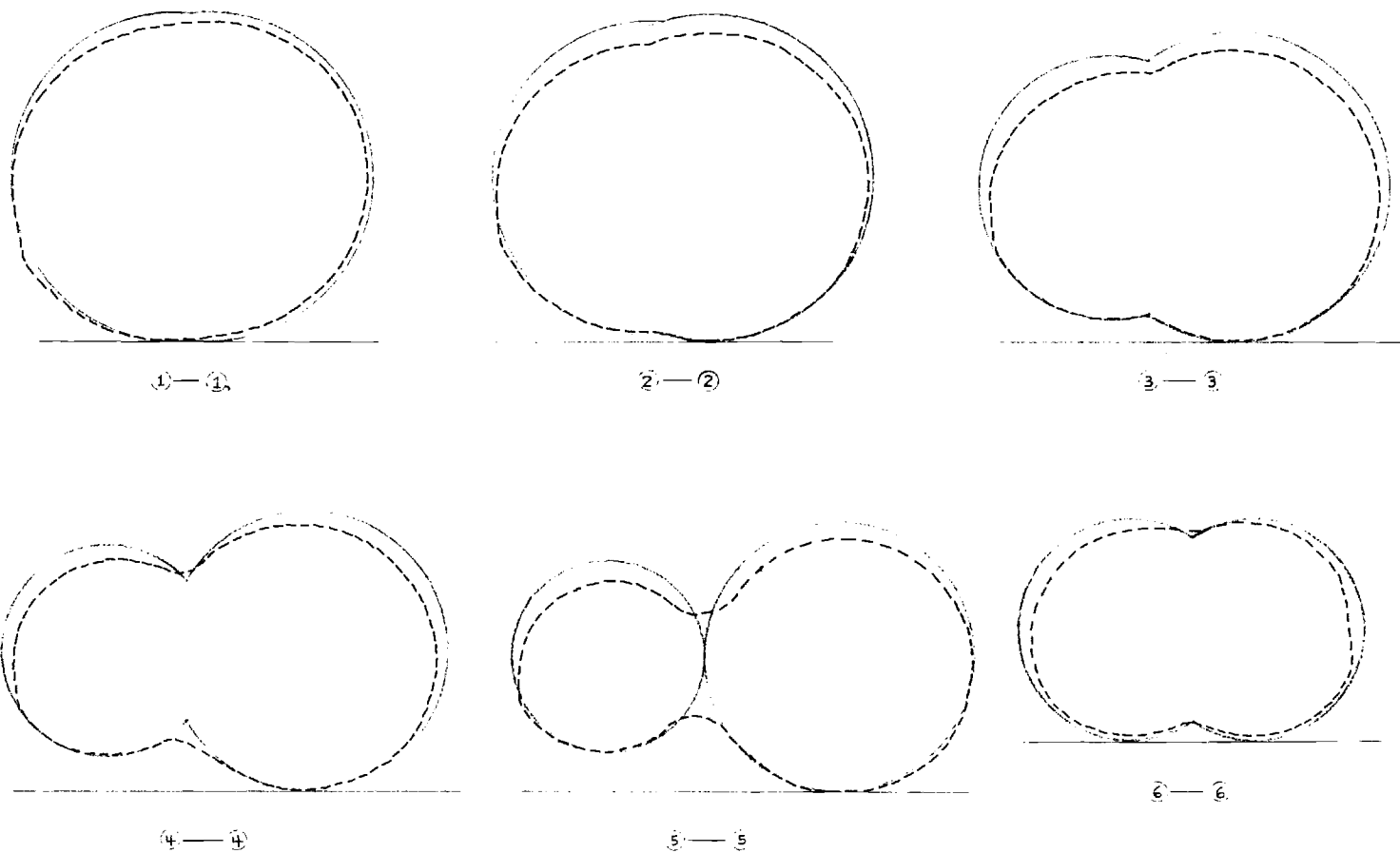


Exhibit 84.(Contd.) Design Drawings and Model Cross
Sections for Scheme A-1.

— DESIGN
--- MODEL AS BUILT